

EDUARDO BASSI SIMONI

**UNVEILING PLANT CELL SIGNALINGS: CELL DEATH RESPONSES AND
AtRGS1 PHOSPHO-BARCODE**

Thesis submitted to the Biochemistry and Biotechnology Graduate Program of the Universidade Federal de Viçosa in partial fulfillment of the requirements for the degree of *Doctor Scientiae*.

Adviser: Pedro Augusto Braga dos Reis

Co-advisers: Elizabeth Pacheco B. Fontes
Alan M. Jones
Célio Cabral Oliveira

**VIÇOSA - MINAS GERAIS
2024**

**Ficha catalográfica elaborada pela Biblioteca Central da Universidade
Federal de Viçosa - Campus Viçosa**

T

S599u
2024
Simoni, Eduardo Bassi, 1995-
Unveiling plant cell signalings: cell death responses and
AtRGS1 phospho-barcode / Eduardo Bassi Simoni. – Viçosa,
MG, 2024.

1 tese eletrônica (83 f.): il. (algumas color.).

Orientador: Pedro Augusto Braga dos Reis.

Tese (doutorado) - Universidade Federal de Viçosa,
Departamento de Bioquímica e Biologia Molecular, 2024.

Referências bibliográficas: f. 38-43.

DOI: <https://doi.org/10.47328/ufvbbt.2024.117>

Modo de acesso: World Wide Web.

1. Plantas - Biologia celular. 2. Plantas - Efeito do stress.
3. Fosforilação. 4. Proteínas G. 5. Morte celular. I. Reis, Pedro
Augusto Braga dos, 1985-. II. Universidade Federal de Viçosa.
Departamento de Bioquímica e Biologia Molecular. Programa de
Pós-graduação em Bioquímica Aplicada. III. Título.

CDD 22. ed. 571.6


EDUARDO BASSI SIMONI

**UNVEILING PLANT CELL SIGNALINGS: CELL DEATH RESPONSES AND
AtRGS1 PHOSPHO-BARCODE**


Thesis submitted to the Biochemistry and
Biotechnology Graduate Program of the
Universidade Federal de Viçosa in partial
fulfillment of the requirements for the degree
of *Doctor Scientiae*.

APPROVED: January 30, 2024

Assent:

Documento assinado digitalmente
 **EDUARDO BASSI SIMONI**
Data: 07/03/2024 17:42:30-0300
Verifique em <https://validar.iti.gov.br>

Eduardo Bassi Simoni
Author

Documento assinado digitalmente
 **PEDRO AUGUSTO BRAGA DOS REIS**
Data: 08/03/2024 12:44:42-0300
Verifique em <https://validar.iti.gov.br>

Pedro Augusto Braga dos Reis
Advisor

ACKNOWLEDGEMENTS

To God, for providing the strength and health necessary to reach this point, for shaping everything I am and have;

To my parents, my sister, and my family, for their unwavering support, unconditional love, and for doing everything to see me where I am;

To my beloved Paula, for being the best companion I could ever imagine having, for making me so happy, and for always supporting me in everything I do;

To Professor Pedro Augusto, for the guidance, patience, and trust. I appreciate every demand for results that allowed me to reach this point, in addition to the beautiful friendship we built over these years. I am very grateful to have had you as my mentor;

To Professor Elizabeth Fontes, for allowing me to be part of your laboratory, for all the teachings over the years, and for being an example of success in science. It is wonderful to be close and learn from such an intelligent and dedicated person;

To Professor Alan M. Jones, for welcoming me so well into your laboratory, for all the trust and opportunities invested in me. I cannot express how grateful I am; people like you are rare in the world;

To Jing, for all her kindness and attention to the laboratory and to me;

To the great friends who share with me the daily struggles and successes, especially Celio, not only for our collaborative work but also for the genuine friendship we share;

To the amazing friends that Viçosa and UFV/LBMP provided me, I miss you every day;

To my brothers from SJDR, I don't remember a moment, good or bad, when we weren't together;

To the Federal University of Viçosa, BIOAGRO, the Nucleus of Microscopy and Microanalysis, and INCTIPP for the structure made available for the execution of this work;

To the Coordination for the Improvement of Higher Education Personnel (CAPES) for granting the scholarship;

This study was partially financed by the Coordination for the Improvement of Higher Education Personnel – Brazil (CAPES) – Finance Code 001. Additional financial support was provided by CNPq, FAPEMIG, NIGMS, and NSF.

RESUMO

SIMONI, Eduardo Bassi, D.Sc., Universidade Federal de Viçosa, janeiro de 2024. **Revelando sinalizações celulares em plantas: Respostas à morte celular e o código de barras de fosforilação de AtRGS1.** Orientador: Pedro Augusto Braga dos Reis. Coorientadores: Elizabeth Pacheco Batista Fontes, Alan M. Jones e Célio Cabral Oliveira.

A adaptação/aclimatização de plantas depende do ajuste perfeito da interação entre o organismo e o ambiente, necessitando de uma cooperação complexa e robusta entre diferentes componentes. Alterações nessa interação podem perturbar a homeostase celular, ativando uma variedade de respostas. Desde a percepção de sinais até a regulação da expressão gênica e, posteriormente, o controle do destino celular, sofisticadas cascatas de sinalização desempenham papéis essenciais nesses processos, facilitando a comunicação entre diversas organelas. No presente trabalho, buscamos descrever e elucidar fatores envolvidos em sinalização celular específica, bem como sua função na percepção, propagação e resposta a um sinal ambiental. No primeiro capítulo, intitulado "Sinalização de morte celular a partir do estresse do retículo endoplasmático: características específicas de plantas e conservação evolutiva", revisamos os principais aspectos da sinalização do estresse do retículo endoplasmático (ER) e sua conservação evolutiva em diferentes organismos, concentrando-nos nas sinalizações de morte celular ativadas por respostas ao estresse do ER. O ER é uma organela importante responsável pelo controle do correto enovelamento e modificação pós-traducional de proteínas secretórias, homeostase de Ca^{2+} e controle de qualidade de proteínas. Sob condições normais, a dinâmica proteica do ER é estabilizada pela taxa de síntese/enovelamento e pelo sistema de armazenamento da organela. No entanto, quando o equilíbrio correto é perturbado, começam a se acumular proteínas mal dobradas e, assim, desencadeiam vias de sinalização para restaurar a condição normal, como via de resposta a proteínas mal dobradas (UPR). A acumulação de proteínas mal dobradas pode ser desencadeada por diferentes condições, como estresses bióticos e abióticos. Para restaurar o equilíbrio perfeito no ER, quatro processos principais são estimulados: diminuição da taxa de síntese de proteínas; aumento da expressão gênica de chaperonas do ER; modulação positiva de genes ERAD; expansão da capacidade interna do ER. Esses mecanismos podem ser modulados por dois ramos principais associados a proteínas

ancoradas na membrana do ER: IRE1 e transfatores bZIP. A chaperona molecular BiP também desempenha um papel importante na modulação da sinalização, atuando como chaperona e sensor do estresse. Assim, a combinação de diferentes fatores e respostas permite que a célula lide com o estresse do ER para manter a função e a sobrevivência celular. No entanto, condições de estresse prolongado que não podem ser sanadas, podem desencadear respostas de autofagia ou morte celular programada (PCD) originadas no ER, permitindo a sobrevivência do organismo às custas de células específicas. A PCD de plantas compartilha vias de sinalização conservadas e únicas capazes de modular, ativar e executar o processo de morte celular. Uma resposta única de plantas envolve os módulos da família de fatores de transcrição NAC (NAN/ATAF/CUC), que podem incluir: o módulo de morte celular mediado por DCD/NRP; o módulo de morte celular mediado por bZIP28/bZIP60-ANAC089; o módulo ANAC013/ANAC017. Coletivamente, esses mecanismos diversos são importantes na homeostase celular, percebendo, propagando e ativando respostas específicas para manter a sobrevivência do organismo. Da mesma forma, outra via de sinalização conservada foi estudada no Capítulo 2, intitulado "Revelando o impacto da fosforilação de resíduos em AtRGS1 na sinalização celular de plantas". Neste capítulo, buscamos entender o efeito de modificações pós-traducionais em RGS1 e seu papel na estrutura e função de AtRGS1. Proteínas G heterotriméricas, vitais para crescimento, desenvolvimento, respostas ao estresse e defesa contra patógenos, são negativamente reguladas pelo regulador de sinalização sete transmembranas de proteínas G (7TM-RGS), em vez de GPCRs encontrados em animais. AtRGS1 de *Arabidopsis*, com sua região de *cluster* de fosforilação de serina no C-terminal, se separa da subunidade alfa da proteína G (AtGPA1) após a fosforilação, ativando a endocitose, semelhante a beta-arrestina e as cascatas de sinalização G. Além da região de *cluster*, AtRGS1 possui resíduos de serina no domínio denominado *RGSbox* (Ser417) e na região de *linker* (Ser278), muitas vezes negligenciados devido ao foco em formas truncadas. Nossas simulações de dinâmica molecular (MD) em um modelo de membrana plasmática de planta mostram que a fosforilação na região do *linker* controla o posicionamento do domínio RGS via ligações de hidrogênio com resíduos do *RGSbox*. Este mecanismo, consistente no fosfo-mutante S278E, também é observado em lycophytes, sugerindo um padrão regulatório conservado. Ensaio *in vivo* de Split Firefly Luciferase (SFluc) revelaram que o mutante S278E, mimetizando a fosforilação de S278, exibe interação reduzida

com AtGPA1 em comparação com o tipo selvagem. Análises adicionais de MD e SFluc com vários mutantes fosfomiméticos de ambas as proteínas indicaram que a fosforilação simultânea de S278 em AtRGS1 e Y166 em AtGPA1 é necessária para uma interação estável, apontando para uma complexa relação de eventos de fosforilação na regulação da proteína G em plantas. Nossas descobertas também demonstram que a fosforilação de S278 é um modulador crucial nos processos de internalização, estabilidade e translocação nuclear. Assim, o resíduo S278 desempenha um papel importante na resposta do sistema imunológico antibacteriano. Coletivamente, esses resultados sugerem que o padrão de fosforilação de AtRGS1, especialmente S278 e do *cluster*, age como um código de barras direcionando respostas de vários elicitadores, influenciando o posicionamento do domínio da membrana e os processos gerais de sinalização.

Palavras-chave: UPR; Estresse do ER; Morte celular programada; RGS1; Sinalização G; Fosforilação; Estrutura; Internalização.

ABSTRACT

SIMONI, Eduardo Bassi, D.Sc., Universidade Federal de Viçosa, January, 2024. **Unveiling plant cell signaling: Cell death responses and AtRGS1 phospho-barcode.** Advisor: Pedro Augusto Braga dos Reis. Co-advisors: Elizabeth Pacheco Batista Fontes, Alan M. Jones and Celio Cabral Oliveira.

Plant adaptation/acclimatation relies on the perfect adjustment of the organism and the environment interaction, requiring a complex and robust cooperation among different players. Any alteration in this interaction can disrupt the cell homeostasis, activating various responses. From signal perception to gene expression regulation and subsequently cell fate control, intricate signaling cascades play essential roles in these processes, facilitating communication among diverse organelles. In the present work, we aimed to describe and seek elucidating factors that are involved in specific cell signaling, as well as their function in the perception, propagation, and the response to an environmental signal. Firstly, in the first chapter titled "Cell death signaling from endoplasmic reticulum stress: plant-specific and conserved features", we reviewed the main aspects of the endoplasmic reticulum (ER) stress signaling and its evolutionary conservation in plant organisms, focusing on the different cell death signaling activated by ER stress responses. The ER is an important organelle responsible for controlling the correct folding and post-translational modification of secretory proteins, Ca²⁺ homeostasis and protein quality control. Under normal conditions the ER protein dynamic is stabilized by the rate of synthesis/folding and organelle loading system. However, when the correct balance is disrupted, it starts accumulating unfolded proteins and, thus, triggers signaling pathways to restore the normal condition, such as the unfolded protein response (UPR). The unfolded protein accumulation can be triggered by many different conditions, such as biotic and abiotic stresses. To restore the perfect balance in the ER four main processes are stimulated: decreasing the protein synthesis rate; an increase in the ER chaperone expression; positive modulation of ERAD genes; expansion of ER internal capacity. Those mechanisms can be modulated by two main branches that are associated with ER-membrane-bound proteins: IRE1 and bZIP transactors. The molecular chaperone BiP, also plays an important role in the signaling modulation, acting as chaperone and sensor of the stress. Thus, the combination of different factors and responses allow the cell to cope with ER stress in order to maintain the cell function and survival. However, prolonged

stress conditions that cannot be restored may trigger autophagy or programmed cell death (PCD) responses originating from the ER, enabling organism survival at the expense of specific cells. Plant PCD shares conserved and unique signaling pathways capable of modulating, activating, and executing the cell death process. A unique plant response involves NAC (NAN/ATAF/CUC) transcription factor family modules, which can include: the DCD/NRP-mediated cell death component; bZIP28/bZIP60-ANAC089-mediated cell death component; ANAC013/ANAC017 component. Collectively, these diverse mechanisms are important in cell homeostasis, by perceiving, propagating, and activating specific responses in order to maintain the organism's survival. Likewise, another conserved signaling pathway was studied in Chapter 2 titled "Revealing the impact of AtRGS1 residues phosphorylation in the plant cell signaling". In this chapter we seek to understand the effect of post-translational modifications on RGS1, and their role on the structure and function of AtRGS1. Heterotrimeric G-proteins, vital for growth, development, stress responses, and pathogen defense, are negatively regulated by the seven-transmembrane Regulator of G-protein signaling (7TM-RGS) instead of GPCRs found in animals. Arabidopsis AtRGS1, with its C-terminus serine phosphorylation cluster, detaches from the G-protein alpha subunit (AtGPA1) upon phosphorylation, activating beta-arrestin-like endocytosis and G-signaling cascades. Beyond the cluster, AtRGS1 has serine residues at the RGSbox terminus (Ser417) and linker region (Ser278), often overlooked due to the focus on truncated forms. Our molecular dynamics simulations (MDS) on a plant plasma membrane model show that phosphorylation in the linker region controls RGS domain positioning via hydrogen bonds with RGSbox residues. This mechanism, consistent in the phospho-mutant S278E, is also seen in lycophytes, suggesting a conserved regulatory pattern. *In vivo* Split Firefly Luciferase (SFluc) assays revealed that the S278E variant, mimicking phosphorylated S278, exhibits reduced interaction with AtGPA1 compared to wild type. Additional MDS and SFluc analysis with several phosphomimetic mutants of both proteins indicated that concurrent phosphorylation of S278 in AtRGS1 and Y166 in AtGPA1 is necessary for stable interaction, pointing to a complex interplay of phosphorylation events in plant G protein regulation. Our findings also demonstrate that phosphorylation of S278 is a pivotal modulator in the internalization, stability and nuclei translocation processes. Finally, S278 residue has an important role in the anti-bacterial immune system response. Collectively, these results suggest that the phosphorylation pattern of

AtRGS1, especially S278 and cluster, acts as a barcode directing responses to various elicitors, influencing membrane domain positioning and overall signaling processes.

Keywords: UPR; ER-stress; Programmed cell-death; RGS1; G-signaling; Phosphorylation; Structure; Internalization.

SUMMARY

GENERAL INTRODUCTION	12
REFERENCES.....	15
Chapter I – Cell Death Signaling From Endoplasmic Reticulum Stress: Plant-Specific and Conserved Features	19
Chapter II – Revealing the Impact of AtRGS1 Residues Phosphorylation in the Plant Cell Signaling	36
INTRODUCTION.....	37
MATERIAL AND METHODS.....	40
RESULTS.....	45
DISCUSSION.....	62
REFERENCES.....	67
SUPPLEMENTARY MATERIAL.....	76
GENERAL CONCLUSION	83

GENERAL INTRODUCTION

Throughout different periods, agriculture has been and remains a pivotal activity crucial for the socio-economic development of populations. Agricultural and livestock practices stand as economic pillars in several countries, including Brazil, covering approximately 7.6% of the national territory (IBGE, 2020). Projections for agribusiness in the upcoming decade unveil an immense growth potential within this sector. It is estimated that grain and meat production should escalate by 24.1% and 22.4%, respectively, compared to the country's output in 2022-2023 (MAPA, 2023). Beyond its significant contribution to the Gross Domestic Product (GDP), agriculture generates employment, propels economic activity in rural areas, and positions Brazil as a leading global producer and exporter of agricultural commodities such as soybeans, beef, and sugar (Brasil Escola, 2022). Investment in cutting-edge technologies and sustainable practices, encompassing biotechnology, has proven pivotal in driving productivity, mitigating environmental impacts, and ensuring food security.

Characterized as sessile organisms, plants possess alternative adaptation/acclimatization mechanisms to confront both biotic and abiotic threats. Notably, the modulation of cellular signaling pathways stands out, where plants detect stimuli and respond through a complex signaling network. This process involves the activation of various components such as phytohormones, microbial pattern receptors, and the expression of defense-related genes. These processes are pivotal for plant resistance against pathogens, herbivores, and adverse environmental conditions (Delplace *et al.*, 2022).

Maintaining cellular homeostasis relies on the precise functioning of the endoplasmic reticulum (ER), given its involvement in critical processes like protein folding and maturation. Even under typical conditions, protein processing can fail, resulting in the formation of misfolded or unfolded proteins (Liu and Howell, 2016). In adverse environmental conditions or situations of high protein secretion, the need for protein folding may surpass the capacity of the folding and degradation systems. Consequently, cells can accumulate misfolded proteins within the ER lumen, inducing conditions of ER stress (Bao, Bassham and Howell, 2019).

The unfolded protein response (UPR) is a signaling pathway that has been preserved throughout evolution and is triggered in response to ER stress. In plants, this signaling occurs through signal transducers comprising two main pathways: One

pathway comprises membrane-associated transcription factors, notably BASIC LEUCINE ZIPPER 17 (bZIP17) and bZIP28, while the other pathway involves an RNA splicing factor known as INOSITOL REQUIRING ENZYME1 (IRE1) (Bao and Howell, 2017). Normally, the accumulation of misfolded proteins within the ER initiates cellular signaling, prompting genetic reprogramming to restore organismal equilibrium (Ruberti and Brandizzi, 2018). However, given the intensity or duration of the disturbance, reparative mechanisms may prove insufficient, triggering pathways toward programmed cell death.

Recent advances in comprehending the molecular mechanisms behind plant ER stress responses are extensively detailed in Chapter I, titled “Cell Death Signaling From Endoplasmic Reticulum Stress: Plant-Specific and Conserved Features”. This chapter, a published review available at *Frontiers in Plant Science* by Simoni *et al.* (2022), primarily focuses on (a) plant ER stress elicitation and conserved features of plant UPR; (b) conserved features of the ER stress-induced cell death in plants; (c) ER stress-induced plant-specific cell death signaling: mechanisms and regulation; (d) ER stress-mediated autophagy; (e) ER stress-induced PCD in plant immunity.

Plant adaptation to adverse environmental conditions relies on a complex interplay of diverse mechanisms that operate simultaneously, each designed to discern specific signals and trigger precise responses. Besides ER-associated signaling, the Heterotrimeric G complex orchestrates another pivotal signaling cascade, serving as a crucial mechanism for transducing a broad spectrum of signals across diverse organisms (Mohanasundaram and Pandey, 2023). In addition to their involvement in stress signaling, numerous studies conducted over the years have highlighted the substantial role of G-proteins in several processes, including growth, development, germination, cell division, and hormonal responses (Cho *et al.*, 2015; Wu and Urano, 2018; Pandey and Vijayakumar, 2018; Pandey, 2019; Liu *et al.*, 2021; Ofoe, 2021; Mohanasundaram and Pandey, 2023).

The canonical form of the G complex comprises a $G\alpha$, a $G\beta$, and a $G\gamma$ protein, with the complex's activity regulated by the nucleotide bound to the $G\alpha$ protein (Gilman, 1987). While bound to GDP, $G\alpha$ remains coupled with the $G\beta\gamma$ dimer. However, upon signal-driven activation, a conformational change allows $G\alpha$ to substitute GTP for GDP. This substitution prompts $G\alpha$ to disassociate from the heterotrimeric complex, initiating a specific response for the required signaling (Johnston *et al.*, 2007).

In contrast to animals, plants regulate the activation/deactivation process through the action of the Regulator of G-protein signaling 1 (RGS1) (Jones *et al.*, 2011). The structure of RGS1 comprises a GPCR-like seven-transmembrane barrel domain at the N-terminus, followed by a disordered linker region, a conserved RGS domain, and a C-terminal tail that contains a cluster of five phosphoserines residues (Johnston *et al.*, 2007; Watkins *et al.*, 2021). Besides the serine-cluster residues located in the C-terminal tail, RGS1 also includes a serine residue at the end of RGSbox (Ser417) and another within the linker region (Ser278) (Tunc-Ozdemir *et al.*, 2017; Oliveira *et al.*, 2022).

Widely acknowledged, post-translational modifications stand as crucial mechanisms guiding signaling pathways across various physiological processes in response to a diverse stimulus (Kown *et al.*, 2006; Withers and Dong, 2017). Considering the aforementioned points, Chapter II, titled "Revealing the impact of AtRGS1 residues phosphorylation in the plant cell signaling" primarily explores the effect of AtRGS1 phosphorylation on its dynamics and function. Consistent data highlight the significant influence of phosphorylation patterns on various protein features, including stability, subcellular localization, bacterial responses and protein interactions.

REFERENCES

Bao, Y., Bassham, D. C., & Howell, S. H. (2019). A Functional Unfolded Protein Response Is Required for Normal Vegetative Development. *Plant physiology*, 179(4), 1834–1843. <https://doi.org/10.1104/pp.18.01261>

Bao, Y., & Howell, S. H. (2017). The Unfolded Protein Response Supports Plant Development and Defense as well as Responses to Abiotic Stress. *Frontiers in plant science*, 8, 344. <https://doi.org/10.3389/fpls.2017.00344>

Brasil Escola. Agricultura no Brasil. Disponível em: <https://brasilecola.uol.com.br/brasil/agricultura.htm> . Acesso em: 29/11/23.

Chen, J. G., & Jones, A. M. (2004). AtRGS1 function in *Arabidopsis thaliana*. *Methods in enzymology*, 389, 338–350. [https://doi.org/10.1016/S0076-6879\(04\)89020-7](https://doi.org/10.1016/S0076-6879(04)89020-7)

Cho, Y., Yu, C. Y., Iwasa, T., & Kanehara, K. (2015). Heterotrimeric G protein subunits differentially respond to endoplasmic reticulum stress in *Arabidopsis*. *Plant signaling & behavior*, 10(10), e1061162. <https://doi.org/10.1080/15592324.2015.1061162>

Delplace, F., Huard-Chauveau, C., Berthomé, R., & Roby, D. (2022). Network organization of the plant immune system: from pathogen perception to robust defense induction. *The Plant journal: for cell and molecular biology*, 109(2), 447–470. <https://doi.org/10.1111/tpj.15462>

Gilman A. G. (1987). G proteins: transducers of receptor-generated signals. *Annual review of biochemistry*, 56, 615–649. <https://doi.org/10.1146/annurev.bi.56.070187.003151>

Instituto Brasileiro de Geografia e Estatística (IBGE). Área agrícola cresce em dois anos e ocupa 7,6% do território nacional. Disponível em: <https://agenciadenoticias.ibge.gov.br/agencia-noticias/2012-agencia-de-noticias/noticias/27207-area-agricola-cresce-em-dois-anos-e-ocupa-7-6-do-territorio-nacional> . Acesso em: 29/11/23.

Johnston, C. A., Taylor, J. P., Gao, Y., Kimple, A. J., Grigston, J. C., Chen, J. G., Siderovski, D. P., Jones, A. M., & Willard, F. S. (2007). GTPase acceleration as the rate-limiting step in Arabidopsis G protein-coupled sugar signaling. *Proceedings of the National Academy of Sciences of the United States of America*, 104(44), 17317–17322. <https://doi.org/10.1073/pnas.0704751104>

Jones, J. C., Temple, B. R., Jones, A. M., & Dohlman, H. G. (2011). Functional reconstitution of an atypical G protein heterotrimer and regulator of G protein signaling protein (RGS1) from *Arabidopsis thaliana*. *The Journal of biological chemistry*, 286(15), 13143–13150. <https://doi.org/10.1074/jbc.M110.190355>

Kwon, S. J., Choi, E. Y., Choi, Y. J., Ahn, J. H., & Park, O. K. (2006). Proteomics studies of post-translational modifications in plants. *Journal of experimental botany*, 57(7), 1547–1551. <https://doi.org/10.1093/jxb/erj137>

Liu, Y., Wang, X., Dong, D., Guo, L., Dong, X., Leng, J., Zhao, B., Guo, Y. D., & Zhang, N. (2021). Research Advances in Heterotrimeric G-Protein α Subunits and Unconventional G-Protein Coupled Receptors in Plants. *International journal of molecular sciences*, 22(16), 8678. <https://doi.org/10.3390/ijms22168678>

Liu, J. X., & Howell, S. H. (2016). Managing the protein folding demands in the endoplasmic reticulum of plants. *The New phytologist*, 211(2), 418–428. <https://doi.org/10.1111/nph.13915>

Ministério da Agricultura e Pecuária. Projeções do Agronegócio, Brasil – 2022/2023 a 2032/2033. Disponível em: <https://www.gov.br/agricultura/pt-br/assuntos/politica-agricola/todas-publicacoes-de-politica-agricola/projecoes-do-agronegocio/projecoes-do-agronegocio-2022-2023-a-2032-2033.pdf/> . Acesso em:

Mohanasundaram, B., & Pandey, S. (2023). Moving beyond the arabidopsis-centric view of G-protein signaling in plants. *Trends in plant science*, 28(12), 1406–1421. <https://doi.org/10.1016/j.tplants.2023.07.014>

Ofoe R. (2021). Signal transduction by plant heterotrimeric G-protein. *Plant biology (Stuttgart, Germany)*, 23(1), 3–10. <https://doi.org/10.1111/plb.13172>

Oliveira, C. C., Jones, A. M., Fontes, E. P. B., & Reis, P. A. B. D. (2022). G-Protein Phosphorylation: Aspects of Binding Specificity and Function in the Plant Kingdom. *International journal of molecular sciences*, 23(12), 6544. <https://doi.org/10.3390/ijms23126544>

Pandey S. (2019). Heterotrimeric G-Protein Signaling in Plants: Conserved and Novel Mechanisms. *Annual review of plant biology*, 70, 213–238. <https://doi.org/10.1146/annurev-arplant-050718-100231>

Pandey, S., & Vijayakumar, A. (2018). Emerging themes in heterotrimeric G-protein signaling in plants. *Plant science: an international journal of experimental plant biology*, 270, 292–300. <https://doi.org/10.1016/j.plantsci.2018.03.001>

Ruberti, C., & Brandizzi, F. (2018). Unfolded Protein Response in Arabidopsis. *Methods in molecular biology (Clifton, N.J.)*, 1691, 231–238. https://doi.org/10.1007/978-1-4939-7389-7_18

Simoni, E. B., Oliveira, C. C., Fraga, O. T., Reis, P. A. B., & Fontes, E. P. B. (2022). Cell Death Signaling From Endoplasmic Reticulum Stress: Plant-Specific and Conserved Features. *Frontiers in plant science*, 13, 835738. <https://doi.org/10.3389/fpls.2022.835738>

Tunc-Ozdemir, M., Li, B., Jaiswal, D. K., Urano, D., Jones, A. M., & Torres, M. P. (2017). Predicted Functional Implications of Phosphorylation of Regulator of G Protein Signaling Protein in Plants. *Frontiers in plant science*, 8, 1456. <https://doi.org/10.3389/fpls.2017.01456>

Watkins, J. M., Ross-Elliott, T. J., Shan, X., Lou, F., Dreyer, B., Tunc-Ozdemir, M., Jia, H., Yang, J., Oliveira, C. C., Wu, L., Trusov, Y., Schwochert, T. D., Krysan, P., & Jones, A. M. (2021). Differential regulation of G protein signaling in Arabidopsis through two

distinct pathways that internalize AtRGS1. *Science signaling*, 14(695), eabe4090. <https://doi.org/10.1126/scisignal.abe4090>

Withers, J., & Dong, X. (2017). Post-translational regulation of plant immunity. *Current opinion in plant biology*, 38, 124–132. <https://doi.org/10.1016/j.pbi.2017.05.004>

Wu, T. Y., & Urano, D. (2018). Genetic and Systematic Approaches Toward G Protein-Coupled Abiotic Stress Signaling in Plants. *Frontiers in plant science*, 9, 1378. <https://doi.org/10.3389/fpls.2018.01378>

CHAPTER I

CELL DEATH SIGNALING FROM ENDOPLASMIC RETICULUM STRESS: PLANT-SPECIFIC AND CONSERVED FEATURES

Published article

Eduardo Bassi Simoni, Celio Cabral Oliveira, Otto Teixeira Fraga, Pedro Augusto Braga dos Reis, Elizabeth Pacheco Batista Fontes (2022). Cell Death Signaling From Endoplasmic Reticulum Stress: Plant-Specific and Conserved Features. *Frontiers in Plant Science*. 3(13):835738. doi: 10.3389/fpls.2022.835738.

Pages 20 to 35



Cell Death Signaling From Endoplasmic Reticulum Stress: Plant-Specific and Conserved Features

Eduardo B. Simoni[†], Célio C. Oliveira[†], Otto T. Fraga[†], Pedro A. B. Reis and Elizabeth P. B. Fontes^{*}

Department of Biochemistry and Molecular Biology, BIOAGRO, National Institute of Science and Technology in Plant-Pest Interactions, Universidade Federal de Viçosa, Viçosa, Brazil

OPEN ACCESS

Edited by:

Lingrui Zhang,
Purdue University, United States

Reviewed by:

Yan Bao,
Shanghai Jiao Tong University, China
Aiming Wang,
Agriculture and Agri-Food
Canada (AAFC), Canada

*Correspondence:

Elizabeth P. B. Fontes
bbfontes@ufv.br

[†]These authors have contributed
equally to this work

Specialty section:

This article was submitted to
Plant Cell Biology,
a section of the journal
Frontiers in Plant Science

Received: 14 December 2021

Accepted: 10 January 2022

Published: 03 February 2022

Citation:

Simoni EB, Oliveira CC, Fraga OT,
Reis PAB and Fontes EPB (2022) Cell
Death Signaling From Endoplasmic
Reticulum Stress: Plant-Specific and
Conserved Features.
Front. Plant Sci. 13:835738.
doi: 10.3389/fpls.2022.835738

The endoplasmic reticulum (ER) stress response is triggered by any condition that disrupts protein folding and promotes the accumulation of unfolded proteins in the lumen of the organelle. In eukaryotic cells, the evolutionarily conserved unfolded protein response is activated to clear unfolded proteins and restore ER homeostasis. The recovery from ER stress is accomplished by decreasing protein translation and loading into the organelle, increasing the ER protein processing capacity and ER-associated protein degradation activity. However, if the ER stress persists and cannot be reversed, the chronically prolonged stress leads to cellular dysfunction that activates cell death signaling as an ultimate attempt to survive. Accumulating evidence implicates ER stress-induced cell death signaling pathways as significant contributors for stress adaptation in plants, making modulators of ER stress pathways potentially attractive targets for stress tolerance engineering. Here, we summarize recent advances in understanding plant-specific molecular mechanisms that elicit cell death signaling from ER stress. We also highlight the conserved features of ER stress-induced cell death signaling in plants shared by eukaryotic cells.

Keywords: endoplasmic reticulum, cell death signaling, autophagy, plant immunity, ER stress, programmed cell death, unfolded protein response

INTRODUCTION

The endoplasmic reticulum (ER) is the gateway of synthesized proteins by ER membrane-bound polysomes to the secretory pathway. It is a multitask intracellular organelle that provides the functional apparatus for translocation of the newly synthesized secretory proteins to the lumen of the organelle, protein folding, and protein post-translational modifications. These protein processing activities allow nascent proteins to their destination in the secretory pathway. Under normal conditions, the rate of protein processing in the ER lumen is balanced with the protein synthesis rate and loading into the organelle. Stress conditions that disturb this equilibrium and promote the accumulation of unprocessed, misfolded protein in the organelle promote ER dysfunction, a process known as ER stress. To minimize the deleterious effect of misfolded proteins and prevent their translocation further in the secretory pathway, a protein quality

control machinery monitors protein folding. It addresses misfolded proteins to degradation *via* either the ER-associated degradation (ERAD) system or autophagy. The perturbations in the ER function activate signaling cascades that allow ER communication with the cytoplasm, nucleus, and, under chronically prolonged ER stress, mitochondria, and vacuole to restore ER homeostasis or ultimately cause programmed cell death (PCD).

The unfolded protein response (UPR) is an evolutionarily conserved signaling pathway activated in response to ER stress. Plant UPR is transduced as a well-characterized bipartite signaling module consisting of the ER membrane-associated transducers inositol-requiring protein 1 (IRE1) and bZIP (basic leucine zipper) transmembrane transactivation factors. In *Arabidopsis*, two copies of IRE1, *Arabidopsis thaliana* (At)IRE1a and AtIRE1b, and two copies of the transmembrane bZIP, AtbZIP28, and AtbZIP17, with partially overlapping functions operate in UPR. The functional conservation of these UPR transducers has been examined in other plant species and extends to include eukaryotes from other kingdoms. Under physiological conditions, the luminal domain of AtbZIP28 is bound to the ER-resident molecular chaperone binding protein (BiP) that prevents its activation. Under ER stress conditions, the demand for the chaperone function of BiP is increased, then BiP dissociates from bZIP28, allowing its translocation to the Golgi where it is proteolytically processed to release the bZIP domain from the membrane and promote its translocation to the nucleus. ER stress also activates the kinase and endonuclease domains of the second UPR transducer IRE1, which promotes unconventional splicing of AtbZIP60 RNA to delete a transmembrane motif-encoding segment of the AtbZIP60u unspliced RNA. The IRE-mediated unconventional splicing results in the translation of AtbZIP60s spliced RNA into a soluble transactivation factor that is translocated to the nucleus. AtbZIP60 is the primary downstream component of the IRE1 signaling module, which acts in concert with AtbZIP28 to induce the expression of ER protein processing-related genes involved in the ER protein folding machinery and PCD system. Furthermore, the nuclease activity of IRE1 degrades mRNA encoding secretory proteins, a process known as Regulated IRE1-Dependent RNA Decay (RIDD), to reduce protein loading into the lumen, thereby decreasing protein folding demands within the organelle. However, extensive and acute ER stress directs the UPR toward activating cell death-triggering pathways.

This review describes recent advances in understanding the molecular mechanisms underlying the ER stress responses in plants. It focuses primarily on (a) plant UPR and their connections with cell death mechanisms; (b) ER stress-induced plant-specific cell death signaling; (c) ER stress-mediated autophagy; and (d) ER stress-induced PCD in plant immunity.

PLANT ER STRESS ELICITATION AND CONSERVED FEATURES OF PLANT UPR

The precise operation of the ER is essential to maintaining cellular homeostasis as the ER is involved in several crucial

processes, such as protein folding and maturation. Protein processing can fail even under normal conditions, leading to misfolded/unfolded proteins. To minimize the accumulation of unfolded proteins, two systems play essential roles, the ER quality control (ERQC) system and the ERAD system (reviewed in Liu and Howell, 2016). Nevertheless, under adverse environmental conditions or conditions of intense protein secretion, the demand for protein folding can exceed the efficiency of the folding and degradation systems, thereby, the cells might accumulate misfolded proteins in the ER lumen, leading the ER stress conditions (Liu and Howell, 2016).

Different biotic and abiotic stresses have been shown capable of causing ER stress. In the plant cells, ER stress can be induced by adverse environmental conditions, such as heat, salt, and drought (Liu et al., 2007b; Deng et al., 2011; Parra-Rojas et al., 2015). Similarly, pathogen diseases can also trigger an imbalance in ER functioning, leading to ER stress. Moreno et al. (2012), Ye et al. (2013), and Park and Park (2019). Furthermore, studies have shown that the plant hormones salicylic acid (SA) and ABA may be associated with ER stress (Yang et al., 2013; Nagashima et al., 2014; Zhou et al., 2015). In addition, certain chemical compounds, including tunicamycin (TM), dithiothreitol (DTT), and 1-azetidine-2-carboxylic acid (AZC), can trigger ER stress. While TM prevents N-linked glycosylation of secreted glycoproteins, DTT interferes with the formation of disulfide bonds and, as an inhibitor of the ER calcium pump, AZC affects the primary components of the ER protein-folding apparatus, calnexin, and calreticulin, which are calcium-dependent, thereby, all of them are capable of disrupting the correct folding of proteins (Nawkar et al., 2018). How all elicitors work is not fully understood, but presumably, they may hinder the ER function in some way to indirectly affect protein folding (Howell, 2017).

The accumulation of misfolded proteins in the ER lumen establishes the condition known as ER stress that stimulates UPR. UPR is a conserved cytoprotective signaling pathway among eukaryotes (Wan and Jiang, 2016). This pathway is activated primarily to restore ER homeostasis through (i) an increase in ER chaperone synthesis for protein folding; (ii) upregulation of lipid synthesis to expand ER capacity; (iii) repression of global translation to control protein loading into the organelle; and (iv) upregulation of ERAD genes to attenuate unfolded protein accumulation in the ER lumen (Nawkar et al., 2018; Pastor-Cantizano et al., 2020).

ER stress perception and, subsequently, UPR activation are mediated by membrane-associated sensors first identified in yeast and mammals (Fu and Gao, 2014). In yeast, the UPR is regulated by the inositol-requiring transmembrane kinase/ endonuclease p, a type I transmembrane ER protein that removes an intron of 252 nucleotides from HAC1 mRNA, forming the mature mRNA Hac1p (Figure 1, Sidrauski and Walter, 1997; Maldonado-Bonilla, 2020). Hac1p encodes a transcription factor of 238 amino acids (Figure 2) that plays an essential role in the UPR signaling, regulating downstream UPR genes including *KAR2*, *PDII*, *EUG1*, and *LHS1* (Xia, 2019). In metazoans, the UPR signaling pathway is modulated by three ER stress-sensing and transducing proteins (Figure 1). One branch of UPR

signaling involves the bifunctional kinase and endoribonuclease IRE 1 (α and β subunits), which splices the mRNA of bZIP-like transcription factor X box-binding protein-1 (XBP1; **Figure 2**). A second branch is mediated by membrane-tethered activating transcription factor 6 (ATF6), transported to the Golgi to be processed by site 1 and site 2 proteases (S1P and S2P). In the third signaling branch, the global translation is regulated by ER-associated kinase R-like endoplasmic reticulum kinase (PERK), which phosphorylates and inactivates the translation initiation factor eIF2 α (Wan and Jiang, 2016; Ruberti et al., 2018). These ER sensors are regulated by the ER-resident molecular chaperone BiP. Under normal conditions, BiP associates with the luminal portion of these receptors, keeping them inactive. Accumulation of misfolded proteins in the ER causes BiP to dissociate from these transducers to serve as a molecular

chaperone. The BiP release promotes the activation of these receptors (Pincus et al., 2010; Srivastava et al., 2013; Li et al., 2017).

Plant functional homologs of ATF6 (bZIP17 and bZIP28) and IRE1 (IRE1a and IRE1b), but not PERK, have been described (Ruberti and Brandizzi, 2014). bZIP17 and bZIP28 are type II transmembrane proteins with a cytosolic N-terminal portion containing the bZIP transcription factor (TF) domain and an ER luminal C-terminus with amino acid signals for ER retention (**Figure 1**; Liu et al., 2007a). In non-stressed cells, BiP interacts with the luminal domain of bZIP17/28, keeping them retained in the ER (**Figure 1**). Upon ER stress, however, BiP disconnects from bZIP17/28 to act on misfolded proteins and, thus, allowing the translocation of these TFs from ER toward the Golgi complex (Srivastava et al., 2013). Once on the Golgi, an unidentified

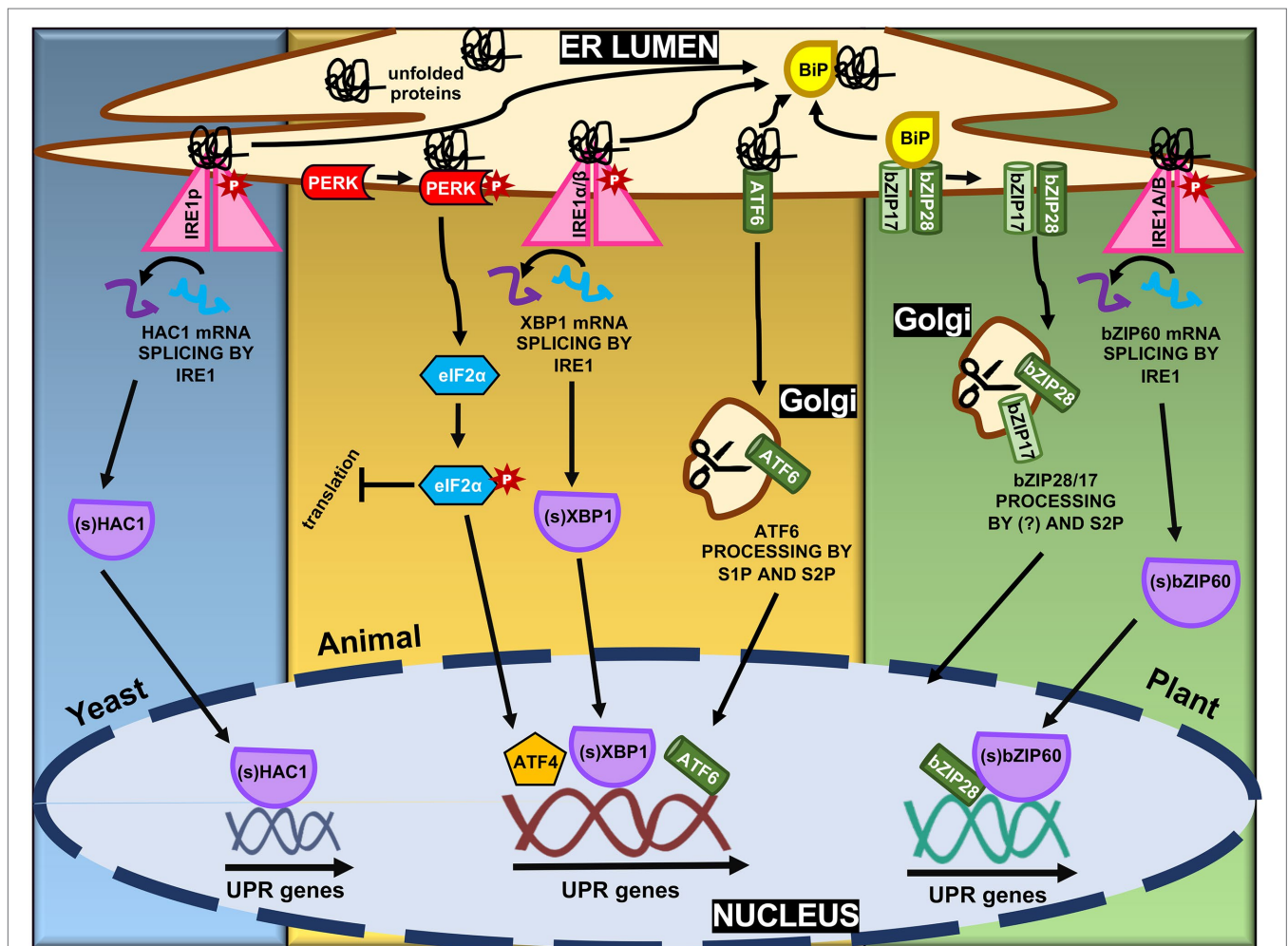
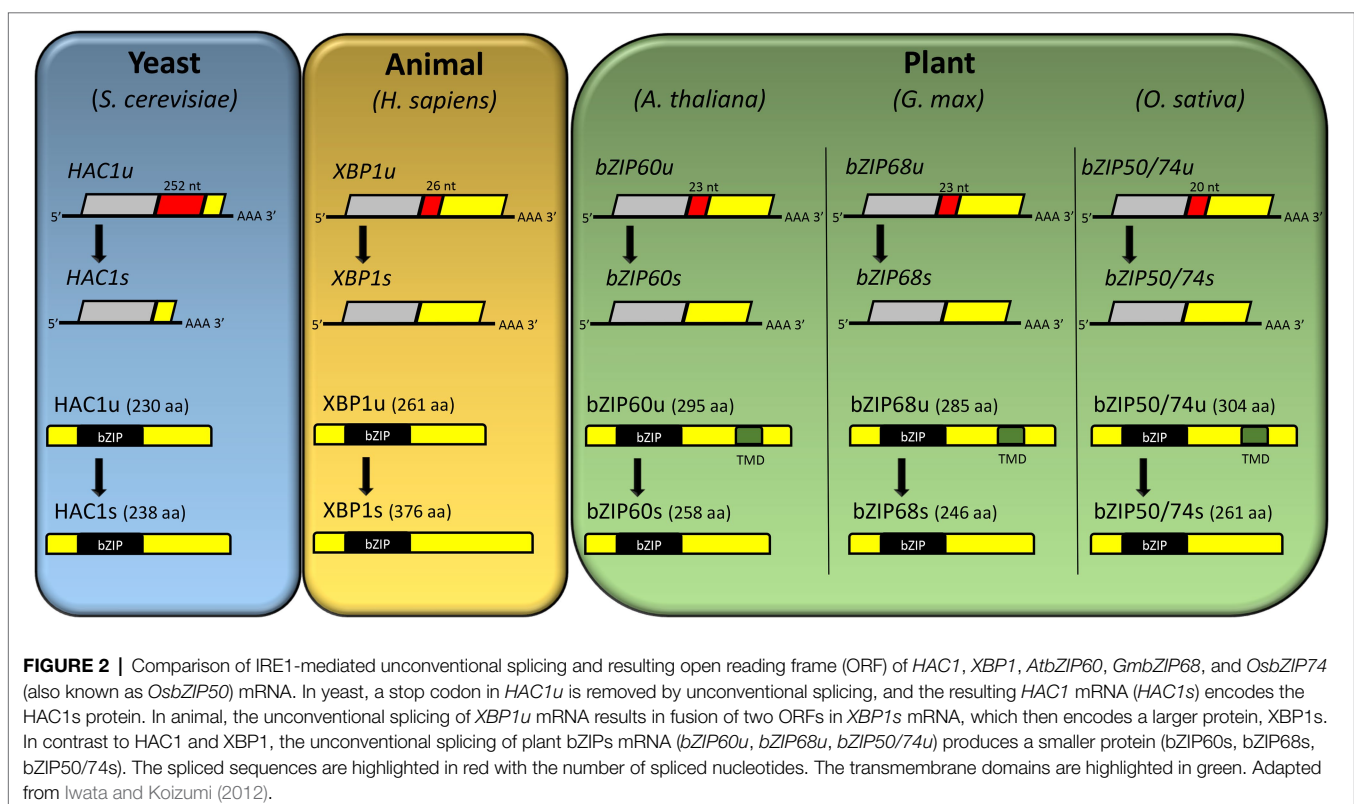


FIGURE 1 | Molecular mechanisms of ER stress-induced unfolded protein response (UPR) signaling in yeast, animal, and plant. The ER stress transducers, Ire1 α/β , PERK, and activating transcription factor 6 (ATF6) form the three branches of the UPR pathways in mammals. PERK oligomerizes and phosphorylates eIF2 α to decrease overall translation while increasing specific translation of genes, including ATF4. Upon ER stress, ATF6-BiP complex dissociates and ATF6 is packaged and translocated to Golgi apparatus, where it is processed to create an active transcription factor. Ire1 α/β , releasing from BiP and sensing misfolded proteins, oligomerizes and phosphorylates itself, leading to the activation of the XBP1 transcription factor by splicing the XBP1u mRNA to create XBP1s mRNA. All three transcription factors lead to the upregulation of UPR genes. In plants, with similar mechanisms, only Ire1 α/β and ATF6 branches are identified, Ire1a/b and bZIP17/28, respectively. Yeast have only the Ire1 α/β branch, represented by Ire1p.

protease(s) first cleaves the bZIP28 at its transmembrane domain, thereby allowing S2P to function. Although the luminal portion has the consensus S1P recognition motif, S1P is not involved in bZIP28 processing (Iwata et al., 2017). In contrast, bZIP17 appears to suffer the action of S1P (Liu et al., 2007b). Once cleaved, the TF can reallocate to the nucleus forming a transcriptional complex with the nuclear factor- κ B TFs to activate the UPR genes (Liu and Howell, 2010). In most cases, bZIP17 and bZIP28 exhibit similar properties and are induced by ER stress inducers (TM, DTT), environmental and developmental conditions. However, the induction kinetics, specific activation, and modulated target genes are not necessarily identical (Liu et al., 2007a,b; Duwi Fanata et al., 2013; Henriquez-Valencia et al., 2015; Li et al., 2017; Park and Park, 2019). For instance, bZIP17, but not bZIP28, is induced, processed, and relocated into the nucleus upon salt stress conditions. Kim et al. (2018) showed that the double mutant *bzip17/28* exhibited root growth impairment and constitutive overexpression of the *bZIP60* gene. These results indicate that either bZIP17 and bZIP28 function redundantly or act together to modulate cell growth and root development, besides the UPR activity (Kim et al., 2018). Likewise, bZIP17 functions in concert with IRE1a and IRE1b in normal plant development as the *bzip17/ire1a/ire1b* triple mutant displays severe vegetative and reproductive growth defects (Bao et al., 2018). IRE's role in normal plant development was associated with IRE RIDD activity on secretory protein mRNAs but uncoupled to the bZIP60 mRNA splicing, whereas bZIP17 might activate UPR unrelated genes in response to developmental stimuli. Moreover, both bZIP17 and bZIP28 genes, along with the IRE/bZIP60 signaling arm, are induced by

virus infection in *Arabidopsis* and *Nicotiana benthamiana* (Gayral et al., 2020; Li and Howell, 2021).

The second branch of plant UPR relies on the ER receptor IRE1 (Figure 1). In many eukaryotes, IRE1-mediated unconventional splicing of mRNA is the most conserved branch of the UPR (Ruberti et al., 2015). Like in metazoan, plant IRE1 is an ER membrane protein with dual functions. As an endoribonuclease, it catalyzes mRNA splicing; as a serine/threonine-protein kinase, IRE1 initiates autophosphorylation, forming oligomers upon ER stress (Wan and Jiang, 2016). As a central player in the UPR, IRE1 mediates two signaling pathways, the unconventional splicing of its typical substrate, bZIP60, and an alternative pathway that cleaves other RNAs by RIDD to control translational overload (Hollien et al., 2009; Mishiba et al., 2013). The IRE1 receptor configuration harbors an N-terminal signal-sensing portion facing the ER lumen, followed by an internal transmembrane segment and a cytosolic signal-transducing C-terminal domain. The N-terminal region senses misfolded proteins to trigger signaling. The C-terminal region plays a role as an RNA processing enzyme, acting at the unconventional splicing of bZIP60 transcription factor, another essential regulator of the ER stress response (Sidrauski and Walter, 1997; Deng et al., 2011; Wakasa et al., 2012). Although well-characterized in yeast, the exact mechanism of the IRE1 stress-sensing process in plants has not been elucidated yet (Zhang et al., 2016). The most accepted hypothesis is that similarly to bZIP17/28, BiP detaches from the luminal portion of the IRE1, and once released, this region interacts with misfolded proteins, activating the pathway (Kimata et al., 2003;



Gardner and Walter, 2011; Li and Howell, 2021). Upon ligand-induced activation, IRE1 undergoes dimerization and autophosphorylation followed by oligomerization and cluster formation (Wan and Jiang, 2016; Nawkar et al., 2018). The RNase activity of IRE1 processes the mRNA encoding unspliced bZIP60 (bZIP60u) to produce an active TF, spliced bZIP60 (bZIP60s), which has 23bp less (Figure 2; Howell, 2013). The two ends of bZIP60 mRNA in Arabidopsis are joined by a tRNA ligase RLG1 (Nagashima et al., 2016). Likewise, this process is conserved in soybean and rice, in which GmbZIP68 and OsbZIP50/74 mRNAs are processed upon ER stress induction (Figure 2). The active form of bZIP60 without the transmembrane domain translocates toward the nucleus and modulates the expression of UPR target genes to overcome ER stress (Deng et al., 2011). The Arabidopsis bZIP60 splicing is induced by a variety of conditions that cause the ER stress and, unlike other eukaryotes, the spliced and unspliced forms are present in any stressful condition; the extent of this processing is affected by the organ nature (Parra-Rojas et al., 2015). Moreover, bZIP60u protein has been shown to undergo constant activation by the proteasome system, and its function remains elusive.

Among plant species, IRE1 may be represented by one or more isoforms depending on the species; for example, the rice genome encodes a single *IRE1* isoform, while Arabidopsis and soybean genomes encode two and four isoforms, respectively (Nagashima et al., 2011; Wakasa et al., 2012; Silva et al., 2015; Howell, 2021). Besides the two full-length isoforms, the Arabidopsis genome also has a third *IRE1* gene (*IRE1c*), which generates a truncated protein lacking the sensor domain and might play a role beyond the ER stress responses. This interpretation is supported by the finding that *IRE1c*, together with *IRE1a* and *IRE1b*, is essential for plant development since the triple knockout mutant *ire1a/b/c* is lethal (Mishiba et al., 2019). However, introducing a heterozygous IREc allele into the triple mutant generated the *ire1a/ire1b/ire1c* (-/+) mutant and caused a typical phenotype, linking *IRE1c* to male gametogenesis (Pu et al., 2019).

A specific and alternative plant UPR branch involves two NAC proteins that also require the bZIP60 function (Figure 1). The bZIP60-ANAC062/ANAC103 module is activated to amplify the transcriptional signals that ensure cell survival under ER stress conditions. Under accumulation of misfolded proteins into the ER lumen, the transmembrane segment-less bZIP60 is translated from the processed bZIP60 mRNA and directed to the nucleus, where it binds to the cis-element UPRE III on the ANAC062 and ANAC103 promoter region and induces the expression of these target genes (Sun et al., 2013; Yang et al., 2014a). The plasma membrane-associated transcription factor ANAC062 has a transmembrane domain, processed under ER stress, leading to the ANAC062 relocation from the plasma membrane to the nucleus (Yang et al., 2014a). Besides protein synthesis and traffic, the endoplasmic reticulum produces lipids and sterols, crucial for ER and plasma membrane biogenesis. Possibly, the ER stress affects the composition and fluidity of the plasma membrane, which in turn regulates the dissociation of ANAC062. Accordingly, the proteolytic processing of ANAC062 under cold is triggered by cold-induced changes in membrane

fluidity (Seo et al., 2010; Degenkolbe et al., 2012). The nuclear-localized transcription factor ANAC103 and the processed form of ANAC062 bind the promoter region of UPR downstream genes as BiP, calnexin, reticulon, and PDI (Sun et al., 2013; Yang et al., 2014a). Although the activation mechanism of bZIP60/HAC1/XBP1 is conserved among eukaryotic cells, plant cells seem to have evolved new specific transmembrane components, such as ANAC062/ANAC103, to strengthen and perhaps amplify the pro-survival function of plant UPR.

CONSERVED FEATURES OF THE ER STRESS-INDUCED CELL DEATH IN PLANTS

Severe and persistent ER stress jeopardizes cell stability either due to an excess of unfolded proteins or Ca²⁺ imbalance, thereby, PCD is activated to maintain the integrity of the whole system (Jäger et al., 2012). Although ER-induced cell death occurs *via* apoptosis or autophagy, a crosstalk between the two pathways has been described in mammals (Maiuri et al., 2007). Autophagy can inhibit cysteine protease activities, including apoptosis-associated caspases, whereas apoptosis induces the degradation of autophagy-related proteins (ATG). Nevertheless, autophagy can also strengthen apoptosis processes in some cases, leading to a complex interplay of these processes upon ER stress (Song et al., 2017). In maize, autophagy responses range from pro-survival effects, reducing the oxidative stress response, to pro-death responses, by upregulating the Cep1-like cysteine protease (Srivastava et al., 2018).

In mammalian cells, the transmembrane mammalian ER sensors IRE1, ATF6, and PERK, in addition to functioning in ER homeostasis recovery, in critical cases, activate PCD (Nirmala and Lopus, 2020). However, the mechanisms coordinating pro-survival or apoptotic signaling have yet to be fully elucidated. In addition to inducing pro-survival related genes (Cross et al., 2012), IRE1 signaling also activates the apoptotic signaling kinase 1 and, in a tumor necrosis factor receptor-associated factor 2-dependent manner, it activates the Jun-N-terminal kinase (JNK), the main protein of a pathway described to be apoptotic in late ER stress responses but antiapoptotic in earlier responses. The IRE1-mediated JNK activation acts upstream of XBP splicing (Urano et al., 2000; Brown et al., 2016). The RIDD activity selectively degrades mRNA encoding foldases; thereby, prolonged activation of RIDD signaling promotes cell death (Han et al., 2009; Hollien et al., 2009).

In Arabidopsis, *IRE1a* and *IRE1b* isoforms are localized in the perinuclear ER, and concomitant with bZIP60 splicing, *IRE1* exhibits degradation RIDD activity on another ribosome-associated mRNA in the ER (Li and Howell, 2021). Tunicamycin-induced RIDD activity of ZmIRE1 leads to the downregulation of various peroxidase genes in the early phase of stress; however, along with other ZmIRE1 antiapoptotic activities, the RIDD activity is attenuated during the late phase. There are several proposed mechanisms of plant *IRE1* attenuation, including the formation of an ERdj4/*IRE1*/BiP complex (Amin-Wetzel et al., 2017; Srivastava et al., 2018).

Like XBP-1, the Golgi-matured ATF6 activates the expression of UPR genes during mild stress and, in case of persistent stress, upregulates PCD genes, including the pro-death bZIP transcription factor CHOP (Yang et al., 2020). In Arabidopsis, although the activation mechanism of the transcription factors bZIP17 and bZIP28 under UPR shares conservation with the ER-Golgi traffic-mediated activation of ATF6, the role of the plant transcriptional factors during PCD has not been fully uncovered (Sanchez et al., 2000; Eichmann and Schäfer, 2012). The endoplasmic reticulum (ER)-resident transmembrane protein Bax inhibitor-1 (BI-1) is a cell death regulator in plants (Sanchez et al., 2000), which has been recently shown to modulate ER stress-induced PCD by attenuating the pro-survival function of bZIP28 during ER stress recovery (Ruberti et al., 2018). BI-1 acts in parallel to the UPR pathway to modulate ER stress-mediated PCD in Arabidopsis (Watanabe and Lam, 2008). The BI-1-mediated cell death regulation is activated by physical interactions with key modulators of Ca^{+2} signaling and lipid metabolism (Ishikawa et al., 2011; Nagano et al., 2019). Despite the BI-1 pro-survival role, new studies have been shown that BI-1 can interact with ATG6 to induce autophagy and PCD (Xu et al., 2017). Interestingly, in Arabidopsis, plant BI1 antagonizes bZIP28 function, and unlike mammalian BI1, it does not suppress the IRE1-ribonuclease activity demonstrating unique features in the modulation of the UPR signaling-mediated PCD modules (Ruberti et al., 2018). The third mammalian ER sensor, the transmembrane protein kinase (PERK), which shuts down global translation by phosphorylating eIF2 α , has not been identified in plants. Nonetheless, under cold stress, the proteins AtGCN1 and AtGCN2 are involved in the plant eIF2 α phosphorylation (Wang et al., 2017).

As the central calcium storage organelle, the ER has calcium-dependent resident foldases, making a Ca^{2+} balance critical for protein synthesis homeostasis. High levels of calcium release can also lead to the accumulation of the cation in the mitochondria, leading to oxidative stress and hence activation of PCD (Marchi et al., 2018). Therefore, the cell also has calcium regulators like Bcl-2, a calcium sensor that modulates its release from the ER and regulates mammalian apoptosis (Pinton and Rizzuto, 2006). Interestingly, plants do not have Bcl-2 at a DNA level, but mammalian Bcl-2 and other homologs conserve their function when expressed in plants (Dickman et al., 2001). The ability of heterologous Bcl-2 in protecting the plant cell from death during severe biotic and abiotic stresses suggests conservation with a putative plant Bcl-2 at a structural level (Williams et al., 2014).

The Bcl-2-associated athanogene (BAG) family is another example of conservation beyond the sequence level in plants (Williams et al., 2014). BAG proteins are a multifunctional group of cochaperones with diverse subcellular locations (Thantrige et al., 2020). An interaction screening for Bcl-2 partners identified the first BAG protein (Takayama et al., 1995). BAG1 is a cytoprotective protein that activates Bcl-2 to protect mitochondrial integrity by Ca^{2+} sensing, permeability, and regulation. The protein also has a conserved-Hsp70 binding domain that activates the chaperone leading to the inhibition of apoptosome formation (Planchamp et al., 2008).

Although BAG family homologs have not been identified in the Arabidopsis genome *via* multiple sequence alignment, more robust structural comparison methods have uncovered seven putative plant BAGs (Doukhanina et al., 2006). Four of the seven BAG family members have domain organization similar to the mammalian counterparts, whereas three copies in the Arabidopsis genome possess a divergent calmodulin-binding domain (Li and Dickman, 2016). The endoplasmic reticulum resident BAG7 has been shown to play a central regulatory role in the UPR pathway under ER, cold, and heat stress (Williams et al., 2010). Furthermore, the hypersensitivity phenotype of BAG7 mutants to autophagy inducers indicates that BAG7 may regulate autophagy pathways (Williams et al., 2010). BAG7 binds to the Hsp70 paralog BiP2, a molecular marker of UPR and one of the negative regulators of the plant-specific NRP-mediated cell death pathway (Williams et al., 2010; Reis et al., 2016). In normal conditions, the cell death suppressor BAG7 binds bZIP28 and BiP2 in the ER. Under ER stress, BAG7 is sumoylated and dissociates with bZIP28 from BiP2, and both are proteolytically processed to relocate to the nucleus. In the nucleus, sumoylated BAG7 interacts with WRK29 to induce the expression of BAG7 and other UPR genes (Li et al., 2017). Therefore, plant BAGs retain several biochemical properties reminiscent of mammalian BAGs that suggest similar inhibitory roles in cell death events.

ER STRESS-INDUCED PLANT-SPECIFIC CELL DEATH SIGNALING: MECHANISMS AND REGULATION

The plant cell can trigger pro-survival or pro-death signaling pathways to dictate the cell fate in response to ER stress. The NAC (NAM/ATAF/CUC) transcription factors constitute one of the main components of this second layer of the signaling response. As plant-specific transactivator factors, NACs are involved in plant-specific mechanisms underlying ER stress-induced cell death response, often associated with prolonged ER stress conditions (Figure 3). The NAC module of transducers and other cell death regulators are represented by: (i) the DCD/NRP-NAC-VPE (vacuolar processing enzyme) cell death signaling circuit, (ii) the (bZIP28/bZIP60)-ANAC089 cell death signaling module, and (iii) the ER-mitochondria crosstalk mediated by ANAC013/ANAC017.

The NRP-NAC-VPE cell death signaling module, also known as development and cell death domain-containing N-rich protein (DCD/NRP)-mediated cell death signaling, integrates osmotic and ER stress into a signaling cascade that leads to a cell death fate (reviewed in Fraga et al., 2021). The ER and osmotic stress stimuli induce Glycine max (Gm)ERD15 expression that activates the DCD/NRP promoters (Alves et al., 2011). The small-sized, acidic, and hydrophilic transcription factor GmERD15 (Early Dehydration Responsive) belongs to a PAM2 domain-containing protein family, first identified due to its rapid response to drought stress (Kiyosue et al., 1994). GmERD15 can recognize

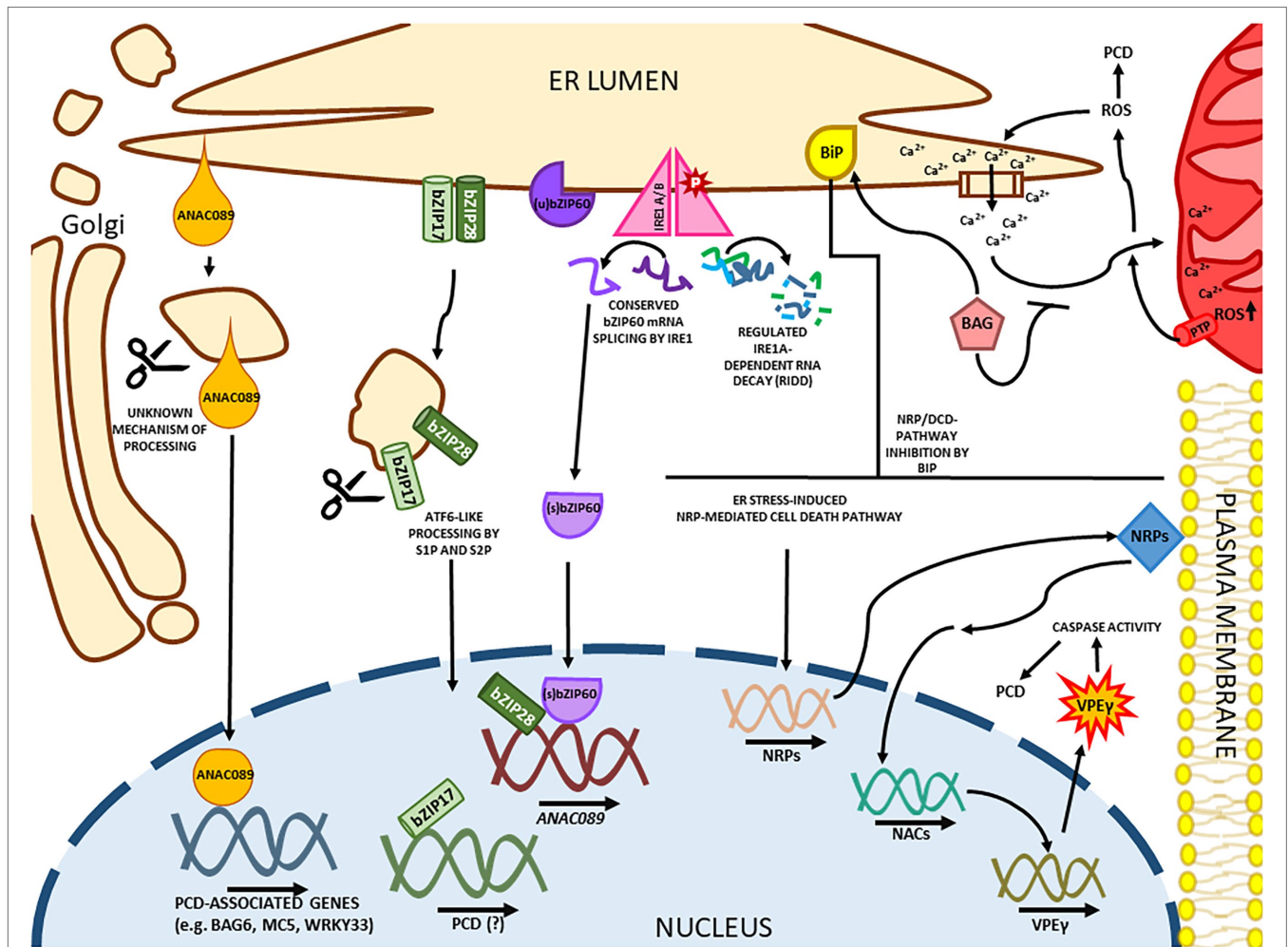


FIGURE 3 | ER stress-induced cell death in plants. In a mammalian-conserved mechanism, IRE1 is responsible for the splicing of bZIP60, which loses its transmembrane domain causing a relocation to the nucleus. IRE1A has an unspecific ribonuclease function during cell death, promoting the Regulated IRE1a-dependent RNA Decay. Like the ATF6 factor in mammals, the transmembrane ER sensors bZIP17 and bZIP28 are processed in the Golgi apparatus. Both bZIP28 and bZIP60 matured transcription factors have pro-survival functions in the nucleus but also upregulate pro-apoptotic genes like ANAC089 in Arabidopsis. ANAC089 is a plant-specific NAC-containing factor that is processed in the Golgi in a S1P/S2P-independent mechanism. Without its transmembrane domain, ANAC089 upregulates programmed cell death (PCD)-associated genes. Another plant-specific arm of ER-induced PCD is the developmental cell death (DCD) domain-containing asparagine-rich protein (NRP)-mediated cell death response, where the NRP genes are upregulated and induce the expression of ANAC036 in Arabidopsis, culminating in the expression of the cell death executor gammaVPE. The NRP/DCD pathway is attenuated by the expression of the molecular chaperone BiP. Prolonged ER stress also promotes the Calcium release from the organelle and accumulation in the mitochondria. The cation accumulation in the mitochondria leads to a ROS burst and the formation of mitochondrial PTPs. The mitochondrial ROS leakage promotes the Calcium release from the ER creating a positive feedback loop. A few BAG proteins are BiP binding partners, and this protein family acts as calcium sensors, inhibiting the ion accumulation in the mitochondria.

the palindromic sequence –511AGCAnnnnnTGCT–500 on the NRP-B promoter (Kiyosue et al., 1994; Alves et al., 2011).

The GmERD15-mediated induction of two plant-specific DCD/N-rich proteins, GmNRP-A and GmNRP-B, leads to enhanced cell death markers *in planta*, including chlorophyll loss, DNA fragmentation, caspase-3-like activity, malondialdehyde production, and leaf yellowing (Costa et al., 2008; Reis et al., 2011, 2016). This cell death response is initiated by induction of the GmNRPs, which activate a signaling cascade culminating with GmNAC030 and GmNAC081 induced expression (Faria et al., 2011; Mendes

et al., 2013). These transcription factors, GmNAC081 and GmNAC030, form a heterodimer that binds to cis-regulatory sequences and activates target promoters from hydrolytic enzyme-encoding genes, including VPE, a caspase-1-like vacuolar processing enzyme, which is an effector of cell death (Mendes et al., 2013; Pimenta et al., 2016). The vacuole-localized cysteine protease (VPE) can be self-activated through a hydrolytic cleavage step and, in turn, mediates activation of vacuolar enzymes, crucial to the vacuolar collapse-mediated cell death, a plant-specific PCD event (Hara-Nishimura et al., 2005; Hatsugai et al., 2015).

First identified in soybean, the NRP-NAC-VPE module is conserved in other plant species. The Arabidopsis orthologs AtNRP1, AtNRP2, ANAC036, and γ VPE induce cell death in *N. benthamiana* leaves, and their knockout lines display enhanced tolerance to ER stress and cell death (Figure 3; Reis et al., 2016; de Camargos et al., 2019). Furthermore, stress-mediated induction of ANAC036 and γ VPE requires the NRP1 function (Reis et al., 2016). These interpretations have been challenged by recent studies conducted with the double mutant *nrp1/nrp2* in Arabidopsis (Yang et al., 2021). In contrast to the cell death resistant phenotype displayed by 15 days-old *nrp1* knockout seedlings (Reis et al., 2016), the *nrp1/nrp2* double mutant exhibits enhanced ER stress-induced cell death response at 7 days after germination (Yang et al., 2021). The apparent contradiction between these studies may suggest that specific pathways regulating the NRP-mediated cell death signaling cascade might operate in different stages of plant development. While the pro-survival function of NRPs culminates with inhibition of cell death-related metacaspases under ER stress conditions, the pro-death function of NRP1 has been linked to the induction of the ANAC036-VPE signaling module (Reis et al., 2016; Yang et al., 2021). More recently, a Cd²⁺-mediated cell death response was associated with induction of both ER stress and the NRPs-GmNACs-VPE signaling module in soybean at the vegetative and reproductive developmental stages (Quadros et al., 2021). Nevertheless, the ER stress-mediated activation of the NRPs-GmNACs-VPE signaling module has not been investigated in soybean seedlings or during germination, and the possibility that NRPs activate specific signaling modules under differential developmental programs remains enigmatic. The molecular chaperone BiP attenuates the NRP/DCD-mediated cell death response by modulating their components expression and activity in soybean, tobacco, and Arabidopsis (Valente et al., 2009; Reis et al., 2011).

Contradictory results have also been reported for Arabidopsis AGB1-mediated signaling events that trigger UPR-associated cell death in plants (Wang et al., 2007; Chen and Brandizzi, 2012). AGB1 is the G β subunit of the heterotrimeric G protein, which has been demonstrated to associate partially with the ER membrane. Inactivation of the single-copy gene *AGB1* has been shown to impair ER stress-induced cell death and attenuate the induction of UPR-specific target genes in grown plants (Wang et al., 2007). In contrast, a more recent report demonstrated that three AGB1 mutants, *agb1-1*, *agb1-2*, and *agb1-3*, displayed oversensitivity to ER stress during germination (Chen and Brandizzi, 2012). Although the underlying mechanism for AGB1-mediated cell death remains unsolved, whether AGB1 would associate with different signaling modules at different developmental stages has not been investigated.

Another plant-specific transcriptional factor from the Arabidopsis NAC family, ANAC089, uses a different signaling module to mediate ER stress-mediated cell death responses (Figure 3). Under severe ER stress conditions, the ER membrane-anchored transcription factor ANAC089 relocates from the ER membrane to the Golgi, where it undergoes proteolytic cleavage by a yet-to-be-identified protease (Ai et al., 2021). The C-terminal ER lumen small size tail of ANAC089 has no canonical S1P

cutting site, and loss of S2P function does not impair the correct ANAC089 processing in the Golgi (Liu et al., 2007a; Yang et al., 2014b). The processed ANAC089 is redirected to the nucleus to promote the induction of caspase-like activities, the NRP-ANAC-VPE cell death module, and downstream PCD-associated genes, including BAG6 (Bcl-2-associated athanogene family member), MC5 (metacaspase 5), WRKY33 (autophagy-related gene), and aspartyl protease A39 (Yang et al., 2014b). Accordingly, the overexpression of truncated ANAC089 without the transmembrane domain induces PCD, whereas the ANAC089 RNAi plants display ER stress tolerance (Yang et al., 2014b). Under ER stress conditions, ANAC089 is induced by bZIP28 and bZIP60, which bind to the UPR-I element on the ANAC089 promoter. Besides the increase in ANAC089 protein levels, the ANAC089 proteolytically processed form is tightly controlled and only activated under severe ER stress (Yang et al., 2014b). Accordingly, tobacco mosaic virus and phytophthora infections induce ANAC089 expression, and the ER stress-induced immune signal promotes the ANAC089 relocation to the nucleus to activate genes involved in PCD (Li et al., 2018; Ai et al., 2021).

The crosstalk between organelles is essential for maintaining cellular homeostasis. The ER can cooperate with mitochondria and chloroplast through inter-organelle communication that triggers specific signaling pathways to promote cell survival or death events (Liu and Li, 2019). Ca²⁺, ROS, MECP, and the ER-anchored transcription factors ANAC013/ANAC017 are implicated as the core components of this inter-organelle crosstalk. ANAC013 and ANAC017 have been shown to be involved in retrograde mitochondrial regulation during stressful conditions (De Clercq et al., 2013; Ng et al., 2013). Under ER stress, ANAC017 also plays a protective role in ER stress tolerance, inducing the expression of molecular chaperones, bZIP60, and ER stress-responsive genes (Chi et al., 2017). The disruption of ER and mitochondrial homeostasis might activate unknown proteases to process the two ER-anchored NAC proteins and hence relocate them from the ER membrane to the nucleus. Together, the ER-anchored ANAC013 and ANAC017 integrate the mitochondria and chloroplast ROS signaling through interaction with a nuclear protein Radical-induced Cell Death1 (Shapiguzov et al., 2019).

The ER serves as intracellular storage of Ca²⁺, and the ER lumen concentration of Ca²⁺ is vital to facilitate the activity of ER chaperones and foldases (Berridge, 2002). Mitochondria and ER can communicate through Ca²⁺ mobilization. Furthermore, perturbation in ER functions promotes the release of Ca²⁺ to mitochondria, resulting in a mitochondrial permeability transition pore (PTP), which triggers a cell death signaling pathway that intensifies ER Ca²⁺ release by a positive feedback loop, decreasing ER protein-folding capacity (Williams et al., 2014). In addition to chloroplast and mitochondria, ROS also can be produced in the ER lumen to provide an oxidizing environment for PDI disulfide bond formation (Ozgun et al., 2015). The H₂O₂ permeability of the ER membrane allows the ER to influence mitochondrial ROS production, and the mitochondrial ROS can induce ER Ca²⁺ mobilization and expression of UPR components (Ramming et al., 2014;

Ozgur et al., 2018). Furthermore, the plastidial metabolite MEcPP has been shown to directly trigger the induction of selected UPR genes, coupling the chloroplast and ER homeostasis (Walley et al., 2015).

ER STRESS-MEDIATED AUTOPHAGY

Occasionally, the efforts of the UPR pathway and the ERQC and ERAD systems under extreme circumstances cannot restore the ER balance. In this case, the ER stress might lead to autophagy, cell death, or even the death of the whole plant (Wan and Jiang, 2016). Autophagy (meaning “self-eating”), conserved in all eukaryotes, is a cell-sparing process and represents a macromolecule degradation process, in which cells recycle cytoplasmic contents, whole or pieces of organelles through the lysosomes in metazoans, or the vacuole in yeast and plants (Liu and Bassham, 2012; Wan and Jiang, 2016). Under optimal growth conditions, this process is kept at basal levels but is highly upregulated by a wide variety of biotic and abiotic stresses, such as nutrient starvation, pathogen infection, heat, or drought stress (Liu et al., 2009; Li et al., 2015; Gomez et al., 2021). Autophagy may also be triggered by ER stress through ER stress inducers, such as TM and DTT (Liu et al., 2012), leading to engulfment of ER membranes (ER-phagy; Grumati et al., 2018). Macromolecules resulting from autophagic degradation are reused by the cell to reestablish basal metabolism and stimulate the plant’s acclimatization and resistance to adverse environmental conditions (Minina et al., 2018). Three main types of autophagy have been described based on their mechanisms and membrane dynamics: macroautophagy (Yang and Klionsky, 2010), microautophagy (Oku and Sakai, 2018), and autophagy mediated by direct target translocation across the lysosomal membrane, such as chaperone-mediated autophagy (Orenstein and Cuervo, 2010). In plants, macroautophagy and microautophagy have already been described (Bassham, 2007).

Autophagy is a self-destructive process that engulfs non-essential or damaged cellular components, including organelles, in characteristic double-membrane vesicles known as autophagosomes with subsequent cargo delivery to the vacuole where they are degraded or recycled. Into the vacuole, the outer membrane of the autophagosome fuses with the tonoplast, and the inner membrane with the cargo is degraded by vacuolar hydrolases (Pu and Bassham, 2013). A set of autophagy-related genes (ATG) and proteins is essential for this process (Mizushima et al., 2011). In yeast, more than 30 ATG genes have been identified, and many of them are also present in mammals and plants (Mizushima et al., 2011; Liu and Bassham, 2012). These genes can be divided into several functional groups (Yang and Klionsky, 2010; Bao and Bassham, 2020): the ATG1-ATG13 complex, which senses the signal and initiates autophagosome formation through ATG9 recruitment; ATG9 and associated proteins that acquire lipids for the expansion of the phagophore (a cup-shaped double-membrane that expands to form an autophagosome); the phosphoinositide 3-kinase complex, which, together with ATG9, is required for the

initiation of autophagosome formation; and two ubiquitin-like conjugation systems, ATG5-ATG12/ATG16 and ATG8-phosphatidylethanolamine (PE). The first system acts as an E3 ligase and mediates the covalent conjugation of ATG8 to a PE. The second one is required to complete autophagosome formation and cargo selection. Two types of markers have been frequently used to monitor autophagosomes in plants: green fluorescent protein-ATG8 fusion proteins, because the ATG8 essential role in autophagosome formation and its stable localization in both sides of autophagosome membranes (Zeng et al., 2019); and monodansylcadaverine staining, an acidotropic dye that stains acidic membrane compartments (Contento et al., 2005).

As mentioned before, upon continuous ER stress, ER-phagy is triggered to degrade some of the misfolded/unfolded proteins accumulated in the ER (Grumati et al., 2018). In yeast and plants, autophagy is closely associated with the ER, which provides autophagosome membranes and is a target for autophagy during ER stress (Marshall and Vierstra, 2018; Zeng et al., 2019). In ER-phagy, specific cargo receptors are needed to interact with both ATG8 and the target for degradation. The yeast ER-phagy pathway requires the receptors ATG39 and ATG40, two ER membrane proteins that load the ER subdomains into autophagosomes (Mochida et al., 2015). In mammals, the ER-phagy receptors, including FAM134B, RTN3, ATL3, TEX264, CCPG1, and Sec62, were identified through an inefficient proteasomal function of ERAD under the UPR (Khaminets et al., 2015; Fumagalli et al., 2016; Grumati et al., 2017; Smith et al., 2018; An et al., 2019; Chen et al., 2019;). The first plant ER-phagy receptors reported were the *A. thaliana* ATG8-interacting proteins ATI1 and ATI2 (Honig et al., 2012). Localized in the ER membrane under normal conditions, these single transmembrane domain receptors possess an ATG8 interacting motif and do not have homologs in yeast and mammals. Under carbon starvation, ATI1 and ATI2 are transported to the vacuole upon interaction with ATG8 (Honig et al., 2012). Although plant receptors for autophagy are largely unknown, some homologs of mammalian receptors are encoded by the plant genomes, including Lnp1, calnexin, ATL3, and Sec62 (Zeng et al., 2019). Whether they have a similar function in autophagy remains obscure. For instance, Arabidopsis SEC62 is an ER transmembrane protein that co-localizes with ATG8 in autophagosomes, and the *atsec62* mutant is hypersensitive to ER stress, while overexpression of AtSEC62 confers ER stress tolerance (Hu et al., 2020). Thus, AtSEC62 might be an ER-phagy receptor in plants. Despite the lack of knowledge of these receptors, IRE1 has been proved indispensable for plant ER stress-induced ER-phagy.

IRE1 is generally involved in the ER stress-induced autophagy, although it is differently regulated in yeast (Bernales et al., 2006), animals (Ogata et al., 2006), and plants (Liu et al., 2012). In yeast, the biosynthesis of ATG8p, an essential component of autophagosome formation, relies on the splicing of HAC1 by IRE1 (Yorimitsu et al., 2006) and, hence, yeast autophagy is dependent on the RNase function of IRE1. Differently, mammals require the kinase function of IRE1 as the c-JNK pathway responsible for triggering autophagy depends on IRE1

activity (Urano et al., 2000; Ogata et al., 2006). Unlike yeast, autophagy in plants is also dependent on the IRE1 RNase function; however, the splicing of bZIP60, homologous to HAC1, is irrelevant to the process. More specifically, IRE1b, but not IRE1a, has been shown to be required for ER stress-induced autophagy (Liu et al., 2012). Both *Arabidopsis* *ire1a* and *ire1b* null mutants display similar expression profiles of autophagy-related genes and similar levels of autophagosome formation as wild-type plants under nutrient deficiency conditions. However, the autophagosome formation is abolished under treatment with the ER stress inducers TUN and DTT in *ire1b* plants, but not in *ire1a* knockout lines (Liu et al., 2012). Other studies have shown that the RIDD function of AtIRE1b, but not its protein kinase activity or splicing target bZIP60, is responsible for regulating this event (Bao et al., 2018). Furthermore, 3 out of 12 RIDD targets potentially repress autophagy during normal conditions, while during ER stress, they are degraded to release this repression. Although IRE1b is not necessarily the direct elicitor of autophagy, it may promote the RNA degradation of transcription factors that interfere with the induction of autophagy (Bao et al., 2018). Nevertheless, further investigations are needed better to understand ER stress-induced autophagy and its components in plants.

ER STRESS-INDUCED PCD IN PLANT IMMUNITY

ER function is associated with plant innate immunity on several levels. ER plays an essential role in processing antimicrobial proteins delivered to the site of the microbial attack by the secretory pathway *via* vesicle-mediated transport. Non-expressor of PR genes 1 (NPR1) coordinately controls the upregulation of PR genes and genes encoding proteins of the secretory pathway during salicylic acid (SA)-dependent systemic acquired resistance (SAR). Exogenous SA induces the processing of bZIP28 and splicing of bZIP60 in *Arabidopsis* and rice, linking the IRE1 activation to defense responses, which may represent a second branch regulating SA-dependent ER marker genes independently of NPR1 (Nagashima et al., 2014). A more recent report has demonstrated that an SA-independent ER stress-induced redox may promote the translocation of NPR1 to the nucleus, where it suppresses the transcriptional role of bZIP60 and bZIP28 in the UPR (Lai et al., 2018).

Consistent with the interpretation that IRE1 may be a positive regulator of SA-mediated defense responses in *Arabidopsis*, *ire1a* and *bzip60* mutants display enhanced susceptibility to the hemibiotrophic pathogen *Pseudomonas syringae* and attenuated SAR (Moreno et al., 2012). Likewise, the UPR branch IRE1/bZIP60 plays an essential role in turnip mosaic virus (TuMV; genus Potyvirus) and plantago asiatica mosaic virus (PIAMV; genus Potexvirus) infection (Zhang et al., 2015; Gagancela et al., 2016). Viral pathogenesis is enhanced in the *bzip60-2* mutant and the *ire1a/ire1b* double mutant, consistent with the induced bZIP60 splicing in response to TuMV and PIAMV infection. The potyvirus membrane-binding protein 6K2 and potexvirus triple gene block 3 are the effectors that

induce the IRE1/bZIP60 pathway. More recently, the bZIP17/28 branch of UPR has also been shown to be activated upon potyvirus and potexvirus infection in *Arabidopsis* (Gayral et al., 2020) and in response to rice streak virus (RSV) infection in *N. benthamiana* (Li et al., 2021). Expression of the membrane-associated viral effectors NSvc2 and NSvc4 induces the proteolytic cleavage of bZIP17/28 and the expression of UPR-related genes. Silencing NbbZIP17/28 significantly inhibited RSV infection. Likewise, the plant susceptibility factor Resistance to *Phytophthora parasitica* 1 (RTP1) has been recently shown to be involved in ER stress sensing (Qiang et al., 2021). RTP1 negatively modulates the IRE1/bZIP60 splicing activity and binds to bZIP28. In response to *P. parasitica* infection, *rtp1bzip60* and *rtp1bzip28* mutant plants display decreased resistance, along with attenuated induction of ER stress-responsive immune genes, suggesting that *rtp1*-mediated resistance to *P. parasitica* is coordinately regulated with UPR. Collectively these results indicated that both UPR signaling branches are linked to immune responses and provide some insights into the mechanisms by which UPR signaling cascades are coordinated with immunity.

Additionally, ER monitors the synthesis and controls the quality of several immune receptors. Specific components of ERQC mediate the processing of the pattern recognition receptors (PRR), Elongation-factor Tu (EF-Tu) receptor, which undergoes pathogen-associated molecular pattern (PAMP)-induced oligomerization with coreceptors to activate PAMP-triggered immunity (Li et al., 2009; Nekrasov et al., 2009; Saijo et al., 2009). Additional examples of plasma membrane immune receptors, which depend on ERQC for proper function, include glycosylated *Cf* proteins, linked to race-specific resistance to the fungal pathogen *Cladosporium fulvum* (Liebrand et al., 2012), the rice PRR XA21 involved in resistance to *Xanthomonas oryzae* pv. *oryzae* (Park et al., 2010), and the induced receptor kinase, implicated in N-mediated resistance of tobacco to tobacco mosaic virus (Caplan et al., 2009).

While ERQC loss-of-function mutants display enhanced susceptibility to ER stress inducers and pathogens (Wang et al., 2005; Li et al., 2009; Lu et al., 2009; Nekrasov et al., 2009; Saijo et al., 2009), the inactivation of ER-QC components enhances colonization of the mutualistic fungus *Piriformospora indica* in *Arabidopsis* roots (Qiang et al., 2012). The improved growth of *P. indica* displayed by ERQC mutants occurs only during cell death-dependent but not biotrophic colonization. *P. indica* activates an ER-PCD, associated with enhanced VPE/ caspase 1-like activities and vacuole collapse-mediated PCD. Loss-of-function VPE mutants confirmed that the fungus depends on the VPE-mediated ER-PCD to colonize *Arabidopsis* roots successfully. In contrast, VPE activity has been associated with enhanced resistance to bacterial pathogens (Carvalho et al., 2014). VPE also mediates vacuolar collapse and execution of virus-induced cell death (hypersensitive response) in *Nicotiana tabacum*, which restricts virus spread to the site of infection (Hatsugai et al., 2004). Therefore, as an executioner of PCD, VPE may function dually as a susceptibility or resistance factor depending on whether the pathogen benefits from cell death or is restricted by PCD.

A recently characterized mechanism underlying ER stress-triggered PCD in immunity relies on activating the ER stress-induced membrane-anchored TF NAC089 (Yang et al., 2014b; Ai et al., 2021). In response to PAMPs from *Phytophthora capsica* and *P. syringae*, NAC089 translocates from the ER membrane to the nucleus via a proteolytic cleavage in the Golgi. Inside the nucleus, truncated NAC089 activates PCD-related genes (BAG6, MC5, WRKY33, aspartyl protease A39, VPE) to assemble cell death programs and restrict pathogen infection. Therefore, as an ER stress immunity regulator, NAC089 positively controls host resistance against the oomycete pathogen *P. capsica* and the bacterial pathogen *P. syringae*.

CONCLUSION

The endoplasmic reticulum is an essential component of the cellular organism and is vital for synthesizing, folding, and quality control of proteins, lipid biosynthesis, and calcium storage. In plants, diverse abiotic stressors and biotic agents can disturb the ER operation and homeostasis, leading to ER stress conditions. The exact mechanism by which each kind of stress promotes ER stress is not known, but it is conceptually accepted that they can interfere with the ER function in some way related to protein folding. Further investigations are needed to prove this point. In response to ER stress, the plant cell can trigger pro-survival or pro-cell death pathways to restore correct cell function. Many cell strategies to alleviate ER stress have been described, including the induction of ERQC and ERAD system, UPR pathway, and under situations of prolonged stress, autophagy, and cell death signaling. However, the mechanisms underlying the coordination of recovery or death responses are still largely undescribed.

The plant UPR are transduced by a bipartite signaling module, involving the ER membrane-anchored stress sensors bZIP17/28 and IRE1 (through specific splicing of bZIP60), which are responsible for upregulating ER-resident chaperones and stress-responsive genes. Despite all knowledge about this signaling pathway, there are still some missing details regarding the molecular mechanisms of UPR in plants. For instance, we still do not know the exact protease responsible for the first cleavage of bZIP28 in its transmembrane domain, and the mechanisms of the IRE1 stress-sensing process remain to be elucidated. Other topics worth investigating involve the

function of bZIP60u and IRE1c under normal and stressful situations and the role of plant transcriptional factors during PCD.

If these cytoprotective pathways cannot stabilize and alleviate the ER stress, autophagy or PCD may occur. Autophagy is a self-destructive but cell-sparing process that, although described in plant cells, some components have yet to be identified. For example, what are the plant receptors for autophagy? If IRE1b is not necessarily the direct elicitor that promotes autophagy, what induces autophagy in response to stress? Important to mention that, although autophagy is considered a pro-survival mechanism, it can also strengthen apoptosis processes in some cases, raising the question of how the decision of life-to-death is taken.

Similarly, NRPs, the upstream components of a plant-specific ER stress-induced cell death signaling, have been shown to display both pro-death and pro-survival activities. The possibility that NRPs activate specific signaling modules under different developmental stages needs to be investigated. Not less importantly, some orthologs of the plant-specific NRP-mediated cell death pathway still need to be identified in Arabidopsis and other plant species.

A relevant question arises from all these signaling profiles. What situations and circumstances determine the turning point at which the cell switch on the pro-survival profile to pro-death modules? Addressing these questions is needed for a better understanding of the plant physiological response to ER stresses, such that this knowledge can be applied for genetically engineering superior crops.

AUTHOR CONTRIBUTIONS

ES, OF, and CO wrote the drafts. EF and PR conceived and supervised the review topics. All authors contributed to the article and approved the submitted version.

FUNDING

This work was partially funded by CAPES finance code 001, CNPq, FAPEMIG, and the National Institute of Science and Technology in Plant-Pest interactions. ES and CO are recipients of a CAPES graduate fellowship, and OF is supported by a FAPMIG graduate fellowship.

REFERENCES

- Ai, G., Zhu, H., Fu, X., Liu, J., Li, T., Cheng, Y., et al. (2021). Phytophthora infection signals-induced translocation of NAC089 is required for endoplasmic reticulum stress response-mediated plant immunity. *Plant J.* 108, 67–80. doi: 10.1111/tbj.15425
- Alves, M. S., Reis, P. A., Dadalto, S. P., Faria, J. A., Fontes, E. P., and Fietto, L. G. (2011). A novel transcription factor, ERD15 (early responsive to dehydration 15), connects endoplasmic reticulum stress with an osmotic stress-induced cell death signal. *J. Biol. Chem.* 286, 20020–20030. doi: 10.1074/jbc.M111.233494
- Amin-Wetzel, N., Saunders, R. A., Kamphuis, M. J., Rato, C., Preissler, S., Harding, H. P., et al. (2017). A J-protein co-chaperone recruits BiP to monomerize IRE1 and repress the unfolded protein response. *Cell* 171, 1625–1637.e13. doi: 10.1016/j.cell.2017.10.040
- An, H., Ordureau, A., Paulo, J. A., Shoemaker, C. J., Denic, V., and Harper, J. W. (2019). TEX264 is an endoplasmic reticulum-resident ATG8-interacting protein critical for ER remodeling during nutrient stress. *Mol. Cell* 74, 891–908.e10. doi: 10.1016/j.molcel.2019.03.034
- Bao, Y., and Bassham, D. C. (2020). ER-Phagy and its role in ER homeostasis in plants. *Plan. Theory* 9:1771. doi: 10.3390/plants9121771
- Bao, Y., Pu, Y., Yu, X., Gregory, B. D., Srivastava, R., Howell, S. H., et al. (2018). IRE1B degrades RNAs encoding proteins that interfere with the induction of autophagy by ER stress in *Arabidopsis thaliana*. *Autophagy* 14, 1562–1573. doi: 10.1080/15548627.2018.1462426
- Bassham, D. C. (2007). Plant autophagy—more than a starvation response. *Curr. Opin. Plant Biol.* 10, 587–593. doi: 10.1016/j.pbi.2007.06.006

- Bernales, S., McDonald, K. L., and Walter, P. (2006). Autophagy counterbalances endoplasmic reticulum expansion during the unfolded protein response. *PLoS Biol.* 4:e423. doi: 10.1371/journal.pbio.0040423
- Berridge, M. J. (2002). The endoplasmic reticulum: a multifunctional signaling organelle. *Cell Calcium* 32, 235–249. doi: 10.1016/s0143416002001823
- Brown, M., Strudwick, N., Suwara, M., Sutcliffe, L. K., Mihai, A. D., Ali, A. A., et al. (2016). An initial phase of JNK activation inhibits cell death early in the endoplasmic reticulum stress response. *J. Cell Sci.* 129, 2317–2328. doi: 10.1242/jcs.179127
- Caplan, J. L., Zhu, X., Mamillapalli, P., Marathe, R., Anandalakshmi, R., and Dinesh-Kumar, S. P. (2009). Induced ER chaperones regulate a receptor-like kinase to mediate antiviral innate immune response in plants. *Cell Host Microbe* 6, 457–469. doi: 10.1016/j.chom.2009.10.005
- Carvalho, H. H., Silva, P. A., Mendes, G. C., Brustolini, O. J., Pimenta, M. R., Gouveia, B. C., et al. (2014). The endoplasmic reticulum binding protein BiP displays dual function in modulating cell death events. *Plant Physiol.* 164, 654–670. doi: 10.1104/pp.113.231928
- Chen, Y., and Brandizzi, F. (2012). AtIRE1A/AtIRE1B and AGB1 independently control two essential unfolded protein response pathways in Arabidopsis. *Plant J.* 69, 266–277. doi: 10.1111/j.1365-313X.2011.04788.x
- Chen, Q., Xiao, Y., Chai, P., Zheng, P., Teng, J., and Chen, J. (2019). ATL3 is a tubular ER-Phagy receptor for GABARAP-mediated selective autophagy. *Curr. Biol.* 29, 846–855.e6. doi: 10.1016/j.cub.2019.01.041
- Chi, Y. H., Melencion, S., Alinapon, C. V., Kim, M. J., Lee, E. S., Paeng, S. K., et al. (2017). The membrane-tethered NAC transcription factor, AtNLT7, contributes to ER-stress resistance in Arabidopsis. *Biochem. Biophys. Res. Commun.* 488, 641–647. doi: 10.1016/j.bbrc.2017.01.047
- Contento, A. L., Xiong, Y., and Bassham, D. C. (2005). Visualization of autophagy in Arabidopsis using the fluorescent dye monodansylcadaverine and a GFP-AtATG8e fusion protein. *Plant J.* 42, 598–608. doi: 10.1111/j.1365-313X.2005.02396.x
- Costa, M. D., Reis, P. A., Valente, M. A., Irsigler, A. S., Carvalho, C. M., Loureiro, M. E., et al. (2008). A new branch of endoplasmic reticulum stress signaling and the osmotic signal converge on plant-specific asparagine-rich proteins to promote cell death. *J. Biol. Chem.* 283, 20209–20219. doi: 10.1074/jbc.M802654200
- Cross, B. C., Bond, P. J., Sadowski, P. G., Jha, B. K., Zak, J., Goodman, J. M., et al. (2012). The molecular basis for selective inhibition of unconventional mRNA splicing by an IRE1-binding small molecule. *Proc. Natl. Acad. Sci. U. S. A.* 109, E869–E878. doi: 10.1073/pnas.1115623109
- de Camargos, L. F., Fraga, O. T., Oliveira, C. C., da Silva, J., Fontes, E. P., and Reis, P. A. (2019). Development and cell death domain-containing asparagine-rich protein (DCD/NRP): an essential protein in plant development and stress responses. *Theor. and Exp. Plant Physiol.* 31, 59–70. doi: 10.1007/S40626-018-0128-Z
- De Clercq, I., Vermeirssen, V., Van Aken, O., Vandepoele, K., Murcha, M. W., Law, S. R., et al. (2013). The membrane-bound NAC transcription factor ANAC013 functions in mitochondrial retrograde regulation of the oxidative stress response in Arabidopsis. *Plant Cell* 25, 3472–3490. doi: 10.1105/tpc.113.117168
- Degenkolbe, T., Gialvalisco, P., Zuther, E., Seiwert, B., Hinch, D. K., and Willmitzer, L. (2012). Differential remodeling of the lipidome during cold acclimation in natural accessions of *Arabidopsis thaliana*. *Plant J.* 72, 972–982. doi: 10.1111/tj.12007
- Deng, Y., Humbert, S., Liu, J. X., Srivastava, R., Rothstein, S. J., and Howell, S. H. (2011). Heat induces the splicing by IRE1 of a mRNA encoding a transcription factor involved in the unfolded protein response in Arabidopsis. *Proc. Natl. Acad. Sci. U. S. A.* 108, 7247–7252. doi: 10.1073/pnas.1102117108
- Dickman, M. B., Park, Y. K., Oltersdorf, T., Li, W., Clemente, T., and French, R. (2001). Abrogation of disease development in plants expressing animal antiapoptotic genes. *Proc. Natl. Acad. Sci. U. S. A.* 98, 6957–6962. doi: 10.1073/pnas.091108998
- Doukhanina, E. V., Chen, S., van der Zalm, E., Godzik, A., Reed, J., and Dickman, M. B. (2006). Identification and functional characterization of the BAG protein family in *Arabidopsis thaliana*. *J. Biol. Chem.* 281, 18793–18801. doi: 10.1074/jbc.M511794200
- Duwi Fanata, W. I., Lee, S. Y., and Lee, K. O. (2013). The unfolded protein response in plants: a fundamental adaptive cellular response to internal and external stresses. *J. Proteome* 93, 356–368. doi: 10.1016/j.jpro.2013.04.023
- Eichmann, R., and Schäfer, P. (2012). The endoplasmic reticulum in plant immunity and cell death. *Front. Plant Sci.* 3:200. doi: 10.3389/fpls.2012.00200
- Faria, J. A., Reis, P. A., Reis, M. T., Rosado, G. L., Pinheiro, G. L., Mendes, G. C., et al. (2011). The NAC domain-containing protein, GmNAC6, is a downstream component of the ER stress- and osmotic stress-induced NRP-mediated cell-death signaling pathway. *BMC Plant Biol.* 11:129. doi: 10.1186/1471-2229-11-129
- Fraga, O. T., de Melo, B. P., Quadros, I. P. S., Reis, P. A. B., and Fontes, E. P. B. (2021). Senescence-associated Glycine max (gm)NAC genes: integration of natural and stress-induced leaf senescence. *Int. J. Mol. Sci.* 22:8287. doi: 10.3390/ijms22158287
- Fu, X. L., and Gao, D. S. (2014). Endoplasmic reticulum proteins quality control and the unfolded protein response: the regulative mechanism of organisms against stress injuries. *Biofactors* 40, 569–585. doi: 10.1002/biof.1194
- Fumagalli, F., Noack, J., Bergmann, T. J., Cebollero, E., Pisoni, G. B., Fasana, E., et al. (2016). Translocon component Sec62 acts in endoplasmic reticulum turnover during stress recovery. *Nat. Cell Biol.* 18, 1173–1184. doi: 10.1038/ncb3423
- Gaguancela, O. A., Zúñiga, L. P., Arias, A. V., Halterman, D., Flores, F. J., Johansen, I. E., et al. (2016). The IRE1/bZIP60 pathway and Bax inhibitor 1 suppress systemic accumulation of Potyvirus and Potexvirus in *Arabidopsis* and *Nicotiana benthamiana* plants. *Mol. Plant-Microbe Interact.* 29, 750–766. doi: 10.1094/MPMI-07-16-0147-R
- Gardner, B. M., and Walter, P. (2011). Unfolded proteins are Ire1-activating ligands that directly induce the unfolded protein response. *Science* 333, 1891–1894. doi: 10.1126/science.1209126
- Gayral, M., Arias Gaguancela, O., Vasquez, E., Herath, V., Flores, F. J., Dickman, M. B., et al. (2020). Multiple ER-to-nucleus stress signaling pathways are activated during Platyago Asiatica mosaic virus and turnip mosaic virus infection in *Arabidopsis thaliana*. *Plant J.* 103, 1233–1245. doi: 10.1111/tj.14798
- Gomez, R. E., Lupette, J., Chambaud, C., Castets, J., Ducloy, A., Cacas, J. L., et al. (2021). How lipids contribute to autophagosome biogenesis, a critical process in plant responses to stresses. *Cell* 10:1272. doi: 10.3390/cells10061272
- Grumati, P., Dikic, I., and Stolz, A. (2018). ER-phagy at a glance. *J. Cell Sci.* 131:jcs217364. doi: 10.1242/jcs.217364
- Grumati, P., Morozzi, G., Hölper, S., Mari, M., Harwardt, M. I., Yan, R., et al. (2017). Full length RTN3 regulates turnover of tubular endoplasmic reticulum via selective autophagy. *elife* 6:e25555. doi: 10.7554/eLife.25555
- Han, D., Lerner, A. G., Vande Walle, L., Upton, J. P., Xu, W., Hagen, A., et al. (2009). IRE1alpha kinase activation modes control alternate endoribonuclease outputs to determine divergent cell fates. *Cell* 138, 562–575. doi: 10.1016/j.cell.2009.07.017
- Hara-Nishimura, I., Hatsugai, N., Nakaune, S., Kuroyanagi, M., and Nishimura, M. (2005). Vacuolar processing enzyme: an executor of plant cell death. *Curr. Opin. Plant Biol.* 8, 404–408. doi: 10.1016/j.pbi.2005.05.016
- Hatsugai, N., Kuroyanagi, M., Yamada, K., Meshi, T., Tsuda, S., Kondo, M., et al. (2004). A plant vacuolar protease, VPE, mediates virus-induced hypersensitive cell death. *Science* 305, 855–858. doi: 10.1126/science.1099859
- Hatsugai, N., Yamada, K., Goto-Yamada, S., and Hara-Nishimura, I. (2015). Vacuolar processing enzyme in plant programmed cell death. *Front. Plant Sci.* 6:234. doi: 10.3389/fpls.2015.00234
- Henriquez-Valencia, C., Moreno, A. A., Sandoval-Ibañez, O., Mitina, I., Blanco-Herrera, F., Cifuentes-Esquivel, N., et al. (2015). bZIP17 and bZIP60 regulate the expression of BiP3 and other salt stress responsive genes in an UPR-independent manner in *Arabidopsis thaliana*. *J. Cell. Biochem.* 116, 1638–1645. doi: 10.1002/jcb.25121
- Hollien, J., Lin, J. H., Li, H., Stevens, N., Walter, P., and Weissman, J. S. (2009). Regulated Ire1-dependent decay of messenger RNAs in mammalian cells. *J. Cell Biol.* 186, 323–331. doi: 10.1083/jcb.200903014
- Honig, A., Avin-Wittenberg, T., Ufaz, S., and Galili, G. (2012). A new type of compartment, defined by plant-specific Atg8-interacting proteins, is induced upon exposure of Arabidopsis plants to carbon starvation. *Plant Cell* 24, 288–303. doi: 10.1105/tpc.111.093112
- Howell, S. H. (2013). Endoplasmic reticulum stress responses in plants. *Annu. Rev. Plant Biol.* 64, 477–499. doi: 10.1146/annurev-arplant-050312-120053
- Howell, S. H. (2017). When is the unfolded protein response not the unfolded protein response? *Plant Sci.* 260, 139–143. doi: 10.1016/j.plantsci.2017.03.014

- Howell, S. H. (2021). Evolution of the unfolded protein response in plants. *Plant Cell Environ.* 44, 2625–2635. doi: 10.1111/pce.14063
- Hu, S., Ye, H., Cui, Y., and Jiang, L. (2020). AtSec62 is critical for plant development and is involved in ER-phagy in *Arabidopsis thaliana*. *J. Integr. Plant Biol.* 62, 181–200. doi: 10.1111/jipb.12872
- Ishikawa, T., Watanabe, N., Nagano, M., Kawai-Yamada, M., and Lam, E. (2011). Bax inhibitor-1: a highly conserved endoplasmic reticulum-resident cell death suppressor. *Cell Death Differ.* 18, 1271–1278. doi: 10.1038/cdd.2011.59
- Iwata, Y., Ashida, M., Hasegawa, C., Tabara, K., Mishiba, K. I., and Koizumi, N. (2017). Activation of the Arabidopsis membrane-bound transcription factor bZIP28 is mediated by site-2 protease, but not site-1 protease. *Plant J.* 91, 408–415. doi: 10.1111/tpj.13572
- Iwata, Y., and Koizumi, N. (2012). Plant transducers of endoplasmic reticulum unfolded protein response. *Trends Plant Sci.* 17, 720–727. doi: 10.1016/j.tplants.2012.06.014
- Jäger, R., Bertrand, M. J., Gorman, A. M., Vandenabeele, P., and Samali, A. (2012). The unfolded protein response at the crossroads of cellular life and death during endoplasmic reticulum stress. *Biol. Cell.* 104, 259–270. doi: 10.1111/boc.201100055
- Khaminets, A., Heinrich, T., Mari, M., Grumati, P., Huebner, A. K., Akutsu, M., et al. (2015). Regulation of endoplasmic reticulum turnover by selective autophagy. *Nature* 522, 354–358. doi: 10.1038/nature14498
- Kim, J. S., Yamaguchi-Shinozaki, K., and Shinozaki, K. (2018). ER-anchored transcription factors bZIP17 and bZIP28 regulate root elongation. *Plant Physiol.* 176, 2221–2230. doi: 10.1104/pp.17.01414
- Kimata, Y., Kimata, Y. I., Shimizu, Y., Abe, H., Farcasanu, I. C., Takeuchi, M., et al. (2003). Genetic evidence for a role of BiP/Kar2 that regulates Ire1 in response to accumulation of unfolded proteins. *Mol. Biol. Cell* 14, 2559–2569. doi: 10.1091/mbc.e02-11-0708
- Kiyosue, T., Yamaguchi-Shinozaki, K., and Shinozaki, K. (1994). Cloning of cDNAs for genes that are early-responsive to dehydration stress (ERDs) in *Arabidopsis thaliana* L.: identification of three ERDs as HSP cognate genes. *Plant Mol. Biol.* 25, 791–798. doi: 10.1007/BF00028874
- Lai, Y. S., Renna, L., Yarema, J., Ruberti, C., He, S. Y., and Brandizzi, F. (2018). Salicylic acid-independent role of NPR1 is required for protection from proteotoxic stress in the plant endoplasmic reticulum. *Proc. Natl. Acad. Sci. U. S. A.* 115, E5203–E5212. doi: 10.1073/pnas.1802254115
- Li, F., Chung, T., Pennington, J. G., Federico, M. L., Kaeppler, H. F., Kaeppler, S. M., et al. (2015). Autophagic recycling plays a central role in maize nitrogen remobilization. *Plant Cell* 27, 1389–1408. doi: 10.1105/tpc.15.00158
- Li, Y., and Dickman, M. (2016). Processing of AtBAG6 triggers autophagy and fungal resistance. *Plant Signal. Behav.* 11:e1175699. doi: 10.1080/15592324.2016.1175699
- Li, Z., and Howell, S. H. (2021). The two faces of IRE1 and their role in protecting plants from stress. *Plant Sci.* 303:110758. doi: 10.1016/j.plantsci.2020.110758
- Li, F., Sun, H. J., Jiao, Y., Wang, F. L., Yang, J., and Shen, L. (2018). Viral infection-induced endoplasmic reticulum stress and a membrane-associated transcription factor NbnAC089 are involved in resistance to virus in *Nicotiana benthamiana*. *Plant Pathol.* 67, 233–243. doi: 10.1111/ppa.12707
- Li, Y., Williams, B., and Dickman, M. (2017). Arabidopsis B-cell lymphoma2 (Bcl-2)-associated athanogene 7 (BAG7)-mediated heat tolerance requires translocation, sumoylation and binding to WRKY29. *New Phytol.* 214, 695–705. doi: 10.1111/nph.14388
- Li, C., Zhang, T., Liu, Y., Li, Z., Wang, Y., Fu, S., et al. (2021). Rice stripe virus activates the bZIP17/28 branch of the unfolded protein response signalling pathway to promote viral infection. *Mol. Plant Pathol.* doi: 10.1111/mpp.13171 [Epub ahead of print].
- Li, J., Zhao-Hui, C., Batoux, M., Nekrasov, V., Roux, M., Chinchilla, D., et al. (2009). Specific ER quality control components required for biogenesis of the plant innate immune receptor EFR. *Proc. Natl. Acad. Sci. U. S. A.* 106, 15973–15978. doi: 10.1073/pnas.0905532106
- Liebrand, T. W., Smit, P., Abd-El-Halim, A., de Jonge, R., Cordewener, J. H., America, A. H., et al. (2012). Endoplasmic reticulum-quality control chaperones facilitate the biogenesis of Cf receptor-like proteins involved in pathogen resistance of tomato. *Plant Physiol.* 159, 1819–1833. doi: 10.1104/pp.112.196741
- Liu, Y., and Bassham, D. C. (2012). Autophagy: pathways for self-eating in plant cells. *Annu. Rev. Plant Biol.* 63, 215–237. doi: 10.1146/annurev-arplant-042811-105441
- Liu, Y., Burgos, J. S., Deng, Y., Srivastava, R., Howell, S. H., and Bassham, D. C. (2012). Degradation of the endoplasmic reticulum by autophagy during endoplasmic reticulum stress in Arabidopsis. *Plant Cell* 24, 4635–4651. doi: 10.1105/tpc.112.101535
- Liu, J. X., and Howell, S. H. (2010). bZIP28 and NF-Y transcription factors are activated by ER stress and assemble into a transcriptional complex to regulate stress response genes in Arabidopsis. *Plant Cell* 22, 782–796. doi: 10.1105/tpc.109.072173
- Liu, J. X., and Howell, S. H. (2016). Managing the protein folding demands in the endoplasmic reticulum of plants. *New Phytol.* 211, 418–428. doi: 10.1111/nph.13915
- Liu, L., and Li, J. (2019). Communications Between the endoplasmic reticulum and other organelles During abiotic stress response in plants. *Front. Plant Sci.* 10:749. doi: 10.3389/fpls.2019.00749
- Liu, J. X., Srivastava, R., Che, P., and Howell, S. H. (2007a). An endoplasmic reticulum stress response in Arabidopsis is mediated by proteolytic processing and nuclear relocation of a membrane-associated transcription factor, bZIP28. *Plant Cell* 19, 4111–4119. doi: 10.1105/tpc.106.050021
- Liu, J. X., Srivastava, R., Che, P., and Howell, S. H. (2007b). Salt stress responses in Arabidopsis utilize a signal transduction pathway related to endoplasmic reticulum stress signaling. *Plant J.* 51, 897–909. doi: 10.1111/j.1365-313X.2007.03195.x
- Liu, Y., Xiong, Y., and Bassham, D. C. (2009). Autophagy is required for tolerance of drought and salt stress in plants. *Autophagy* 5, 954–963. doi: 10.4161/auto.5.7.9290
- Lu, X., Tintor, N., Mentzel, T., Kombrink, E., Boller, T., Robatzek, S., et al. (2009). Uncoupling of sustained MAMP receptor signaling from early outputs in an Arabidopsis endoplasmic reticulum glucosidase II allele. *Proc. Natl. Acad. Sci. U. S. A.* 106, 22522–22527. doi: 10.1073/pnas.0907711106
- Maiuri, M. C., Zalckvar, E., Kimchi, A., and Kroemer, G. (2007). Self-eating and self-killing: crosstalk between autophagy and apoptosis. *Nat. Rev. Mol. Cell Biol.* 8, 741–752. doi: 10.1038/nrm2239
- Maldonado-Bonilla, L. D. (2020). The endoribonuclease domain of IRE1 and its substrate HAC1 are structurally linked components of the unfolded protein response in fungi. *Am. J. Biochem. Biotechnol.* 16, 482–493. doi: 10.3844/ajbbsp.2020.482.493
- Marchi, S., Patergnani, S., Missiroli, S., Morciano, G., Rimessi, A., Wieckowski, M. R., et al. (2018). Mitochondrial and endoplasmic reticulum calcium homeostasis and cell death. *Cell Calcium* 69, 62–72. doi: 10.1016/j.ceca.2017.05.003
- Marshall, R. S., and Vierstra, R. D. (2018). Autophagy: The master of bulk and selective recycling. *Annu. Rev. Plant Biol.* 69, 173–208. doi: 10.1146/annurev-arplant-042817-040606
- Mendes, G. C., Reis, P. A., Calil, I. P., Carvalho, H. H., Aragão, F. J., and Fontes, E. P. (2013). GmNAC30 and GmNAC81 integrate the endoplasmic reticulum stress- and osmotic stress-induced cell death responses through a vacuolar processing enzyme. *Proc. Natl. Acad. Sci. U. S. A.* 110, 19627–19632. doi: 10.1073/pnas.1311729110
- Minina, E. A., Moschou, P. N., Vetukuri, R. R., Sanchez-Vera, V., Cardoso, C., Liu, Q., et al. (2018). Transcriptional stimulation of rate-limiting components of the autophagic pathway improves plant fitness. *J. Exp. Bot.* 69, 1415–1432. doi: 10.1093/jxb/ery010
- Mishiba, K. I., Iwata, Y., Mochizuki, T., Matsumura, A., Nishioka, N., Hirata, R., et al. (2019). Unfolded protein-independent IRE1 activation contributes to multifaceted developmental processes in Arabidopsis. *Life Sci. Alliance* 2:e201900459. doi: 10.26508/lsa.201900459
- Mishiba, K., Nagashima, Y., Suzuki, E., Hayashi, N., Ogata, Y., Shimada, Y., et al. (2013). Defects in IRE1 enhance cell death and fail to degrade mRNAs encoding secretory pathway proteins in the Arabidopsis unfolded protein response. *Proc. Natl. Acad. Sci. U. S. A.* 110, 5713–5718. doi: 10.1073/pnas.1219047110
- Mizushima, N., Yoshimori, T., and Ohsumi, Y. (2011). The role of Atg proteins in autophagosome formation. *Annu. Rev. Cell Dev. Biol.* 27, 107–132. doi: 10.1146/annurev-cellbio-092910-154005
- Mochida, K., Oikawa, Y., Kimura, Y., Kirisako, H., Hirano, H., Ohsumi, Y., et al. (2015). Receptor-mediated selective autophagy degrades the endoplasmic reticulum and the nucleus. *Nature* 522, 359–362. doi: 10.1038/nature14506
- Moreno, A. A., Mukhtar, M. S., Blanco, F., Boatwright, J. L., Moreno, I., Jordan, M. R., et al. (2012). IRE1/bZIP60-mediated unfolded protein response

- plays distinct roles in plant immunity and abiotic stress responses. *PLoS One* 7:e31944. doi: 10.1371/journal.pone.0031944
- Nagano, M., Kakuta, C., Fukao, Y., Fujiwara, M., Uchimiya, H., and Kawai-Yamada, M. (2019). Arabidopsis Bax inhibitor-1 interacts with enzymes related to very-long-chain fatty acid synthesis. *J. Plant Res.* 132, 131–143. doi: 10.1007/s10265-018-01081-8
- Nagashima, Y., Iwata, Y., Ashida, M., Mishiba, K., and Koizumi, N. (2014). Exogenous salicylic acid activates two signaling arms of the unfolded protein response in Arabidopsis. *Plant Cell Physiol.* 55, 1772–1778. doi: 10.1093/pcp/pcu108
- Nagashima, Y., Iwata, Y., Mishiba, K., and Koizumi, N. (2016). Arabidopsis tRNA ligase completes the cytoplasmic splicing of bZIP60 mRNA in the unfolded protein response. *Biochem. Biophys. Res. Commun.* 470, 941–946. doi: 10.1016/j.bbrc.2016.01.145
- Nagashima, Y., Mishiba, K., Suzuki, E., Shimada, Y., Iwata, Y., and Koizumi, N. (2011). Arabidopsis IRE1 catalyses unconventional splicing of bZIP60 mRNA to produce the active transcription factor. *Sci. Rep.* 1:29. doi: 10.1038/srep00029
- Nawkar, G. M., Lee, E. S., Shelake, R. M., Park, J. H., Ryu, S. W., Kang, C. H., et al. (2018). Activation of the transducers of unfolded protein response in plants. *Front. Plant Sci.* 9:214. doi: 10.3389/fpls.2018.00214
- Nekrasov, V., Li, J., Batoux, M., Roux, M., Chu, Z. H., Lacombe, S., et al. (2009). Control of the pattern-recognition receptor EFR by an ER protein complex in plant immunity. *EMBO J.* 28, 3428–3438. doi: 10.1038/emboj.2009.262
- Ng, S., Ivanova, A., Duncan, O., Law, S. R., Van Aken, O., De Clercq, I., et al. (2013). A membrane-bound NAC transcription factor, ANAC017, mediates mitochondrial retrograde signaling in Arabidopsis. *Plant Cell* 25, 3450–3471. doi: 10.1105/tpc.113.113985
- Nirmala, J. G., and Lopus, M. (2020). Cell death mechanisms in eukaryotes. *Cell Biol. Toxicol.* 36, 145–164. doi: 10.1007/s10565-019-09496-2
- Ogata, M., Hino, S., Saito, A., Morikawa, K., Kondo, S., Kanemoto, S., et al. (2006). Autophagy is activated for cell survival after endoplasmic reticulum stress. *Mol. Cell Biol.* 26, 9220–9231. doi: 10.1128/MCB.01453-06
- Oku, M., and Sakai, Y. (2018). Three distinct types of microautophagy based on membrane dynamics and molecular machineries. *BioEssays* 40:e1800008. doi: 10.1002/bies.201800008
- Orenstein, S. J., and Cuervo, A. M. (2010). Chaperone-mediated autophagy: molecular mechanisms and physiological relevance. *Semin. Cell Dev. Biol.* 21, 719–726. doi: 10.1016/j.semcdb.2010.02.005
- Ozgun, R., Uzilday, B., Iwata, Y., Koizumi, N., and Turkan, I. (2018). Interplay between the unfolded protein response and reactive oxygen species: a dynamic duo. *J. Exp. Bot.* 69, 3333–3345. doi: 10.1093/jxb/ery040
- Ozgun, R., Uzilday, B., Sekmen, A. H., and Turkan, I. (2015). The effects of induced production of reactive oxygen species in organelles on endoplasmic reticulum stress and on the unfolded protein response in Arabidopsis. *Ann. Bot.* 116, 541–553. doi: 10.1093/aob/mcv072
- Park, C. J., Bart, R., Chern, M., Canlas, P. E., Bai, W., and Ronald, P. C. (2010). Overexpression of the endoplasmic reticulum chaperone BiP3 regulates XA21-mediated innate immunity in rice. *PLoS One* 5:e9262. doi: 10.1371/journal.pone.0009262
- Park, C. J., and Park, J. M. (2019). Endoplasmic reticulum plays a critical role in integrating signals generated by Both biotic and abiotic stress in plants. *Front. Plant Sci.* 10:399. doi: 10.3389/fpls.2019.00399
- Parra-Rojas, J., Moreno, A. A., Mitina, I., and Orellana, A. (2015). The dynamic of the splicing of bZIP60 and the proteins encoded by the spliced and unspliced mRNAs reveals some unique features during the activation of UPR in Arabidopsis thaliana. *PLoS One* 10:e0122936. doi: 10.1371/journal.pone.0122936
- Pastor-Cantizano, N., Ko, D. K., Angelos, E., Pu, Y., and Brandizzi, F. (2020). Functional diversification of ER stress responses in Arabidopsis. *Trends Biochem. Sci.* 45, 123–136. doi: 10.1016/j.tibs.2019.10.008
- Pimenta, M. R., Silva, P. A., Mendes, G. C., Alves, J. R., Caetano, H. D., Machado, J. P., et al. (2016). The stress-induced soybean NAC transcription factor GmNAC81 plays a positive role in developmentally programmed leaf senescence. *Plant Cell Physiol.* 57, 1098–1114. doi: 10.1093/pcp/pcw059
- Pincus, D., Chevalier, M. W., Aragón, T., van Anken, E., Vidal, S. E., El-Samad, H., et al. (2010). BiP binding to the ER-stress sensor Ire1 tunes the homeostatic behavior of the unfolded protein response. *PLoS Biol.* 8:e1000415. doi: 10.1371/journal.pbio.1000415
- Pinton, P., and Rizzuto, R. (2006). Bcl-2 and Ca²⁺ homeostasis in the endoplasmic reticulum. *Cell Death Differ.* 13, 1409–1418. doi: 10.1038/sj.cdd.4401960
- Planchamp, V., Bermel, C., Tönges, L., Ostendorf, T., Kügler, S., Reed, J. C., et al. (2008). BAG1 promotes axonal outgrowth and regeneration *in vivo* via Raf-1 and reduction of ROCK activity. *Brain J. Neurol.* 131, 2606–2619. doi: 10.1093/brain/awn196
- Pu, Y., and Bassham, D. C. (2013). Links between ER stress and autophagy in plants. *Plant Signal. Behav.* 8:e24297. doi: 10.4161/psb.24297
- Pu, Y., Ruberti, C., Angelos, E. R., and Brandizzi, F. (2019). AtIRE1C, an unconserved isoform of the UPR master regulator AtIRE1, is functionally associated with AtIRE1B in Arabidopsis gametogenesis. *Plant Direct* 3:e00187. doi: 10.1002/pld3.187
- Qiang, X., Liu, X., Wang, X., Zheng, Q., Kang, L., Gao, X., et al. (2021). Susceptibility factor RTP1 negatively regulates *Phytophthora parasitica* resistance via modulating UPR regulators bZIP60 and bZIP28. *Plant Physiol.* 186, 1269–1287. doi: 10.1093/plphys/kiab126
- Qiang, X., Zechmann, B., Reitz, M. U., Kogel, K. H., and Schäfer, P. (2012). The mutualistic fungus *Piriformospora indica* colonizes Arabidopsis roots by inducing an endoplasmic reticulum stress-triggered caspase-dependent cell death. *Plant Cell* 24, 794–809. doi: 10.1105/tpc.111.093260
- Quadros, I., Madeira, N. N., Loriato, V., Saia, T., Silva, J. C., Soares, F., et al. (2021). Cadmium-mediated toxicity in plant cells is associated with the DCD/NRP-mediated cell death response. *Plant Cell Environ.* doi: 10.1111/pce.14218 [Epub ahead of print].
- Ramming, T., Hansen, H. G., Nagata, K., Ellgaard, L., and Appenzeller-Herzog, C. (2014). GPx8 peroxidase prevents leakage of H₂O₂ from the endoplasmic reticulum. *Free Radic. Biol. Med.* 70, 106–116. doi: 10.1016/j.freeradbiomed.2014.01.018
- Reis, P. A., Carpinetti, P. A., Freitas, P. P., Santos, E. G., Camargos, L. F., Oliveira, I. H., et al. (2016). Functional and regulatory conservation of the soybean ER stress-induced DCD/NRP-mediated cell death signaling in plants. *BMC Plant Biol.* 16:156. doi: 10.1186/s12870-016-0843-z
- Reis, P. A., Rosado, G. L., Silva, L. A., Oliveira, L. C., Oliveira, L. B., Costa, M. D., et al. (2011). The binding protein BiP attenuates stress-induced cell death in soybean via modulation of the N-rich protein-mediated signaling pathway. *Plant Physiol.* 157, 1853–1865. doi: 10.1104/pp.111.179697
- Ruberti, C., and Brandizzi, F. (2014). Conserved and plant-unique strategies for overcoming endoplasmic reticulum stress. *Front. Plant Sci.* 5:69. doi: 10.3389/fpls.2014.00069
- Ruberti, C., Kim, S. J., Stefano, G., and Brandizzi, F. (2015). Unfolded protein response in plants: one master, many questions. *Curr. Opin. Plant Biol.* 27, 59–66. doi: 10.1016/j.pbi.2015.05.016
- Ruberti, C., Lai, Y., and Brandizzi, F. (2018). Recovery from temporary endoplasmic reticulum stress in plants relies on the tissue-specific and largely independent roles of bZIP28 and bZIP60, as well as an antagonizing function of BAX-inhibitor 1 upon the pro-adaptive signaling mediated by bZIP28. *Plant J.* 93, 155–165. doi: 10.1111/tpj.13768
- Saijo, Y., Tintor, N., Lu, X., Rauf, P., Pajeroska-Mukhtar, K., Häwker, H., et al. (2009). Receptor quality control in the endoplasmic reticulum for plant innate immunity. *EMBO J.* 28, 3439–3449. doi: 10.1038/emboj.2009.263
- Sanchez, P., de Torres Zabala, M., and Grant, M. (2000). AtBI-1, a plant homologue of Bax inhibitor-1, suppresses Bax-induced cell death in yeast and is rapidly upregulated during wounding and pathogen challenge. *Plant J.* 21, 393–399. doi: 10.1046/j.1365-313x.2000.00690.x
- Seo, P. J., Kim, M. J., Song, J. S., Kim, Y. S., Kim, H. J., and Park, C. M. (2010). Proteolytic processing of an Arabidopsis membrane-bound NAC transcription factor is triggered by cold-induced changes in membrane fluidity. *Biochem. J.* 427, 359–367. doi: 10.1042/BJ20091762
- Shapiguzov, A., Vainonen, J. P., Hunter, K., Tossavainen, H., Tiwari, A., Järvi, S., et al. (2019). Arabidopsis RCD1 coordinates chloroplast and mitochondrial functions through interaction with ANAC transcription factors. *elife* 8:e43284. doi: 10.7554/eLife.43284
- Sidrauski, C., and Walter, P. (1997). The transmembrane kinase Ire1p is a site-specific endonuclease that initiates mRNA splicing in the unfolded protein response. *Cell* 90, 1031–1039. doi: 10.1016/s0092-8674(00)80369-4
- Silva, P. A., Silva, J. C., Caetano, H. D., Machado, J. P., Mendes, G. C., Reis, P. A., et al. (2015). Comprehensive analysis of the endoplasmic reticulum stress

- response in the soybean genome: conserved and plant-specific features. *BMC Genomics* 16:783. doi: 10.1186/s12864-015-1952-z
- Smith, M. D., Harley, M. E., Kemp, A. J., Wills, J., Lee, M., Arends, M., et al. (2018). CCPG1 is a non-canonical autophagy cargo receptor essential for ER-Phagy and pancreatic ER Proteostasis. *Dev. Cell* 44, 217–232.e11. doi: 10.1016/j.devcel.2017.11.024
- Song, S., Tan, J., Miao, Y., Li, M., and Zhang, Q. (2017). Crosstalk of autophagy and apoptosis: involvement of the dual role of autophagy under ER stress. *J. Cell. Physiol.* 232, 2977–2984. doi: 10.1002/jcp.25785
- Srivastava, R., Deng, Y., Shah, S., Rao, A. G., and Howell, S. H. (2013). BINDING PROTEIN is a master regulator of the endoplasmic reticulum stress sensor/transducer bZIP28 in Arabidopsis. *Plant Cell* 25, 1416–1429. doi: 10.1105/tpc.113.110684
- Srivastava, R., Li, Z., Russo, G., Tang, J., Bi, R., Muppirala, U., et al. (2018). Response to persistent ER stress in plants: A multiphasic process That transitions cells from Prosurvival activities to cell death. *Plant Cell* 30, 1220–1242. doi: 10.1105/tpc.18.00153
- Sun, L., Yang, Z. T., Song, Z. T., Wang, M. J., Sun, L., Lu, S. J., et al. (2013). The plant-specific transcription factor gene NAC103 is induced by bZIP60 through a new cis-regulatory element to modulate the unfolded protein response in Arabidopsis. *Plant J.* 76, 274–286. doi: 10.1111/tbj.12287
- Takayama, S., Sato, T., Krajewski, S., Kochel, K., Irie, S., Millan, J. A., et al. (1995). Cloning and functional analysis of BAG-1: a novel Bcl-2-binding protein with anti-cell death activity. *Cell* 80, 279–284. doi: 10.1016/0092-8674(95)90410-7
- Thanthrige, N., Jain, S., Bhowmik, S. D., Ferguson, B. J., Kabbage, M., Mundree, S., et al. (2020). Centrality of BAGs in plant PCD, stress responses, and host defense. *Trends Plant Sci.* 25, 1131–1140. doi: 10.1016/j.tplants.2020.04.012
- Urano, F., Wang, X., Bertolotti, A., Zhang, Y., Chung, P., Harding, H. P., et al. (2000). Coupling of stress in the ER to activation of JNK protein kinases by transmembrane protein kinase IRE1. *Science* 287, 664–666. doi: 10.1126/science.287.5453.664
- Valente, M. A., Faria, J. A., Soares-Ramos, J. R., Reis, P. A., Pinheiro, G. L., Piovesan, N. D., et al. (2009). The ER luminal binding protein (BiP) mediates an increase in drought tolerance in soybean and delays drought-induced leaf senescence in soybean and tobacco. *J. Exp. Bot.* 60, 533–546. doi: 10.1093/jxb/ern296
- Wakasa, Y., Hayashi, S., Ozawa, K., and Takaiwa, F. (2012). Multiple roles of the ER stress sensor IRE1 demonstrated by gene targeting in rice. *Sci. Rep.* 2:944. doi: 10.1038/srep00944
- Walley, J., Xiao, Y., Wang, J. Z., Baidoo, E. E., Keasling, J. D., Shen, Z., et al. (2015). Plastid-produced interorganelle stress signal MEcPP potentiates induction of the unfolded protein response in endoplasmic reticulum. *Proc. Natl. Acad. Sci. U. S. A.* 112, 6212–6217. doi: 10.1073/pnas.1504828112
- Wan, S., and Jiang, L. (2016). Endoplasmic reticulum (ER) stress and the unfolded protein response (UPR) in plants. *Protoplasma* 253, 753–764. doi: 10.1007/s00709-015-0842-1
- Wang, L., Li, H., Zhao, C., Li, S., Kong, L., Wu, W., et al. (2017). The inhibition of protein translation mediated by AtGCN1 is essential for cold tolerance in *Arabidopsis thaliana*. *Plant Cell Environ.* 40, 56–68. doi: 10.1111/pce.12826
- Wang, S., Narendra, S., and Fedoroff, N. (2007). Heterotrimeric G protein signaling in the Arabidopsis unfolded protein response. *Proc. Natl. Acad. Sci. U. S. A.* 104, 3817–3822. doi: 10.1073/pnas.0611735104
- Wang, D., Weaver, N. D., Kesarwani, M., and Dong, X. (2005). Induction of protein secretory pathway is required for systemic acquired resistance. *Science* 308, 1036–1040. doi: 10.1126/science.1108791
- Watanabe, N., and Lam, E. (2008). BAX inhibitor-1 modulates endoplasmic reticulum stress-mediated programmed cell death in Arabidopsis. *J. Biol. Chem.* 283, 3200–3210. doi: 10.1074/jbc.M706659200
- Williams, B., Kabbage, M., Britt, R., and Dickman, M. B. (2010). AtBAG7, an Arabidopsis Bcl-2-associated athanogene, resides in the endoplasmic reticulum and is involved in the unfolded protein response. *Proc. Natl. Acad. Sci. U. S. A.* 107, 6088–6093. doi: 10.1073/pnas.0912670107
- Williams, B., Verchot, J., and Dickman, M. B. (2014). When supply does not meet demand-ER stress and plant programmed cell death. *Front. Plant Sci.* 5:211. doi: 10.3389/fpls.2014.00211
- Xia, X. (2019). Translation control of HAC1 by regulation of splicing in *Saccharomyces cerevisiae*. *Int. J. Mol. Sci.* 20:2860. doi: 10.3390/ijms20122860
- Xu, G., Wang, S., Han, S., Xie, K., Wang, Y., Li, J., et al. (2017). Plant Bax Inhibitor-1 interacts with ATG6 to regulate autophagy and programmed cell death. *Autophagy* 13, 1161–1175. doi: 10.1080/15548627.2017.1320633
- Yang, Z., and Klionsky, D. J. (2010). Eaten alive: a history of macroautophagy. *Nat. Cell Biol.* 12, 814–822. doi: 10.1038/ncb0910-814
- Yang, Y., Liu, X., Zhang, W., Qian, Q., Zhou, L., Liu, S., et al. (2021). Stress response proteins NRP1 and NRP2 are prosurvival factors that inhibit cell death during ER stress. *Plant Physiol.* 187, 1414–1427. doi: 10.1093/plphys/kiab335
- Yang, Z. T., Lu, S. J., Wang, M. J., Bi, D. L., Sun, L., Zhou, S. F., et al. (2014a). A plasma membrane-tethered transcription factor, NAC062/ANAC062/NTL6, mediates the unfolded protein response in Arabidopsis. *Plant J.* 79, 1033–1043. doi: 10.1111/tbj.12604
- Yang, Y. G., Lv, W. T., Li, M. J., Wang, B., Sun, D. M., and Deng, X. (2013). Maize membrane-bound transcription factor Zmbzip17 is a key regulator in the crosstalk of ER quality control and ABA signaling. *Plant Cell Physiol.* 54, 2020–2033. doi: 10.1093/pcp/pct142
- Yang, H., Niemeijer, M., Van de Water, B., and Beltman, J. B. (2020). ATF6 is a critical determinant of CHOP dynamics during the unfolded protein response. *Science* 23:100860. doi: 10.1016/j.isci.2020.100860
- Yang, Z. T., Wang, M. J., Sun, L., Lu, S. J., Bi, D. L., Sun, L., et al. (2014b). The membrane-associated transcription factor NAC089 controls ER-stress-induced programmed cell death in plants. *PLoS Genet.* 10:e1004243. doi: 10.1371/journal.pgen.1004243
- Ye, C. M., Chen, S., Payton, M., Dickman, M. B., and Verchot, J. (2013). TGBp3 triggers the unfolded protein response and SKP1-dependent programmed cell death. *Mol. Plant Pathol.* 14, 241–255. doi: 10.1111/mpp.12000
- Yorimitsu, T., Nair, U., Yang, Z., and Klionsky, D. J. (2006). Endoplasmic reticulum stress triggers autophagy. *J. Biol. Chem.* 281, 30299–30304. doi: 10.1074/jbc.M607007200
- Zeng, Y., Li, B., Zhang, W., and Jiang, L. (2019). ER-Phagy and ER stress response (ERSR) in plants. *Front. Plant Sci.* 10:1192. doi: 10.3389/fpls.2019.01192
- Zhang, L., Chen, H., Brandizzi, F., Verchot, J., and Wang, A. (2015). The UPR branch IRE1-bZIP60 in plants plays an essential role in viral infection and is complementary to the only UPR pathway in yeast. *PLoS Genet.* 11:e1005164. doi: 10.1371/journal.pgen.1005164
- Zhang, L., Zhang, C., and Wang, A. (2016). Divergence and conservation of the major UPR branch IRE1-bZIP signaling pathway across eukaryotes. *Sci. Rep.* 6:27362. doi: 10.1038/srep27362
- Zhou, S. F., Sun, L., Valdés, A. E., Engström, P., Song, Z. T., Lu, S. J., et al. (2015). Membrane-associated transcription factor peptidase, site-2 protease, antagonizes ABA signaling in Arabidopsis. *New Phytol.* 208, 188–197. doi: 10.1111/nph.13436

Conflict of Interest: The authors declare that the research was conducted in the absence of any commercial or financial relationships that could be construed as a potential conflict of interest.

Publisher's Note: All claims expressed in this article are solely those of the authors and do not necessarily represent those of their affiliated organizations, or those of the publisher, the editors and the reviewers. Any product that may be evaluated in this article, or claim that may be made by its manufacturer, is not guaranteed or endorsed by the publisher.

Copyright © 2022 Simoni, Oliveira, Fraga, Reis and Fontes. This is an open-access article distributed under the terms of the Creative Commons Attribution License (CC BY). The use, distribution or reproduction in other forums is permitted, provided the original author(s) and the copyright owner(s) are credited and that the original publication in this journal is cited, in accordance with accepted academic practice. No use, distribution or reproduction is permitted which does not comply with these terms.

CHAPTER II

REVEALING THE IMPACT OF AtRGS1 RESIDUES PHOSPHORYLATION IN THE PLANT CELL SIGNALING

INTRODUCTION

The heterotrimeric guanine nucleotide-binding protein (G-protein) actively participates in diverse biological processes, several of considerable agronomic importance. Its pivotal role encompasses the regulation of growth, development, stress responses, and the defense mechanism against pathogens (Wang *et al.*, 2019). This heterotrimeric complex consists of $G\alpha$, $G\beta$, and $G\gamma$ subunits. The genome of the model plant *Arabidopsis thaliana* encodes one canonical $G\alpha$ (AtGPA1), three non-canonical extra-large $G\alpha$ (AtXLG1, AtXLG2 and AtXLG3) one $G\beta$ (AtAGB1) and three $G\gamma$ (AtAGG1, AtAGG2 and AtAGG3) subunits (Willard and Siderovski, 2004; Jones *et al.*, 2011a; Urano *et al.*, 2013; Urano and Jones, 2014; Chakravorty *et al.*, 2015). In its inactive state, the $G\alpha$ subunit, bound to GDP, interacts with $G\beta$ and $G\gamma$, forming the $G\alpha\beta\gamma$ heterotetrameric. Upon activation, GDP is replaced by GTP, releasing the $G\beta$ and $G\gamma$ subunits from the $G\alpha\beta\gamma$ complex, generating $G\beta\gamma$ heterodimers. These now-separated subunits modulate signaling pathways (Zhong *et al.*, 2019).

Mammals exhibit a more extensive array of G-protein subunits compared to plants. For example, the human genome harbors four families of $G\alpha$ proteins, each with varying member counts, along with five $G\beta$ and twelve $G\gamma$ subunits (Syrovatkina *et al.*, 2016). Another remarkable difference between these organisms is the dependency of animals on G-protein-coupled receptors (GPCRs) to initiate signaling pathways (Masuho *et al.*, 2020). Meanwhile, plants lack these specific proteins within their genome and employ the Regulator of G-protein signaling 1 (RGS1) as an alternative controller of G-proteins.

RGS1 contains a GPCR-like seven-transmembrane (7TM) barrel domain at the N-terminus, yet despite its structural similarity, there is no data supporting RGS1 acting as a receptor (Chen, 2008). The 7TM domain is followed by a disordered linker region, a conserved RGS domain, and a C-terminal tail (Oliveira *et al.*, 2022). AtRGS1 operates by accelerating GTPase activity of AtGPA1, converting GTP to GDP and subsequently deactivating the complex (Chen *et al.*, 2003; Jones *et al.*, 2011b). This characteristic is essential due to the AtGPA1 nucleotide exchange rate, which exceeds its GTP hydrolysis rate by more than 100-fold (Johnston *et al.*, 2007).

Although not acting as a receptor, receptor-like kinases (RLKs) are described to bind and phosphorylate RGS1 (Fu *et al.*, 2014; Tunc-Ozdemir *et al.*, 2016; Liang *et al.*, 2018) This interaction stands as a crucial step in the uncoupling and internalization process of RGS1, ultimately leading to the activation of G-protein signaling (Urano *et*

al., 2012). Furthermore, AtRGS1 undergoes phosphorylation by cytoplasmic kinases like the WITH-NO-LYSINE kinases (WNKs) in response to elevated sugar levels, which subsequently triggers its internalization (Urano *et al.*, 2012). In the absence of GPCRs in plants, the precise regulation of G-protein signaling may be intricately linked to RLKs through a sophisticated phosphorylation-dependent mechanism. For example, the phosphorylation of AtRGS1 stands as an essential requirement for internalization processes like D-glucose and flg22-triggered endocytosis.

Sugars serve as essential structural components regulating diverse physiological processes. Their forms, concentrations, and energy levels play a pivotal signaling role in growth, development, responses to both biotic and abiotic stresses, and impact the overall energy status of plant cells. Sugar signaling relies on an inherent sensory mechanism and regulatory networks that adapt energy availability and sugar levels to effectively manage plant growth and development under changing environmental conditions (Choudhary *et al.*, 2022). Among the many signaling networks triggered by sugar recognition, a significant pathway is operated through G-protein-dependent mechanisms, involving the phosphorylation of AtRGS1 by WNKs (Urano *et al.*, 2012), as previously highlighted.

The other endocytosis process is governed by flg22, a 22-amino acid pathogen-associated molecular pattern (PAMP) derived from the plant pathogen *Pseudomonas syringae*. This molecule is recognized by plant cells and initiates the innate immunity pathway (Felix *et al.*, 1999; Zipfel *et al.*, 2004). Existing evidence demonstrates that flg22 recognition occurs extracellularly through the formation of a larger complex involving the co-receptors BAK1 and FLS2 alongside the G-protein complex (Sun *et al.*, 2013; Tunc-Ozdemir and Jones, 2017; Jelenska *et al.*, 2017). In essence, in response to flg22 signaling, AtRGS1 interacts with the FLS2/BAK1/BIK1 complex, where phosphorylation at the serine cluster is required for the subsequent internalization of AtRGS1 and the uncoupling from G-proteins. (Liang *et al.*, 2016; Liang *et al.*, 2018).

The C-terminus of AtRGS1 contains multiple di-serine residues, recognized collectively as a cluster. Phosphorylation of RGS1 cluster prompts its dissociation from the heterotrimeric G-protein complex, leading to its subsequent internalization and activation of G signaling (URANO *et al.*, 2012; Watkins *et al.*, 2021). However, while flg22 prompts only the internalization of AtRGS1 through phosphorylation-dependent clathrin-mediated endocytosis (CME), D-glucose-induced internalization activates the

sterol-dependent endocytosis (SDE) pathway as well. Notably, the latter pathway operates independently of the phosphorylation of three C-terminal tail sites in AtRGS1 (Watkins *et al.*, 2021).

Whereas in animals the endocytosis process relies on the activity of β -arrestins (Lhose *et al.*, 1990), higher plants lack the genetic coding for these specific proteins (Alvarez, 2008). Therefore, the retromer proteins VPS26a and VPS26b emerge as potential adaptors, primarily due to the fact these proteins possess an arrestin-like folding (Bologna *et al.*, 2017; Watkins *et al.*, 2021). Both proteins actively participate in AtRGS1 CME-mediated endocytosis when exposed to high sugar concentrations and flg22 induction (Zelazny *et al.*, 2013; Watkins *et al.*, 2021). Notably, the SDE pathway, triggered by sugar but not reliant on cluster phosphorylation, highlights distinct endocytic pathways regulating Arabidopsis G-protein dynamics (Watkins *et al.*, 2021).

In addition to the five serine residues located at the C-terminal tail, RGS1 also features a serine (Ser417) at the terminus of the RGSbox and another within the linker region (Ser278) (Tunc-Ozdemir *et al.*, 2017; Oliveira *et al.*, 2022). Nonetheless, the investigation of residue S278 has been largely overlooked due to the prevalent focus on truncated forms of RGS1 in previous research. The absence of the full-length RGS1 might present a critical oversight in comprehending the phosphorylation-dependent activity of RGS1. Considering this perspective, our approach involved utilizing various AtRGS1 phosphomimetic mutations alongside computational simulations to investigate the mechanisms underlying RGS1. Specifically, we aimed to unveil how its phosphorylation pattern influences and distinguishes G-protein binding, stability, subcellular localization and responses to stress.

MATERIAL AND METHODS

Plasmid construction and site-directed mutagenesis

The clones employed in this study were sourced from Dr. Alan Jones's and Dr. Elizabeth Fontes's laboratories, with additional constructs generated through GatewayTM technology. For site-directed mutagenesis, Q5[®] High-Fidelity DNA Polymerase (New England Biolabs) facilitated end-to-end amplification of the entry vector. Oligonucleotides for mutagenesis, designed for single or multiple codon modifications, featured a free phosphate group added to the 5' end of each primer (Table S1). The resulting linear vector went through ligation using the KLD enzyme mix (New England Biolabs). pENTR/D-TOPO vectors comprising AtRGS1 wild type (AtRGS1^{WT}), AtRGS1^{WT}-HiBiT, AtRGS1^{S428/340/431/435/436A}-HiBiT (clusterA), and AtRGS1^{S428/431/435E S430/436A}-HiBiT (q2q4q6), served as templates for novel constructions. Transformation into *E. coli* DH5 α and subsequent confirmation through sequencing led to the generation of new clones. These cloned genes underwent LR Clonase (Invitrogen) reaction and were transferred to plant expression vectors—specifically, pEarleyGate101, pCAMBIA-CLuc, and pCAMBIA-NLuc. Clones of AtGPA1 on pCAMBIA-CLuc vectors, FAP-tagged AtRGS1^{WT}, along with HiBiT-tagged AtRGS1 overexpressing lines, encompassing both wild type and mutants, were acquired from Jones Lab stocks at The University of North Carolina at Chapel Hill (US) and LBMP stocks at Universidade Federal de Viçosa (BRA) (Oliveira, 2022; Watkins *et al.*, 2023).

Structural modeling and molecular dynamics simulation

To construct the phylogenetic tree, protein sequences of 7AM-RGS were sourced from the 350 plant and green algae species described by Ngou *et al.* (2022). These sequences were aligned using MAFFT 7 software (Kato *et al.*, 2019), and highly gapped (70%) were excluded. The remaining sequences were clustered using Cd-hit (Bhat *et al.*, 2019) with a cutoff of 75%, resulting in a final realignment of 72 sequences. Phylogenetic relationships were assessed using the Maximum Likelihood (ML) method (Nguyen *et al.*, 2014) under the Jones-Taylor-Thornton (JTT) substitution model (Wang *et al.*, 2008) with a gamma distribution of rates between sites, implemented with raxml (Höhler *et al.*, 2022).

For molecular dynamics simulation (MDS), initial structures for dimerization AtRGS1 and AtGPA1 were generated using MULTICOM3. MULTICOM3 serves as an

enhancement module designed to elevate the accuracy of protein tertiary and quaternary structure predictions generated through AlphaFold2 and AlphaFold-Multimer. It achieves this improvement through a comprehensive approach involving diverse multiple sequence alignment sampling, template identification, structural prediction evaluation, and structural prediction refinement. Specifically, it enhances AlphaFold2-based tertiary structure predictions by 8-10% and AlphaFold-Multimer-based quaternary structure predictions by 5-8% (Hou *et al.*, 2020; Liu *et al.*, 2023).

Using the previously resolved AtGPA1 structure (PDB 2XTZ) as a reference, GTP and Mg²⁺ were placed in the protein pocket. Protein/membrane systems were created using CHARMM-GUI (Feng *et al.*, 2023), consisting of a lipid bilayer (DUPC:SITO:CER160, 5:5:1 ratio) solvated with TIP3P water supplemented with NaCl at 0.15 M using the Monte-Carlo method (Toropov and Toropova, 2020). The systems were subjected to 200 or 500 ns simulations with the CHARMM36 force field (Croitoru *et al.*, 2021) on GROMACS v2022.4 (Pronk *et al.*, 2013). Electrostatics were treated with PME, a constant temperature of 303.15 Kelvin maintained. Hydrogen bonds were constrained, and lipid bilayer restraints applied. Subsequent data analysis and representation were conducted using Visual Molecular Dynamics (VMD) (Vieira *et al.*, 2023). Interaction weights of residues were calculated by counting the frames where any atom of a residue came within an 8.0 Å distance of any C α . Protein 3D models were generated using ChimeraX (Meng *et al.*, 2023), Blender v3.6 (Bruns *et al.*, 2020), and Pymol v2.4.1 (Rosignoli *et al.*, 2022).

Split-luciferase complementation assay

CLuc-tagged and HiBiT-NLuc-tagged genes were introduced into *Agrobacterium tumefaciens* strain *GV3101 Agrobacterium* cells, and bacteria cells were resuspended in infiltration buffer (10mM MES, 1M MgCl₂, 200mM Acetosyringone, pH 5.6) followed by leaf co-infiltration in 4 to 5-week-old *Nicotiana benthamiana* plants. Subsequently, approximately 6 leaf disks (6mm) from each of the 16 biological replicates were collected 2 days post-infiltration and combined in a 96-well plate with 100uL of 0.4 mM D-Luciferin or HiBiT reaction mix (Promega). The reaction was kept in the dark for 10 minutes, and light intensity was measured at 570 nm on SpectraMax L. Luciferase activity was then normalized based on the average HiBiT expression level in each leaf.

Plant growth conditions

The *rgs1-2* allele (SALK_074376) of *Arabidopsis thaliana* (Col-0) was acquired from the Arabidopsis Biological Resource Center (ABRC) and Col-0 ecotype was used as the wild type control. Arabidopsis plants were cultivated in a growth chamber under short-day conditions (21°C, 8h/light, 16h/dark) for optimal growth. Seedlings for western blot analysis were disinfected with disinfection solution (ethanol:water:bleach - 4:3:1) per 10 minutes, washed three times with water, germinated on 1/2 strength liquid Murashige and Skoog (MS) medium, and grown for 7 days under low constant light conditions with continuous agitation at 120 rpm.

For YFP-detection confocal microscopy, seedlings were positioned on 1/2 strength solid MS, plated vertically, and etiolated under dark conditions for 4 days. In the case of FAP-detection confocal microscopy, seedlings were placed on 1/2 strength solid MS, plated vertically, and allowed to grow for 6 days under low constant light conditions. One day before treatment, all seedlings on solid medium were transferred to water for acclimatization.

Nicotiana benthamiana plants were germinated in soil and subjected to a half-day photoperiod (25°C, 12h/day, 22°C, 12h/night) for 4 to 5 weeks before infiltration. Dark treatment was administered overnight post-infiltration.

RGS1-YFP and FAP-Beta-RGS1 internalization

In order to monitor the internalization process of RGS1, plants expressing YFP-tagged AtRGS1^{WT}, AtRGS1^{S278A}, AtRGS1^{S278E} and AtRGS1^{S428/431/435/436A} (quadA) were exposed to light for 2 hours and then transferred to dark conditions. Following 4 days of germination, elongated hypocotyl cells underwent a 1-hour exposure to 100 nM flg22. YFP excitation was performed at 514nm, with emission collected in the range of 525-565nm.

To precisely identify the subcellular localization of RGS1 following the internalization process and minimize excessive fluorescence from YFP-tagged plants, Fluorogen Activating Protein (FAP) Technology (SpectraGenetics) was applied. Root cells of FAP-Beta-tagged RGS1^{WT} plants were pretreated for 30 min with 100nM of βGREEN-np membrane impermeant fluorogen, and then exposed to diverse treatment times (30 minutes, 1 hour, 1 hour and a half, 2 hours) of 100nM flg22 and 123μM UDP-glucose after 6 days of germination. The fluorogen was added to the treatment solution

as well in order to guarantee the entire internalization process over time. FAP-BETA excitation was conducted at 509nm, with emission collected close to 530nm.

To validate nuclear localization, root cells were labeled with Hoechst 33342 (ThermoFisher), a nuclear marker, by incorporating the reagent into the treatment solution at a final concentration of 5µg/mL. Hoechst staining involved excitation at 350nm and emission collection at 461nm.

For all experiments, individual cells were examined using a Zeiss LSM880 microscope with a C-Apochromat 40x/1.2NA water immersion objective. Signals from YFP, FAP-Beta, and Hoechst staining were captured across multiple Z-layers at 0.8µm intervals between images. Emission collection on the LSM880 utilized a GaAsP detector. Image processing and quantification were executed following the procedures described in the literature (Watkins *et al.*, 2021).

Immunoblotting analysis of RGS1

To assess stability, 7-day-old seedlings from overexpressing lines underwent a 6-hour time course exposure to 100 nM flg22 and 200µM cycloheximide under constant light and agitation. For phosphorylation detection, 7-day-old seedlings from the same overexpressing lines were treated with 100 nM flg22 for 0, 15, 30, and 45 minutes. Total protein was extracted using RGS1 extraction buffer (50 mM Tris-HCl, pH 7.5, 10% glycerol, 0.5% Triton X-100, 1.5 mM MgCl₂, 1 mM EDTA, 150 mM NaCl, 1 mM PMSF, 1x Roche protease inhibitor cocktail, and 10mM NaF). For phosphorylation detection, YFP-tagged AtRGS1, AtRGS1^{S278E}, AtRGS1^{S278A}, and AtRGS1^{S428/431/435/436A} were purified using the µMACS GFP Isolation Kit (Miltenyi Biotec). Meanwhile, for stability evaluation, pure extract was used.

The extracted proteins were separated into 12% acrylamide gels and directly detected in the gel using the Amersham Typhoon 5 with Cy2 (525BP20) filter. The excitation peak was at 488nm, emission peak at 525nm, 50µM pixel size, and a PMT of 700V. Purified proteins were separated into 12% acrylamide gels and transferred to nitrocellulose membranes. The transcriptional level of Rubisco was used as an internal control. Mitogen-activated protein kinase 1 - MAPK1 (ERK2) and MAPK3 (ERK1) were detected using an anti-p44/42 MAPK antibody (Cell Signaling Technology).

Bacterial pathogen infection assay

Pseudomonas syringae pv. *tomato* (Pst) DC3000 strain was cultured overnight at 28°C in LB medium containing 50 µg/mL rifampicin. Bacteria were harvested by centrifugation, washed, and adjusted to the desired density (OD 10⁻⁴) with 10 mM MgCl₂. Leaves of Col-0, AtRGS1^{WT}, AtRGS1^{S278E}, AtRGS1^{S278A}, AtRGS1^{S428/431/435/436A} and *rgs1-2* plants at 4-week-old were infiltrated with the bacterial suspension using a 1-mL needleless syringe. Subsequently, the leaves were collected to measure bacterial growth. Six leaf discs, separated as three repeats, were ground in 1 mL H₂O, and serial dilutions were plated onto TSA medium (1% Bacto tryptone, 1% sucrose, 0.1% glutamic acid, 1.5% agar) with the appropriate antibiotics. Bacterial colony forming-units were counted after a 2-day incubation at 28°C (Li *et al.*, 2019).

RESULTS

RGS1 structure: Phosphosite conservation suggests the relevance of the linker phosphoserine 278

AtRGS1 is a protein with 459 amino acid residues containing a 7TM domain, a RGSbox domain and a flexible linker region. This protein contains numerous di-serine residues located in its C-terminal region, along with a serine (Ser417) at the terminus of the RGS box and another within the linker region (Ser278) (Oliveira *et al.*, 2022) (Figure 1).

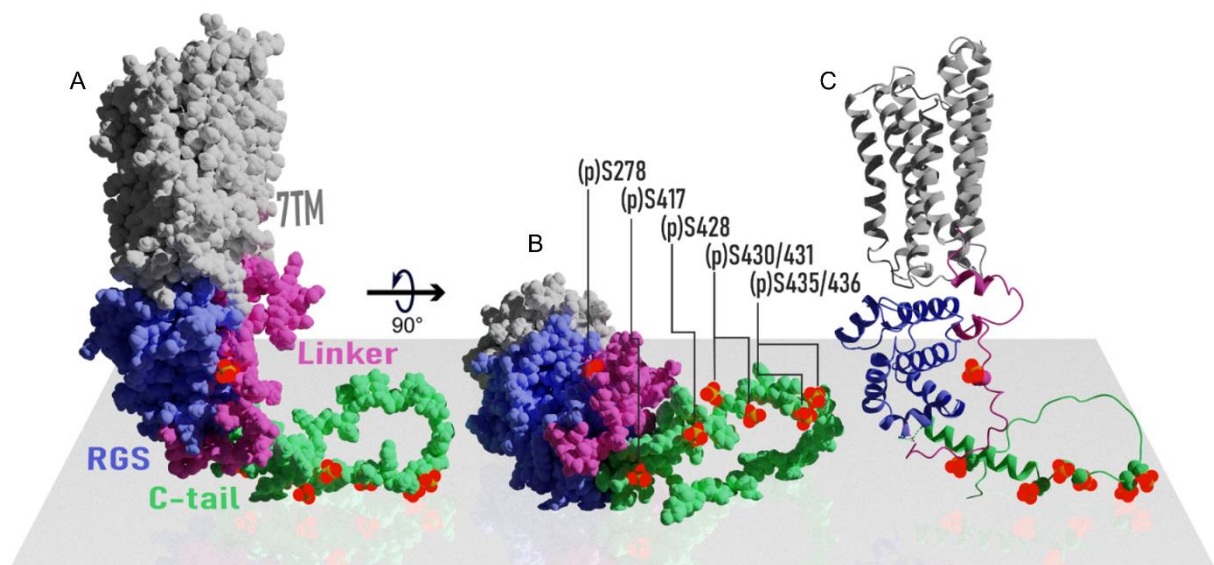


Figure 1 - AtRGS1 structural model. (A) Full-length AtRGS1 has a seven transmembrane domain (gray), a flexible linker region (pink) followed by a conserved RGSbox domain (blue), and a disordered C-terminal tail (green). **(B)** Different phosphosites are present in AtRGS1 and are shown here by red dots. Ser278 is part of a small helix segment located at the linker. C-terminal tail residues are clustered after the RGSbox. **(C)** Backbone structure with domains and regions separated by color as indicated.

Genetic conservation serves as an important feature for understanding protein evolutionary behavior. Conducting a phylogenetic analysis and examining sequence conservation of 7TM-RGS proteins in plants and green algae (Figure 2A-B) revealed the preservation of RGS across diverse families. In a more focused exploration of phosphosites, a larger sequence alignment was performed for a detailed investigation into the conservation and significance of these residues in plants (Figure 2C) (Ngou *et al.*, 2022). Notably, certain residues exhibited higher conservation than others. For instance, S436, S435, and S430, all belonging to the cluster region, displayed a higher conservation proportion among families compared to RGSbox S417 or even the other

cluster serine, S428. Most intriguingly, the residue S278 demonstrated a notably higher conservation percentage among families. This observation is particularly stimulating, not only due to the lack of studies on this residue but also because it resides in a flexible linker region, an uncommon location for a regulatory-capable residue.

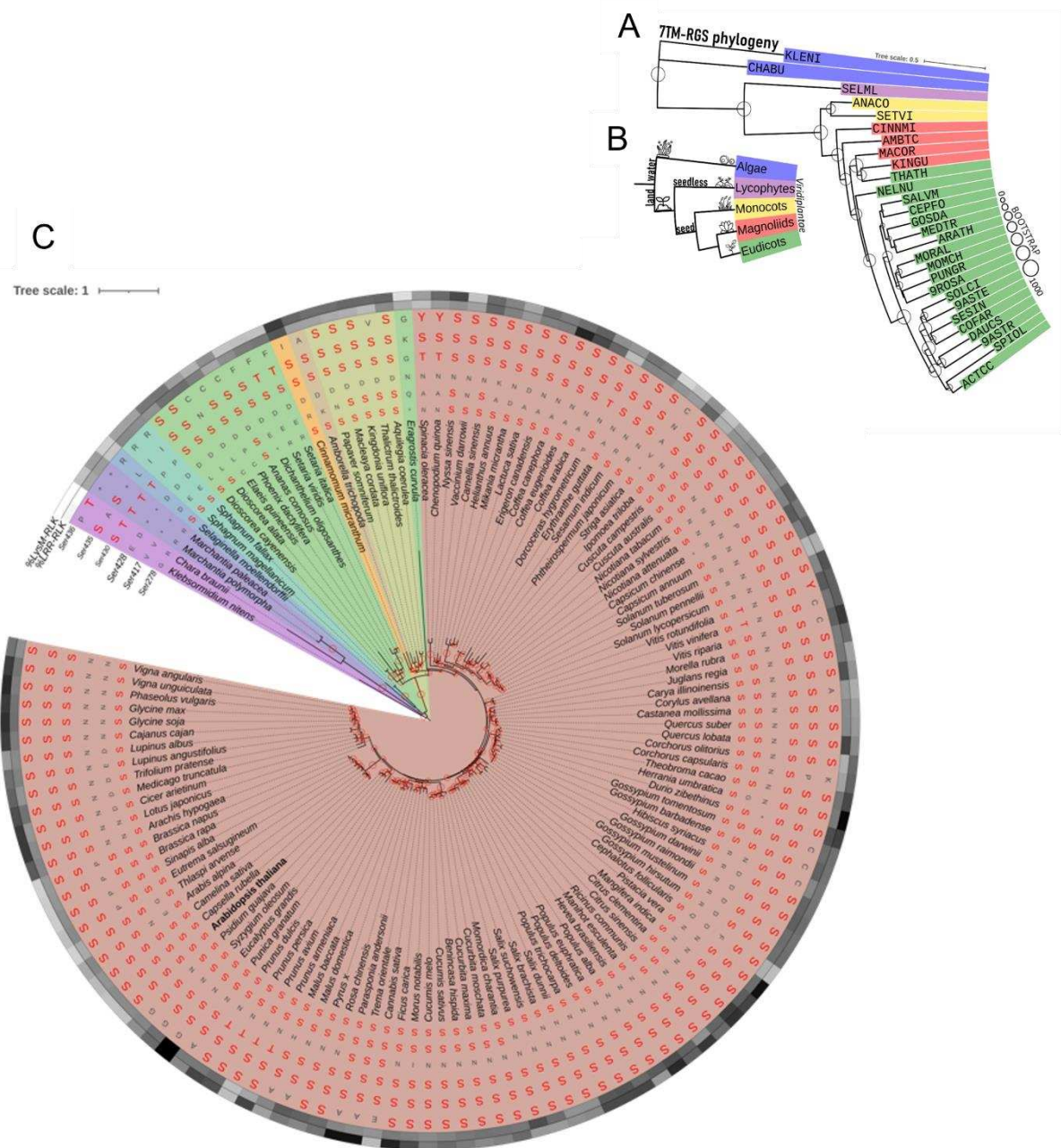
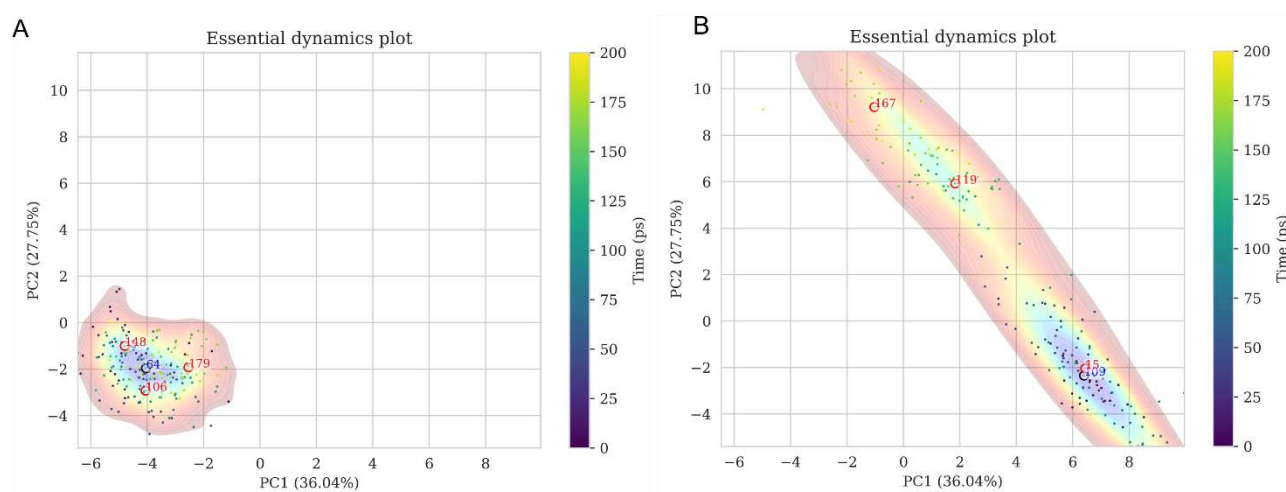


Figure 2 - Phylogenetic analysis and sequence conservation of 7TM-RGS proteins in plants and green algae. (A) Phylogenetic tree of 7TM-RGS proteins from plant and green algae. **(B)** Schematic phylogenetic tree of all the families used. **(C)** Residues conservation map constructed highlighting the serine residues from the linker, RGSbox and cluster regions.

Phospho-S278 modifies RGS1 structure and decreases Linker-C-tail interaction in Molecular Dynamic Simulations

Given the notable conservation of serine-278 across diverse plant families, we investigated the phosphorylation impact of this residue on RGS1 structure and interactions through molecular dynamic simulations. In a comprehensive PCA analysis spanning 500 nanoseconds (ns) (Figure S1A), we observed distinctions between the most representative structures of non-phospho-AtRGS1 (npRGS1) (Figure 3A) and phospho-Ser278-AtRGS1 (pS278) (Figure 3B). These findings suggest that the single phosphorylation of linker serine-278 induces conformational changes in RGS1. Further analysis revealed that this unique phosphorylation not only led to conformational alterations but also impacted interactions between linker and C-tail domains (Figure 3C-D, highlighted in black letters and numbers). Representative structures of npRGS1 exhibited an absence of interactions involving S278 and other residues. In contrast, pS278 structures displayed interactions between this linker residue and three distinct residues of RGSbox. Consequently, interactions between the linker and C-tail were disrupted, with some representative structures showing the nonexistence of a single interaction between these regions, resulting in increased freedom and mobility of the C-tail region (Figure S1B).



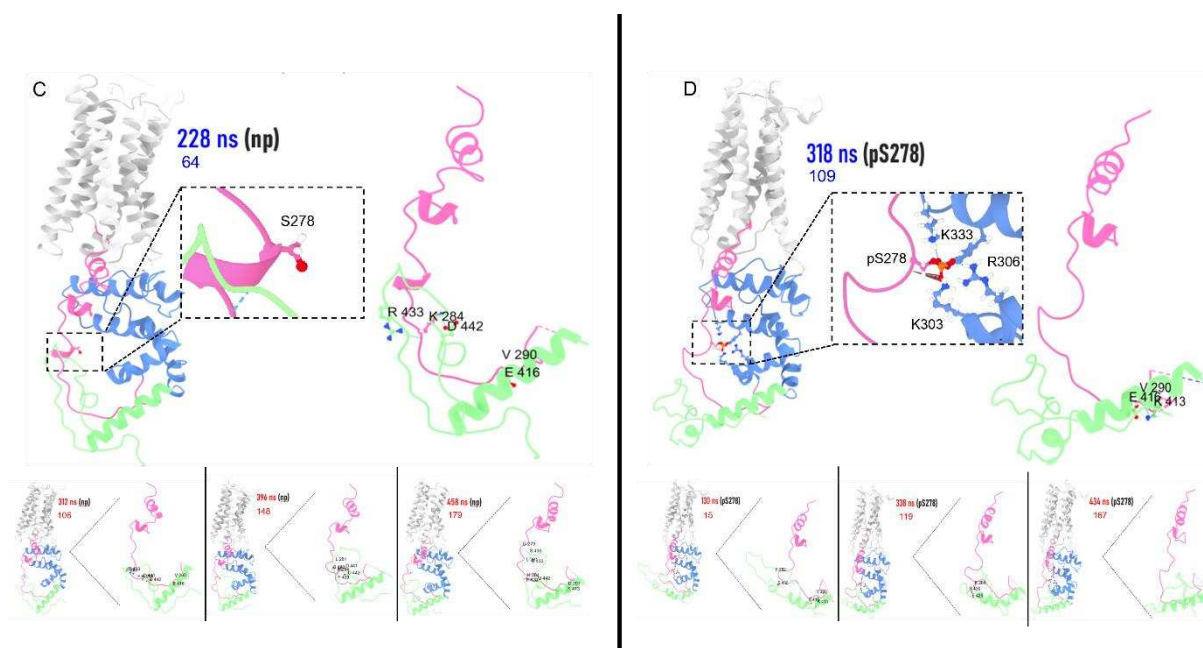


Figure 3 - Molecular Dynamics Simulation Analysis of non-phospho-AtRGS1 and phospho-Ser278-AtRGS1 models. Comparative PCA analysis of non-phospho-AtRGS1 **(A)** and phospho-Ser278-AtRGS1 **(B)** trajectories using MDM-task-web tool. Color gradient of the points indicates frame in nanoseconds, with representative structures and centroids indicated by red or blue circles. **(C)** Representation of 228 ns non-phospho-AtRGS1 with predicted hydrogen bonds extracted from representative PCA frames trajectories. Zoomed-in view of non-phospho-Ser278-AtRGS1. Interacting residues are shown as balls and sticks, while interacting regions are represented as light blue ribbons. Representations from the same analysis in different moments are shown in the bottom as comparison. **(D)** Representation of 318 ns phospho-AtRGS1 with predicted hydrogen bonds extracted from representative PCA frames trajectories. Zoomed-in view of phospho-Ser278-AtRGS1. Interacting residues are shown as balls and sticks, while interacting regions are represented as light blue ribbons. Representations from the same analysis in different moments are shown in the bottom as comparison.

Interestingly, in addition to the conserved nature of S278 residue among various plant families, comparable phosphorylation characteristics emerge in other organisms. PCA analysis spanning 200 nanoseconds (ns) (Figure S2) from the lycophyte *Selaginella moellendorffii*, a distant relative, revealed analogous behavior in the phosphorylation of S273-SELML, the S278 equivalent in Arabidopsis (Figure 4). Distinctions between the most representative structures of npSELML (Figure 4A) and pS273-SELML (Figure 4B) were observed, with no interactions involving S273 in npSELML structures (Figure 4C). However, pS273 structures exhibited interactions between the linker residue and the residues of RGSbox (Figure 4D).

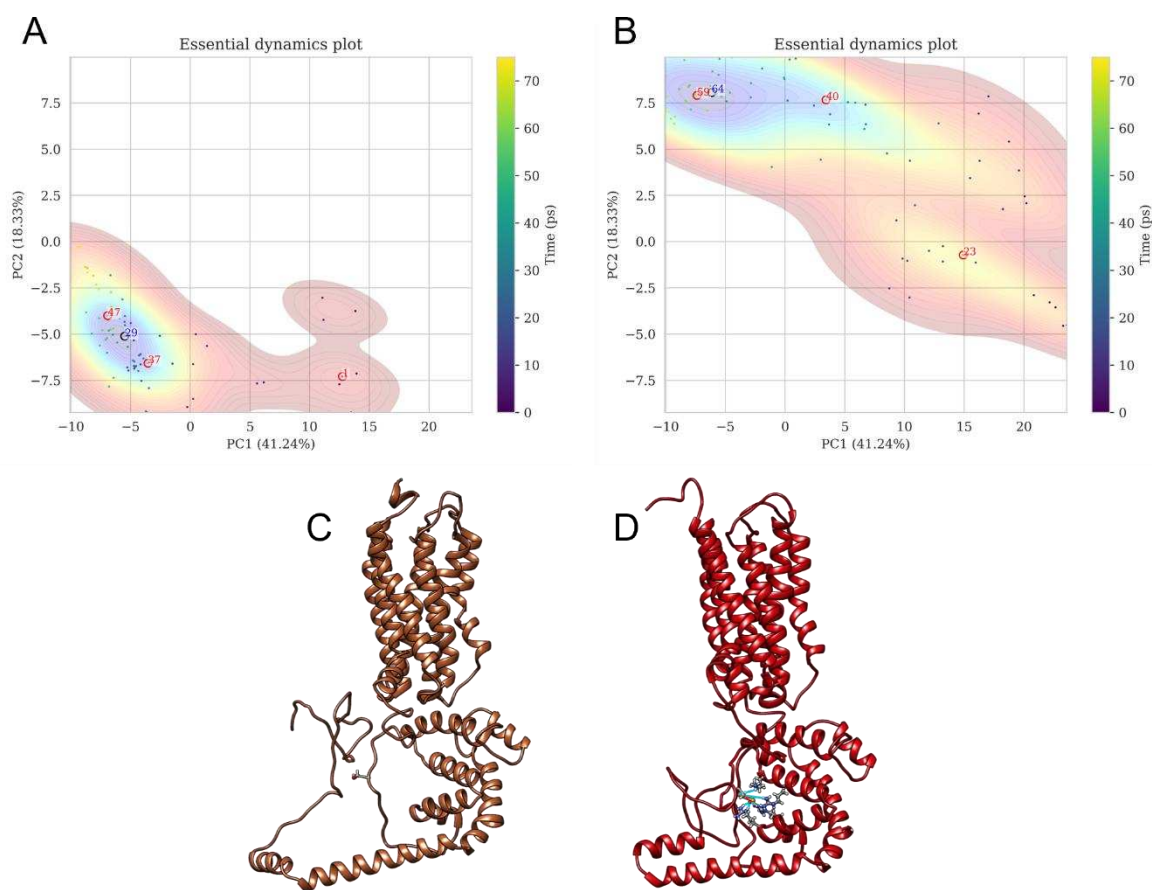


Figure 4 - Molecular Dynamics Simulation Analysis of non-phospho-SELML and phospho-Ser273-SELML models. Comparative PCA analysis of npSELML (A) and pS273-SELML (B) trajectories using MDM-task-web tool. Color gradient of the points indicates frame in nanoseconds, with representative structures and centroids indicated by red or blue circles. (C) Representation of 98 ns npSELML. Interacting residues are shown as balls and sticks, while interacting regions are represented as light blue ribbons. (D) Representation of 168 ns pS273-SELML with predicted hydrogen bonds extracted from representative PCA frames trajectories. Interacting residues are shown as balls and sticks, while interacting regions are represented as light blue ribbons.

Recognizing the crucial role of S278 phosphorylation as a regulatory mechanism, this study employed a set of phospho-mimetic and phospho-null mutants to emulate the phosphorylation pattern of RGS1. To compare the behavior of S278E with pS278, a PCA analysis spanning 200 nanoseconds (ns) was conducted on the mimetic residue (Figure 5A). This analysis revealed a parallel behavior between S278E and pS278, particularly in their ability to engage in similar interactions (Figure 5B). Henceforth, we will refer to the phosphorylated state of S278 as S278E.

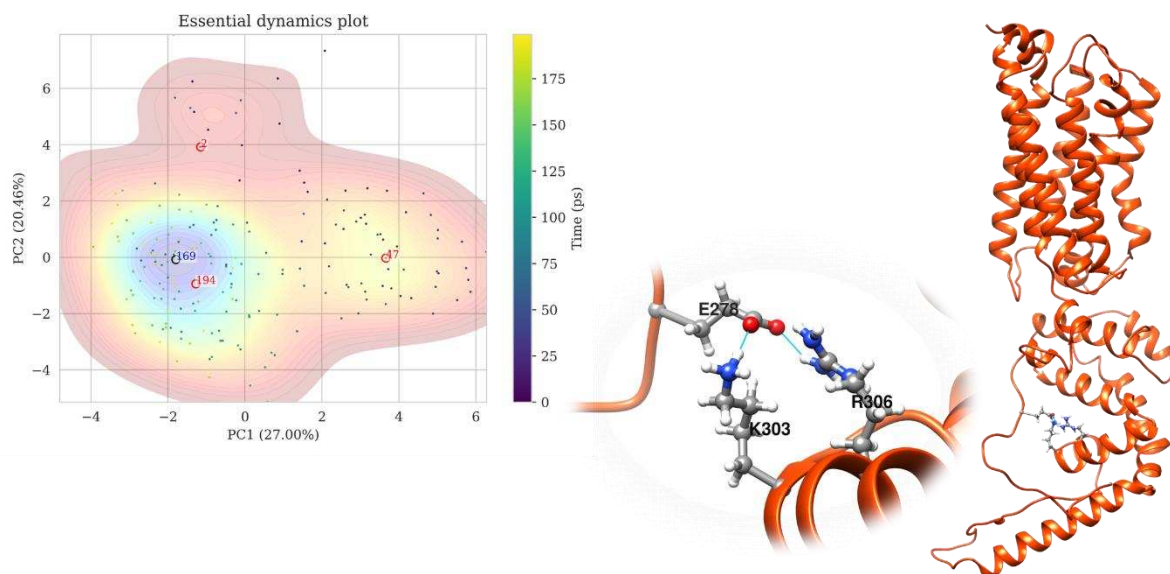


Figure 5 - Molecular Dynamics Simulation Analysis of phospho-mimetic-S278E-AtRGS1 model. Comparative PCA analysis of S278E-AtRGS1 **(A)** trajectories using MDM-task-web tool. Color gradient of the points indicates frame in nanoseconds, with representative structures and centroids indicated by red or blue circles. **(B)** Representation of 169 ns S278E-AtRGS1 with predicted hydrogen bonds extracted from representative PCA frame trajectories. Zoomed-in view S278E-AtRGS1. Interacting residues are shown as balls and sticks, while interacting regions are represented as light blue ribbons.

Phosphorylation of S278-RGS1, but also GPA1, regulates G-protein binding

AtRGS1 regulates G-protein signaling by accelerating GTPase activity of AtGPA1, catalyzing the conversion of GTP to GDP and subsequently deactivating the complex (Chen *et al.*, 2003; Jones *et al.*, 2011b). In turn, the regulation of AtRGS1 is related to its phosphorylation by RLKs (Fu *et al.*, 2014; Tunc-Ozdemir *et al.*, 2016; Liang *et al.*, 2018), a crucial step driving the uncoupling and internalization processes of RGS1 (Urano *et al.*, 2012; Watkins *et al.*, 2021). To comprehend the impact of the S278 phosphorylation status on these internalization pathways, we aimed three important and consecutive features about this entire process: the interaction of AtRGS1 with AtGPA1; the internalization process induced by elicitors; and the stability of RGS1 upon internalization.

To elucidate the interaction between AtRGS1 and AtGPA1 under S278 phosphorylation influence, it is crucial to note that the regulatory phosphorylation is not exclusive to AtRGS1. AtGPA1 can also undergo phosphorylation by various RLKs (Jia *et al.*, 2019). Li and collaborators (2018) have proposed that phosphorylation of Tyr166 in AtGPA1 alters the binding pattern with AtRGS1, consequently modulating the

steady-state rate of the GTPase cycle. Considering this, a molecular dynamic analysis of contacts spanning 210 nanoseconds (ns) between these two proteins under different patterns of phosphorylation was performed (Figure 6A).

This analysis demonstrated that simultaneous phosphorylation of Y166 (pY166-GPA1) and S278 (pS278-RGS1) resulted in a higher interaction between these two proteins. However, the single phosphorylation of one of these residues, with the other represented in the wild type structure, drastically decreases the number of contacts. Notably, the analysis of interactions between fully phosphorylated RGS1 (allP-RGS1) and pY166-GPA1, similar to the interaction between both wild type proteins, exhibited an intermediate number of contacts. These results are consistently reflected in the average analysis of contacts (Figure 6B).

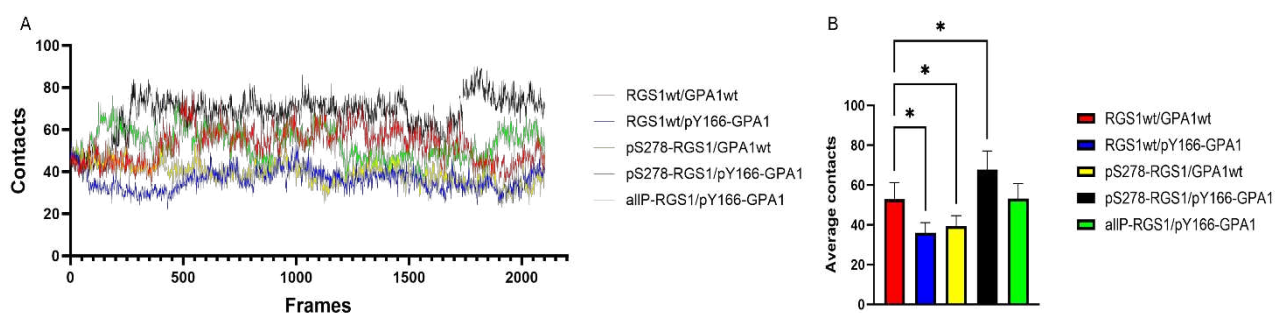


Figure 6 – Molecular Dynamics Simulation Analysis of interaction between RGS1 and GPA1 in different phosphorylation states. (A) MDS of contacts between RGS1 and GPA1 in diverse combinations of phosphostates for S278 and Y166 residues, respectively. The total simulation time is 210 ns with 10 frames per second. (B) Average contacts from the entire trajectory. Statistical significance is represented as * ($P \leq 0.0001$). Error bars indicate standard error of the mean (SEM).

In addition to the insights from molecular dynamics results, we conducted transient expression experiments in *Nicotiana benthamiana* plants to validate the changes in binding affinity of AtRGS1 phosphomimetic mutants compared to the wild type AtGPA1 and the phosphomimetic pY166-AtGPA1 (Y166E). Consistent with the molecular findings, split-luciferase assays revealed a reduced interaction between S278E-RGS1 and GPA1wt, with no significant difference observed with the S278A-RGS1 mutant, both compared to the wild type interaction (Figure 7A). As anticipated, split-luciferase results for the interaction between AtRGS1 mutants and Y166E displayed the opposite pattern (Figure 7B). The interaction between S278E-RGS1 and Y166E no longer exhibited a difference compared to the RGS1^{WT} interaction with GPA1 phosphomimetic. However, the interaction between S278A and Y166E showed

a decrease. These results suggest that not only is the phosphorylation pattern of AtRGS1 crucial for its interaction with GPA1, but also the phosphorylation status of GPA1 plays a pivotal role in this process.

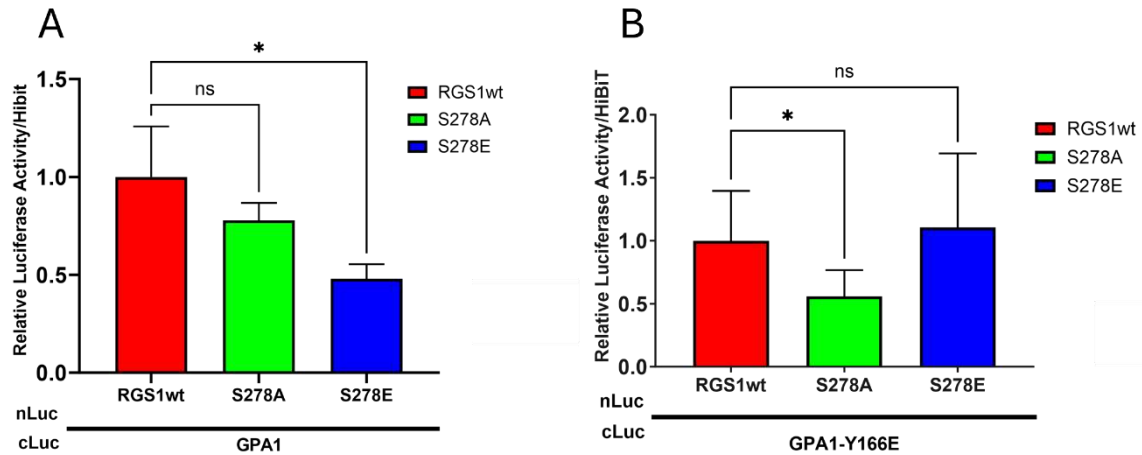


Figure 7 – *In vivo* interaction between phosphomutants of RGS1 and GPA1. Split luciferase-based interaction levels between AtGPA1 (wild type (A) and Y166E (B) and forms) and AtRGS1 mutants, normalized to the wildtype (AtRGS1^{WT}) protein interaction values. Statistical significance is represented as ns ($P > 0.05$) and **** ($P \leq 0.02$). Error bars indicate standard error of the mean (SEM).

Given our understanding that the cluster is involved in the dissociation of RGS1 from GPA1, and since our results indicate that residue S278 also plays a role in this process, we generated additional mutants from cluster phosphomimetics to further understand the regulation of phosphorylation. We created four distinct phosphomutants by combining S278 and clusterA residues: Linker phosphorylated and cluster non-phosphorylated (S278E-clusterA); linker non-phosphorylated and cluster phosphorylated (S278A-q2q4q6); both phosphorylated (S278E-q2q4q6) and both non-phosphorylated (S278A-clusterA) (Figure S3). Subsequently, we assessed the interaction between these mutants and GPA1wt using split-luciferase assays (Figure 8). In summary, clusterA, S278E-q2q4q6, and S278E-clusterA exhibited a reduced interaction with GPA1 compared to the wild type interaction, similar to the behavior observed with S278E.

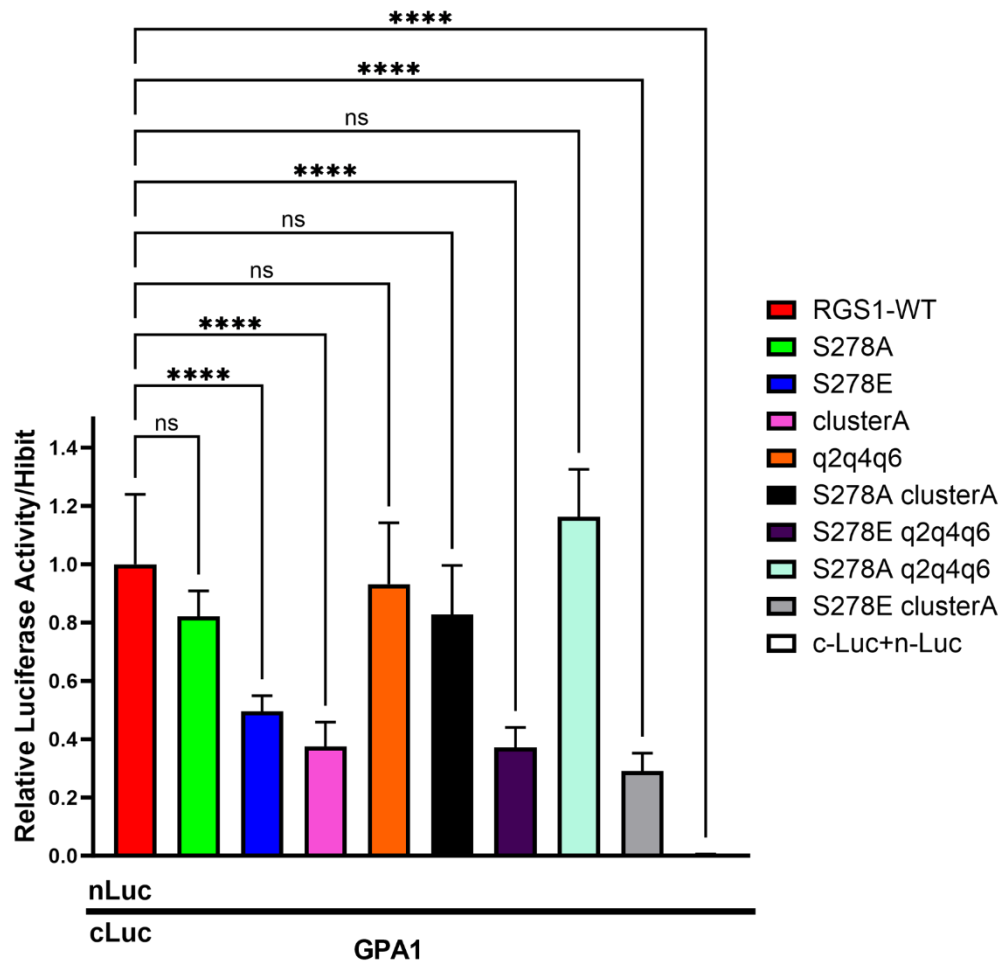


Figure 8 - *In vivo* validation of phosphorylation-mediated regulation of AtRGS1. Split luciferase-based interaction levels between AtGPA1 and AtRGS1 mutants, normalized to the wildtype (AtRGS1^{WT}) protein interaction values. Statistical significance is represented as ns ($P > 0.05$) and **** ($P \leq 0.0001$). Error bars indicate standard error of the mean (SEM). $n \approx 16$.

Ser278 is required for flg22-induced internalization of AtRGS1

The phosphorylation of RGS1, induced by flg22 and UDP-Glucose, has been documented (Urano *et al.*, 2012; Watkins *et al.*, 2021). This phosphorylation triggers the dissociation of RGS1 from the heterotrimeric G-protein complex, initiating subsequent internalization and activation of G signaling. More precisely, the RGS1 cluster plays a crucial role in this process (Urano *et al.*, 2012; Watkins *et al.*, 2021). However, the role of the S278 residue in the internalization pathway induced by elicitors remains insufficiently understood.

To evaluate the involvement of S278, *rgs1-2* plants complemented with AtRGS1^{WT}-YFP, AtRGS1^{S278A}-YFP, AtRGS1^{S278E}-YFP or AtRGS1^{S428/431/435/436A}-YFP (quadA) were utilized for single-cell internalization quantification. Flg22 served as the

infectious signal, and *quadA* served as a control due to its established role in RGS1 internalization (Watkins *et al.*, 2021). Dark-induced elongated hypocotyl cells were treated and observed over time, with pictures taken after one hour of treatment, and the internal YFP signal was quantified relative to membrane-located YFP.

Our data indicate that the phosphorylation of Ser278 is essential for *flg22*-mediated internalization (Figure 9A-B). While only RGS1^{WT}-YFP presented an increase in the internalization rate ($\approx 25\%$), S278A and clusterA mutants exhibited a similar internalization rate in both situations ($\approx 30\%$ and $\approx 20\%$, respectively). Interestingly, even S278E mutant also demonstrated no difference in internalization rate in both situations, this rate was similar to the RGS1^{WT}-YFP rate under *flg22* presence.

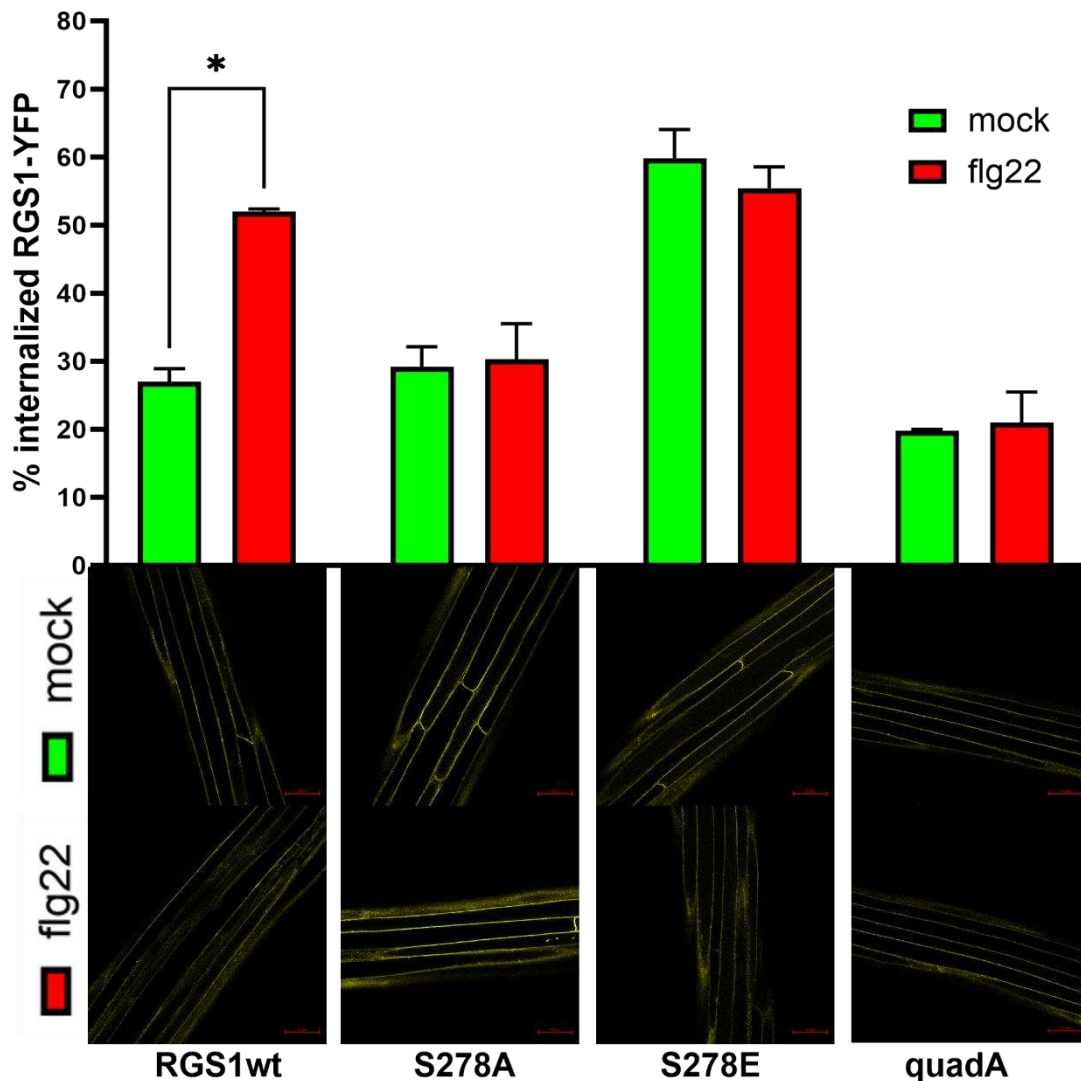


Figure 9 - Ser278 phosphorylation is required for *flg22* signaling. RGS1-YFP internalization on dark-induced elongated hypocotyls under *flg22* treatment. **(A)** Values represent the amount of AtRGS1 that internalized into the cell as a percent of the total YFP fluorescence. **(B)** Image data used to generate

these values. Statistical significance is represented as * ($P \leq 0.0001$). Error bars indicate standard error of the mean (SEM). $n \approx 4$. Scale bar - 50 μm .

RGS1 stability is regulated by a phosphor-barcode in the linker and tail

Following internalization through various distinct endocytic pathways, internalized proteins converge into a similar early/sorting endosome. Subsequently, they diverge along distinct sorting pathways: recycled back to the plasma membrane, directed to the trans-Golgi network, delivered to lysosomes for degradation, or involved in a signal transduction pathway (Elkin *et al.*, 2016).

Upon observing that phosphorylation of S278 stimulated the uncoupling and endocytosis of RGS1, our primary hypothesis was that RGS1 was being targeted for degradation. To evaluate this hypothesis, we decided to monitor the stability of RGS1 wild type and RGS1 phosphomimetics over time, investigating if the phosphorylation state of S278 could impact this characteristic. To achieve this, wild type and mutant seedlings were treated with cycloheximide, a protein synthesis inhibitor, and the samples were collected at various time points for YFP-fluorescence analysis. We conducted extended time courses to precisely determine the optimal duration (Figure S4), and a six-hour time course with sample collection every hour proved to be an appropriate approach for this experiment.

Initially, *rgs1-2* plants complemented with AtRGS1^{WT}-YFP, AtRGS1^{S278A}-YFP, AtRGS1^{S278E}-YFP or AtRGS1^{S428/431/435/436A}-YFP (quadA) were exposed uniquely to cycloheximide for a six-hour time course. Our findings revealed that while S278E mutant demonstrated a decrease in total YFP-fluorescence equivalent to RGS1^{WT}, indicating RGS1 degradation, S278A and clusterA mutants presented a significantly lower decrease compared to RGS1^{WT} (Figure 10A and S5A). These differences become even more evident when examining the slopes, representing the rate of degradation (Figure 10B).

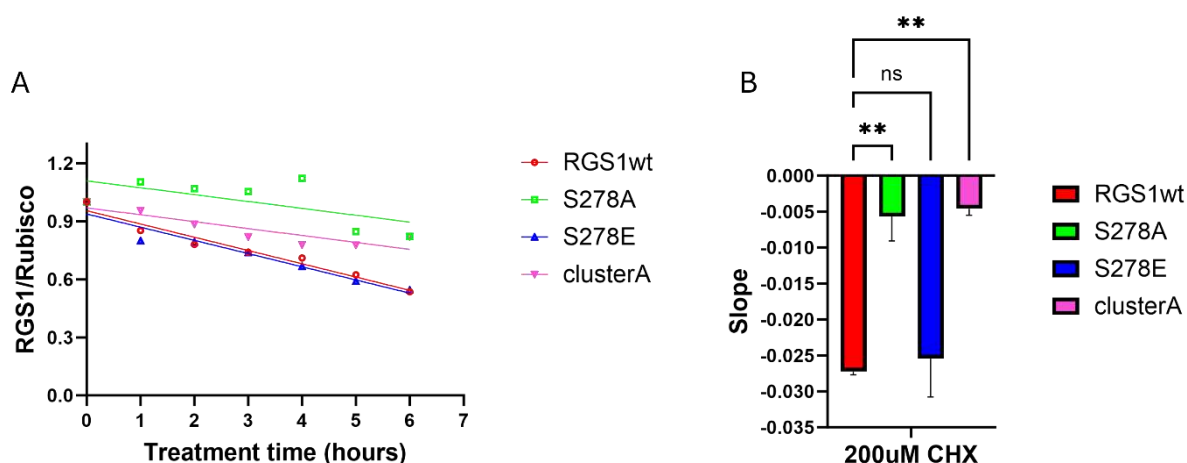


Figure 10 - *In vivo* degradation of AtRGS1. (A) Western blot quantification of AtRGS1 stability over time (6h treatment). Cycloheximide (CHX) was used for protein synthesis inhibition, and Rubisco (RbcL) was used as the loading control. Western blot quantification of AtRGS1 decay comparing inside each treatment group with WT and treatments. (B) Boxed graph displays the line slope, which indicates the degradation rate of AtRGS1 and its mutants. Values were normalized based on WT values. Statistical significance is represented as ns ($P > 0.05$) and ** ($P \leq 0.001$). Error bars indicate standard error of the mean (SEM). $n \approx 3$.

An identical experiment was replicated, but with inclusion of the elicitor flg22 in the cycloheximide treatment to simulate the impact of bacterial presence on RGS1 stability over time. Surprisingly, in the presence of flg22, both RGS1^{WT} and S278E exhibited the same degradation pattern as the S278A and clusterA mutants—indicating increased stability over time (Figure 11A and S5B). These differences become even more evident when examining the slopes (Figure 11B).

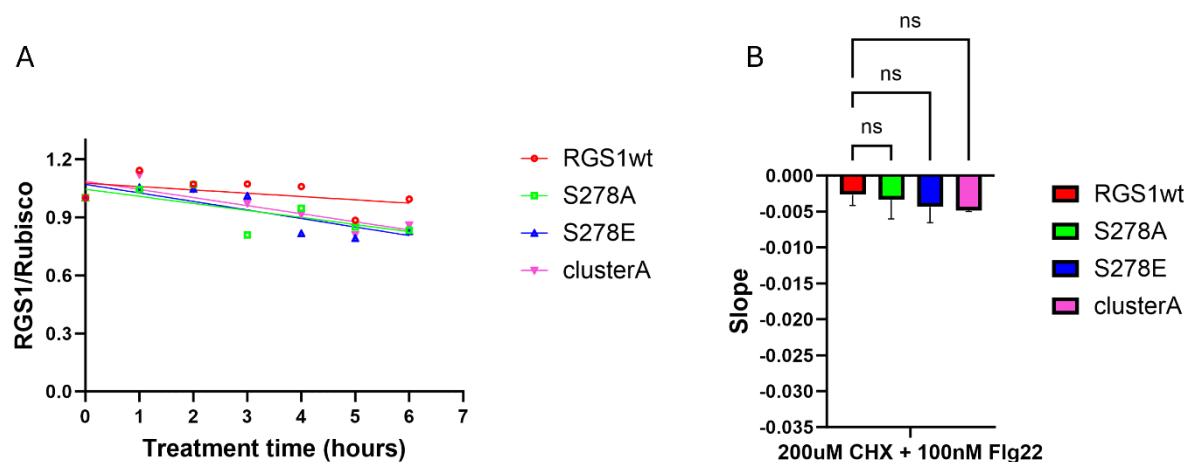


Figure 11 - *In vivo* degradation of AtRGS1 under flg22 exposure. (A) Western blot quantification of AtRGS1 stability over time (6h treatment). Cycloheximide (CHX) was used for protein synthesis inhibition, flg22 was used as a mimetic elicitor, and Rubisco (RbcL) was used as the loading control.

Western blot quantification of AtRGS1 decay comparing inside each treatment group with WT and treatments. **(B)** Boxed graph displays the line slope, which indicates the degradation rate of AtRGS1 and its mutants. Values were normalized based on WT values. Statistical significance is represented as ns ($P > 0.05$). Error bars indicate standard error of the mean (SEM). $n \approx 3$.

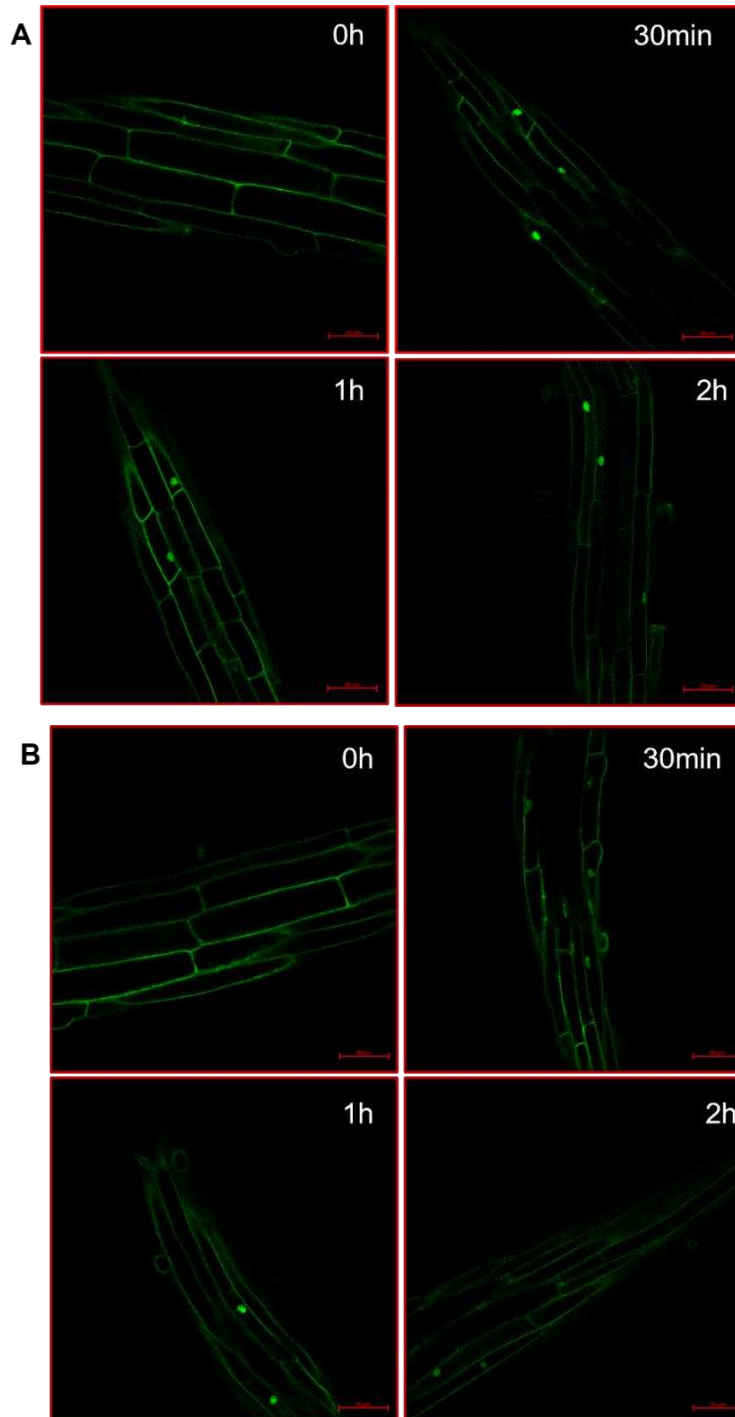
AtRGS1 is localized in the nucleus upon different external signals

Despite the unexpected outcomes in the stability experiments of RGS1, the results were intriguing. Given that RGS1 undergoes uncoupling from the G-protein complex and internalization without degradation upon flg22 exposure, our subsequent focus was on determining the destination of RGS1 post-internalization. To achieve this, we employed Fluorogen Activating Protein (FAP) Technology (SpectraGenetics). In essence, FAP-tags enable the switching of fluorescent signals by the addition or removal of fluorogen (Figure S6). In this study, a membrane-impermeant fluorogen was utilized, ensuring that only AtRGS1 present at the cell surface would be visible. This stands in contrast to standard fluorescent protein fusions, where the entire protein population emits fluorescence, potentially complicating the visualization of the process.

Initially, root cells of FAP-Beta-tagged RGS1^{WT} plants were exposed to different treatment times of 100nM flg22, and individual cells were examined through confocal microscopy. At time 0h, fluorescence was predominantly concentrated in the membranes; however, after 30 minutes of exposure, FAP-B-RGS1^{WT} fluorescence was also evident in the nucleus. This nuclear localization persisted at treatment times of 1 hour and 2 hours (Figure 12A). Subsequently, recognizing that RGS1 internalization is triggered by sugar signals, a parallel experiment was conducted under identical conditions, but this time with a solution containing 123 μ M UDP-glucose. Root cells, in a parallel yet not identical manner, exhibited nuclear localization of FAP-B-RGS1^{WT} at the same treatment durations (Figure 12B). To corroborate the nuclear localization of AtRGS1, root cells were labeled with the nuclear marker Hoechst 33342, confirming the presence of FAP-B-RGS1^{WT} in the nucleus (Figure S7B), as also visualized through the PMT (transparent) channel (Figure S7A). Additional controls were conducted to ensure the accuracy and reliability of the results (Figure S8).

To quantify the nuclear mobilization of RGS1, fluorescent nuclei were counted along the entire root of FAP-B-RGS1 seedlings after 1-hour treatment of 100nM flg22 or 123 μ M UDP-glucose (Figure 12C). This specific treatment time was selected based on higher stability of RGS1-fluorescent nuclear localization among all treatment times.

As evident in the confocal images, exposure to flg22/UDP-Glucose significantly increased the number of RGS1 nuclear localization compared to the mock treatment.



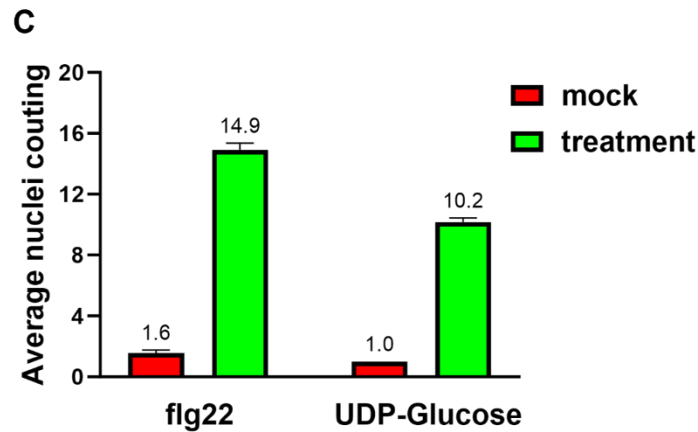


Figure 12 – Flg22/UDP-Glucose stimulates RGS1 internalization and nuclear localization. Representatives processed confocal images of FAP-Beta-RGS1^{WT} cellular localization overtime under (A) Flg22 and (B) UDP-Glucose treatment. (C) Average nuclei quantification among treatments after 1-hour of treatments. Error bars indicate standard error of the mean (SEM). $n \approx 3$. Scale bar - 50 μm .

Unfortunately, the thicker and less flexible hypocotyl walls compared to root walls (Derbyshire *et al.*, 2017) present challenges for the effective uptake of the nuclear marker, making it difficult to assess the nuclear mobilization of YFP-RGS1 overexpressing lines (Figure S9). However, an average nuclear mobilization was measured through observation of nuclear envelope structure in the PMT channel (Figure 13). This careful approach was essential to mitigate potential misinterpretations that could arise from using YFP lines, where the entire protein population emits fluorescence. By doing so, we aimed to minimize miscounting of RGS1-YFP fluorescence in alternative cellular pathways, such as vacuolar degradation or protein synthesis.

The quantitative analysis revealed an increase in the average number of RGS1^{WT} localized in the nucleus in the presence of flg22. Interestingly, the average number of RGS1 phosphomutants remained unchanged under flg22 conditions, but in distinct patterns. Both the S278A and clusterA mutants exhibited a low average number of nuclei, comparable to the mock average of RGS1^{WT}. In contrast, S278E showed a high number of nuclei even without flg22 treatment.

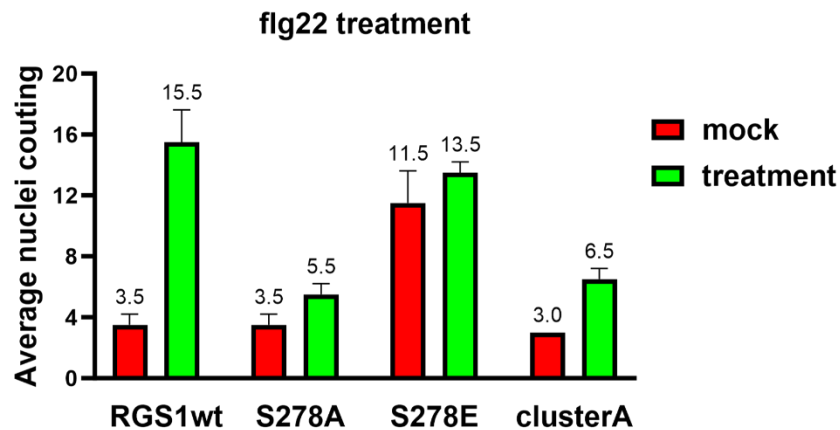


Figure 13 – Phosphorylation of serine residues affects AtRGS1 internalization. Average nuclei quantification of RGS1 phosphomutants after 1-hour flg22 treatment. Error bars indicate standard error of the mean (SEM). $n \approx 3$. Scale bar - 50 μm .

Influence of RGS1 phosphorylation upon pathogen infection

Given the intriguing insights obtained from using flg22 as a bacterial inducer, we extended our investigation to infectious infiltration to comprehend the immune response behavior of RGS1 phosphorylation. For this purpose, we infiltrated *Pseudomonas syringae pv. tomato* (Pst) DC3000 strain into AtRGS1 overexpressing lines and *rgs1-2* leaves. Phenotypic bacterial symptoms were evaluated (Figure 14A and S10), along with quantification of colony-forming units (CFU) (Figure 14B). Our findings revealed that, following an appropriate infection period, both RGS1^{WT} and S278E mutants exhibited a similar response to the Col-0 plants, while *rgs1-2* and *quadA* mutants displayed a reduction in both symptoms and CFU. Nonetheless, the S278A mutant demonstrated increased susceptibility to bacterial infection, as evidenced by elevated symptoms and CFU compared to the Col-0 pattern.

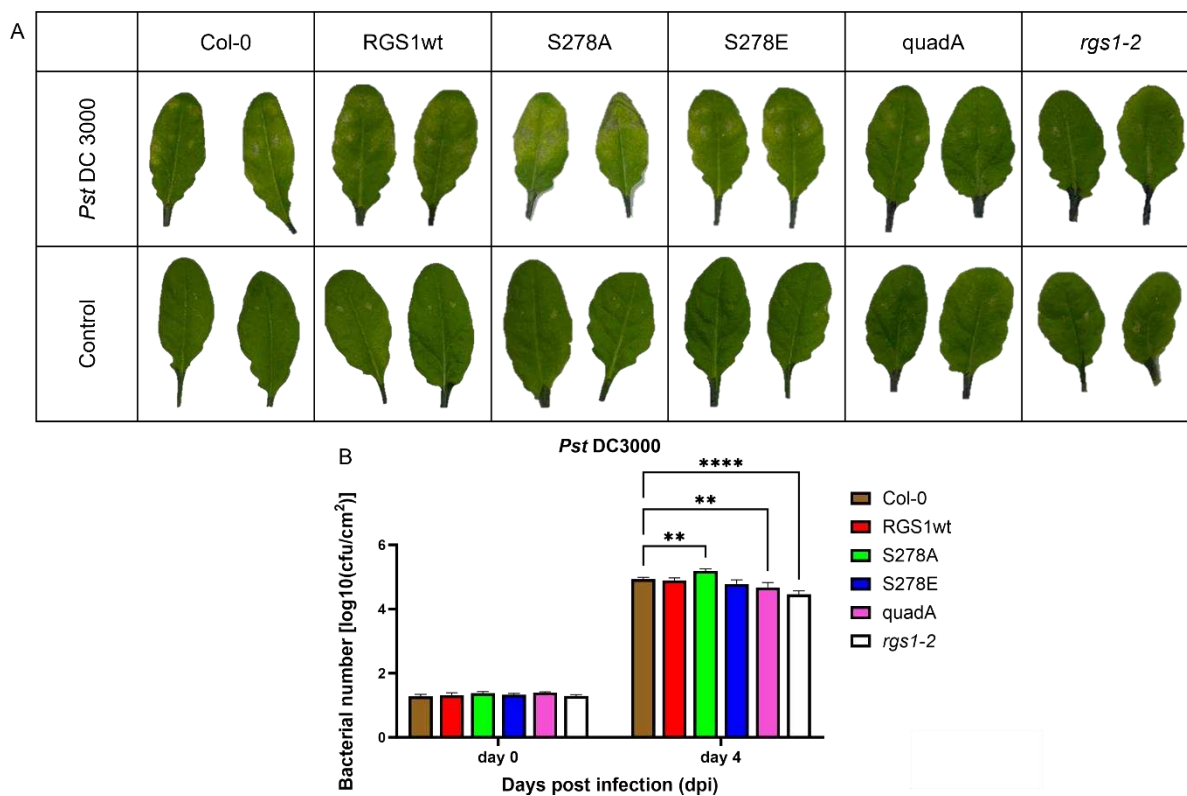


Figure 14 – Phosphorylation of serine residues affects AtRGS1 response to bacterial infection.

(A) Disease symptoms on leaves post *Pst* DC3000 infection. Images were taken at 4 dpi. **(B)** Bacterial growth of *Pst* DC3000 post infection. Leaves of 4-week-old plants Col-0, RGS1^{WT}, S278A, S278E, quadA and *rgs1-2* were hand infiltrated with bacterial suspensions and bacterial populations were quantified at 0 and 4 dpi. Statistical significance is represented as ns ($P > 0.05$), ** ($P \leq 0.004$) and **** ($P \leq 0.0001$). Error bars indicate standard error of the mean (SEM). $n \approx 3$.

DISCUSSION

The in-silico analysis of RGS1 structure and phylogenetic investigation has revealed critical insights into its protein architecture and the conservation of amino acid residues across various plant families, ranging from algae to dicots. Several serine residues, known for their pivotal roles in diverse pathways involving the RGS1 protein (Choudhury and Pandey 2015; Tunc-Ozdemir *et al.*, 2017; Liang *et al.*, 2018; Oliveira, 2022), were identified highly conserved (Figure 2C). Various crucial aspects of the cellular environment were considered during the molecular dynamic simulation (MDS) analysis, including the composition of the bilipid membrane, water content, and concentration of salts. Besides that, dynamic modulation models for protein behavior offer a more intriguing approach compared to steady-state models due to their ability to capture the dynamic and responsive nature of proteins. Unlike steady-state models that assume a static equilibrium, dynamic modulation models consider the temporal fluctuations in protein activity, acknowledging that proteins constantly adapt to various cellular stimuli and environmental changes. This dynamic perspective allows for a more realistic representation of the intricate regulatory mechanisms governing protein behavior, unveiling insights into transient interactions, signal transduction pathways, and adaptive responses.

Molecular dynamic simulation (MDS) analysis demonstrated distinct interaction patterns among specific residues, illustrating that the phosphorylation status of Ser278 induces a conformational change. This change is attributed to the interaction between the linker residue and other residues in the RGS1 box, enhancing the flexibility of the RGS1 C-tail domain (Figure 3C-D). This mechanism is important because it increases the possibility of the linker region participating in distinct processes and interactions, especially considering the serine cluster in this region. In addition to the crucial interaction between S278-AtRGS1 and Y166 residues of the G-protein α subunit (GPA1), recent unpublished MDS analysis indicates a correlation between the tails of both proteins and their overall interaction process. Moreover, this data reveals that, similar to the S278-Y166 interaction already highlighted, the phosphorylation status of the C-tail/cluster also influences the interaction affinity. These findings strongly suggest that a sophisticated phosphorylation system may govern the signaling of RGS1.

Posttranslational modifications are dynamic events that alter protein properties through the addition of modifying groups, such as acetyl, phosphoryl, glycosyl, and methyl, to one or more amino acid residues. These modifications can impact the

activity, localization, and stability of a protein (Ramazi *et al.*, 2020). AtRGS1 has been demonstrated to undergo phosphorylation by various kinases, including RLKs and WNKs (Urano *et al.*, 2012; Fu *et al.*, 2014; Tunc-Ozdemir *et al.*, 2016; Liang *et al.*, 2018; Watkins *et al.*, 2021; Watkins *et al.*, 2023), emphasizing the concept of a signaling code characterized by a diverse array of kinases and distinct phosphorylation patterns across different residues. While there have been studies on the phosphorylation of RGS1 C-tail, the investigation of residue S278 has been largely overlooked. This oversight is attributed to the prevailing focus on truncated forms of RGS1. However, neglecting the full-length RGS1 and overlooking the role of other phosphosites might represent a critical gap in understanding the phosphorylation-dependent activity of RGS1.

In order to abolish the phosphorylation, mutants with alanine substitutions were utilized (S278A and clusterA), while mutants with glutamic acid (Glu) substitutions (S278E and q2q4q6) were employed to mimic phosphorylation. Given our belief that the regulation of RGS1 involves a complex phosphorylation pattern, we systematically generated specific combinations of phosphorylation states for both linker and cluster residues. It is noteworthy that despite acidic residues like Glu being negatively charged and nearly isosteric with pSer, pSer typically carries a double charge at physiological pH, whereas Glu is singly charged (Cooper *et al.*, 1983; Pearlman *et al.*, 2011). However, our MDS revealed that these two proteins exhibit similar behavior.

These phosphomutants were employed in *in vivo* experiments to assess the impact of phosphorylation patterns with GPA1 interaction, given the previous demonstration that such patterns can release the G-protein complex for downstream signaling (Liang *et al.*, 2018). Reinforcing the *in-silico* findings, phosphorylation of S278 reduced the interaction between RGS1 and GPA1 and the interaction between Y166E-GPA1 and S278A-RGS1 also exhibited an interaction decrease. Additionally, the interaction between S278E-RGS1 and Y166E-GPA1 (Figure 7A-B) was consistent with the molecular dynamic simulations, which demonstrate that phosphorylation of Y166-GPA1 enhances the binding affinity of the GDP state of AtGPA1 to AtRGS1 (Li *et al.*, 2018). This is pertinent to the fact that the S278 residue of RGS1 may constantly be found in the phosphorylated form (Watkins *et al.*, 2023).

Interestingly, when examining the interactions of phosphomutants with GPA1, it becomes evident that all matches showing a decrease in the interaction between RGS1 and GPA1 occurred in the presence of S278E, except for the interaction with

the clusterA mutant (Figure 8). However, the exact phosphorylation state of S278 in the clusterA mutant cannot be defined. It cannot be discarded that endogenous kinases may be phosphorylating this residue *in vivo*. Furthermore, as previously mentioned, the phosphorylation state of GPA1 is also crucial for this interaction. This aspect could also justify why the *in vivo* interaction between RGS1^{WT} and GPA1 did not exhibit the same pattern as S278E-GPA1.

To elucidate the role of the S278 residue in the RGS1 internalization process, we assessed the internalization rate of our S278 phosphomutants under flg22-induced endocytosis, using the clusterA mutant as a control (Figure 9) (Watkins *et al.*, 2023). The endocytosis process of the S278A mutant exhibited a rate comparable to the quadA internalization. Intriguingly, the internalization process of the S278E presented the same rate under both conditions, however, it is an internalization rate equivalent to the internalization rate of RGS1^{WT} under flg22 presence. These results suggest that S278 residue is implicated in the RGS1-induced flg22 internalization process independent of cluster phosphorylation. Given that AtRGS1 undergoes internalization in response to flg22 and sugar stimuli, our first hypothesis was if in the presence of these elicitors, RGS1 could be targeted for degradation. To prove that we investigated the stability of phosphomutants in the presence of a protein synthesis inhibitor over a 6-hour time course. Our results demonstrated that the S278 phosphorylation is necessary for RGS1 degradation (Figure 10 and 11). While S278E exhibited the same degradation pattern as RGS1^{WT}, S278A and quadA demonstrated a higher stability over time. Additionally, we introduced flg22 into this experiment, and surprisingly, flg22 increased the stability of both RGS1^{WT} and S278E mutants. Concurrently, recent studies have indicated that in the absence of RGS1 phosphatase (Atb α), the total RGS1 levels were reduced (Watkins *et al.*, 2023). These findings suggest a potential linkage between the degradation pattern observed and RGS1's interaction with other molecules, such as the phosphatase, or even the phosphorylation pattern of other RGS1 residues, like the cluster.

Since AtRGS1 undergoes internalization upon flg22 treatment without highly degradation in sequence, our subsequent objective was to elucidate the destination of RGS1. To address this question, a membrane-impermeant fluorogen was employed to selectively react with RGS1 anchored in the membrane, facilitating the tracking of its localization. Following various treatment periods with flg22 and UDP-glucose, we observed that a portion of RGS1 proteins is directed to the nucleus (Figure 12). This

result, although surprising, finds support in the work of Chen *et al.* (2006), who observed a similar outcome in *Arabidopsis* protoplasts treated with 10 μ M ABA after 16 hours of incubation. Other studies reported that GPCRs continue to signal after internalization and also the translocation of these proteins into the nucleus (Bhosle *et al.*, 2019). For instance, an oxytocin receptor, a member of the rhodopsin-type (class I) family of GPCRs, is translocated into the nucleus of osteoblasts upon stimulation by oxytocin ligands. This translocation was found to play a role in osteoblast maturation (Di Benedetto *et al.*, 2014).

The approach applied to quantify the nuclear localization across treatments involved counting nuclei from the hypocotyl until the distal part of the root. It was verified that the nuclear localization became more evident and widespread throughout the root under flg22 or UDP-Glu treatments. Some other interesting features were observed in our experiment, although articulating these findings is not straightforward. For instance, a higher intensity of nucleus-fluorescence manifested after 1-hour treatment, potentially linked to the stability of this internalization process. Another interesting observation was that the decay of AtRGS1 nuclear fluorescence in response to UDP-Glu compared to flg22, occurring around 2 hours and 3 hours, respectively. This variation may be associated with specificities in each signaling pathway, such as the half-life of elicitors. Furthermore, the examination of Z-stacks in confocal images of individual nucleus cells revealed that FAP-B-RGS1 fluorescence was higher when the nuclear envelope had suboptimal resolution in the PMT channel (Figure S11A). Conversely, the highest resolution of the nuclear envelope coincided with a weaker FAP-B-RGS1 fluorescence (Figure S11B). This observation implies that, following endocytosis, AtRGS1 is positioned in the nuclear membrane. This hypothesis is supported by the fact that GPCRs are also known to localize in the nuclear membrane post-internalization (Di Benedetto *et al.*, 2014).

The visualization of RGS1 localization in YFP plants can be challenging due to the overall YFP-RGS1 fluorescence. However, the new findings about nuclear localization drove us into the attempt to quantify this process upon flg22 induction. Nuclei were counted after a 1-hour treatment (Figure 13). Similar to FAP-B-RGS1^{WT} seedlings, AtRGS1^{WT}-YFP presented an increase of AtRGS1 in the nucleus upon treatment when compared to the mock, proving the influence of flg22 on RGS1 mobilization to the nucleus. S278A and quadA seedlings displayed a consistent response pattern, showing no difference between flg22 and the mock treatments,

indicating the significance of phosphorylation at these residues not only for internalization but also for nuclear localization. While S278E seedlings exhibited similar nucleus counts in both flg22 treatment and the mock, the quantification for both conditions was comparable to AtRGS1^{WT} under flg22 treatment. This result supports the hypothesis that the phosphorylation of these residues is crucial for both internalization and nuclear localization processes. Indeed, this result correlates with S278E internalization response, since even in normal conditions, the internalization rate of this mutant is as high as in the presence of flg22.

To investigate the immune response dynamics influenced by RGS1 phosphorylation, leaves from each one of the phosphomutants were infiltrated with *Pseudomonas syringae pv. tomato (Pst)* DC3000 strain bacteria, and the infectious process was meticulously observed. Col-0, RGS1^{WT} and S278E exhibit similar infection response patterns. Conversely, S278A, clusterA, and rgs1-2 demonstrated distinctive infectious responses when compared to Col-0 (Figure 14). The absence of cluster phosphorylation and the absence of RGS1 displayed a resistant response to infection, while the inability of the S278 residue being phosphorylated aggravated the bacterial infection symptoms. Whereas the response of rgs1-2 has been already demonstrated (Liang *et al.*, 2018), our findings evidenced the pivotal role of S278 and cluster residues' phosphorylation patterns in determining resistance or susceptibility to bacterial infection.

REFERENCES

- Alvarez C. E. (2008). On the origins of arrestin and rhodopsin. *BMC evolutionary biology*, 8, 222. <https://doi.org/10.1186/1471-2148-8-222>
- Bhat, A. H., Prabhu, P., & Balakrishnan, K. (2019). A critical analysis of state-of-the-art metagenomics OTU clustering algorithms. *Journal of biosciences*, 44(6), 148.
- Bologna, Z., Teoh, J. P., Bayoumi, A. S., Tang, Y., & Kim, I. M. (2017). Biased G Protein-Coupled Receptor Signaling: New Player in Modulating Physiology and Pathology. *Biomolecules & therapeutics*, 25(1), 12–25. <https://doi.org/10.4062/biomolther.2016.165>
- Bruns N. (2020). Blender: Universelle 3D-Bearbeitungs- und Animationssoftware [Blender : Universal 3D processing and animation software]. *Der Unfallchirurg*, 123(9), 747–750. <https://doi.org/10.1007/s00113-020-00836-0>
- Chakravorty, D., Gookin, T. E., Milner, M. J., Yu, Y., & Assmann, S. M. (2015). Extra-Large G Proteins Expand the Repertoire of Subunits in Arabidopsis Heterotrimeric G Protein Signaling. *Plant physiology*, 169(1), 512–529. <https://doi.org/10.1104/pp.15.00251>
- Chen, J. G., Willard, F. S., Huang, J., Liang, J., Chasse, S. A., Jones, A. M., & Siderovski, D. P. (2003). A seven-transmembrane RGS protein that modulates plant cell proliferation. *Science (New York, N.Y.)*, 301(5640), 1728–1731. <https://doi.org/10.1126/science.1087790>
- Chen J. G. (2008). Heterotrimeric G-protein signaling in Arabidopsis: Puzzling G-protein-coupled receptor. *Plant signaling & behavior*, 3(12), 1042–1045. <https://doi.org/10.4161/psb.3.12.6064>
- Chen, Y., Ji, F., Xie, H., & Liang, J. (2006). Overexpression of the regulator of G-protein signalling protein enhances ABA-mediated inhibition of root elongation and drought tolerance in Arabidopsis. *Journal of experimental botany*, 57(9), 2101–2110. <https://doi.org/10.1093/jxb/erj167>

Choudhary, A., Kumar, A., Kaur, N., & Kaur, H. (2022). Molecular cues of sugar signaling in plants. *Physiologia plantarum*, 174(1), e13630. <https://doi.org/10.1111/ppl.13630>

Choudhury, S. R., & Pandey, S. (2015). Phosphorylation-Dependent Regulation of G-Protein Cycle during Nodule Formation in Soybean. *The Plant cell*, 27(11), 3260–3276. <https://doi.org/10.1105/tpc.15.00517>

Cooper, J. A., Sefton, B. M., & Hunter, T. (1983). Detection and quantification of phosphotyrosine in proteins. *Methods in enzymology*, 99, 387–402. [https://doi.org/10.1016/0076-6879\(83\)99075-4](https://doi.org/10.1016/0076-6879(83)99075-4)

Croitoru, A., Park, S. J., Kumar, A., Lee, J., Im, W., MacKerell, A. D., Jr, & Aleksandrov, A. (2021). Additive CHARMM36 Force Field for Nonstandard Amino Acids. *Journal of chemical theory and computation*, 17(6), 3554–3570. <https://doi.org/10.1021/acs.jctc.1c00254>

Derbyshire, P., Findlay, K., McCann, M. C., & Roberts, K. (2007). Cell elongation in *Arabidopsis* hypocotyls involves dynamic changes in cell wall thickness. *Journal of experimental botany*, 58(8), 2079–2089. <https://doi.org/10.1093/jxb/erm074>

Elkin, S. R., Lakoduk, A. M., & Schmid, S. L. (2016). Endocytic pathways and endosomal trafficking: a primer. *Wiener medizinische Wochenschrift (1946)*, 166(7-8), 196–204. <https://doi.org/10.1007/s10354-016-0432-7>

Felix, G., Duran, J. D., Volko, S., & Boller, T. (1999). Plants have a sensitive perception system for the most conserved domain of bacterial flagellin. *The Plant journal : for cell and molecular biology*, 18(3), 265–276. <https://doi.org/10.1046/j.1365-313x.1999.00265.x>

Feng, S., Park, S., Choi, Y. K., & Im, W. (2023). CHARMM-GUI Membrane Builder: Past, Current, and Future Developments and Applications. *Journal of chemical theory and computation*, 19(8), 2161–2185. <https://doi.org/10.1021/acs.jctc.2c01246>

Fu, Y., Lim, S., Urano, D., Tunc-Ozdemir, M., Phan, N. G., Elston, T. C., & Jones, A. M. (2014). Reciprocal encoding of signal intensity and duration in a glucose-sensing circuit. *Cell*, 156(5), 1084–1095. <https://doi.org/10.1016/j.cell.2014.01.013>

Höhler, D., Pfeiffer, W., Ioannidis, V., Stockinger, H., & Stamatakis, A. (2022). RAxML Grove: an empirical phylogenetic tree database. *Bioinformatics (Oxford, England)*, 38(6), 1741–1742. <https://doi.org/10.1093/bioinformatics/btab863>

Hou, J., Wu, T., Guo, Z., Quadir, F., & Cheng, J. (2020). The MULTICOM Protein Structure Prediction Server Empowered by Deep Learning and Contact Distance Prediction. *Methods in molecular biology (Clifton, N.J.)*, 2165, 13–26. https://doi.org/10.1007/978-1-0716-0708-4_2

Jelenska, J., Davern, S. M., Standaert, R. F., Mirzadeh, S., & Greenberg, J. T. (2017). Flagellin peptide flg22 gains access to long-distance trafficking in Arabidopsis via its receptor, FLS2. *Journal of experimental botany*, 68(7), 1769–1783. <https://doi.org/10.1093/jxb/erx060>

Jia, H., Song, G., Werth, E. G., Walley, J. W., Hicks, L. M., & Jones, A. M. (2019). Receptor-Like Kinase Phosphorylation of Arabidopsis Heterotrimeric G-Protein $G\alpha$ - Subunit AtGPA1. *Proteomics*, 19(24), e1900265. <https://doi.org/10.1002/pmic.201900265>.

Johnston, C. A., Taylor, J. P., Gao, Y., Kimple, A. J., Grigston, J. C., Chen, J. G., Siderovski, D. P., Jones, A. M., & Willard, F. S. (2007). GTPase acceleration as the rate-limiting step in Arabidopsis G protein-coupled sugar signaling. *Proceedings of the National Academy of Sciences of the United States of America*, 104(44), 17317–17322. <https://doi.org/10.1073/pnas.0704751104>

Jones, J. C., Duffy, J. W., Machius, M., Temple, B. R., Dohlman, H. G., & Jones, A. M. (2011). The crystal structure of a self-activating G protein alpha subunit reveals its distinct mechanism of signal initiation. *Science signaling*, 4(159), ra8. <https://doi.org/10.1126/scisignal.2001446>

Jones, J. C., Temple, B. R., Jones, A. M., & Dohlman, H. G. (2011). Functional reconstitution of an atypical G protein heterotrimer and regulator of G protein signaling protein (RGS1) from *Arabidopsis thaliana*. *The Journal of biological chemistry*, 286(15), 13143–13150. <https://doi.org/10.1074/jbc.M110.190355>

Katoh, K., Rozewicki, J., & Yamada, K. D. (2019). MAFFT online service: multiple sequence alignment, interactive sequence choice and visualization. *Briefings in bioinformatics*, 20(4), 1160–1166. <https://doi.org/10.1093/bib/bbx108>

Li, B., Ferreira, M. A., Huang, M., Camargos, L. F., Yu, X., Teixeira, R. M., Carpinetti, P. A., Mendes, G. C., Gouveia-Mageste, B. C., Liu, C., Pontes, C. S. L., Brustolini, O. J. B., Martins, L. G. C., Melo, B. P., Duarte, C. E. M., Shan, L., He, P., & Fontes, E. P. B. (2019). The receptor-like kinase NIK1 targets FLS2/BAK1 immune complex and inversely modulates antiviral and antibacterial immunity. *Nature communications*, 10(1), 4996. <https://doi.org/10.1038/s41467-019-12847-6>

Li, B., Tunc-Ozdemir, M., Urano, D., Jia, H., Werth, E. G., Mowrey, D. D., Hicks, L. M., Dokholyan, N. V., Torres, M. P., & Jones, A. M. (2018). Tyrosine phosphorylation switching of a G protein. *The Journal of biological chemistry*, 293(13), 4752–4766. <https://doi.org/10.1074/jbc.RA117.000163>

Liang, X., Ma, M., Zhou, Z., Wang, J., Yang, X., Rao, S., Bi, G., Li, L., Zhang, X., Chai, J., Chen, S., & Zhou, J. M. (2018). Ligand-triggered de-repression of *Arabidopsis* heterotrimeric G proteins coupled to immune receptor kinases. *Cell research*, 28(5), 529–543. <https://doi.org/10.1038/s41422-018-0027-5>

Liang, X., Ding, P., Lian, K., Wang, J., Ma, M., Li, L., Li, L., Li, M., Zhang, X., Chen, S., Zhang, Y., & Zhou, J. M. (2016). *Arabidopsis* heterotrimeric G proteins regulate immunity by directly coupling to the FLS2 receptor. *eLife*, 5, e13568. <https://doi.org/10.7554/eLife.13568>

Liu, J., Guo, Z., Wu, T., Roy, R. S., Quadir, F., Chen, C., & Cheng, J. (2023). Enhancing AlphaFold-Multimer-based Protein Complex Structure Prediction with MULTICOM in

CASP15. bioRxiv: the preprint server for biology, 2023.05.16.541055.
<https://doi.org/10.1101/2023.05.16.541055>

Lohse, M. J., Benovic, J. L., Codina, J., Caron, M. G., & Lefkowitz, R. J. (1990). beta-Arrestin: a protein that regulates beta-adrenergic receptor function. *Science (New York, N.Y.)*, 248(4962), 1547–1550. <https://doi.org/10.1126/science.2163110>

Masuho, I., Balaji, S., Muntean, B. S., Skamangas, N. K., Chavali, S., Tesmer, J. J. G., Babu, M. M., & Martemyanov, K. A. (2020). A Global Map of G Protein Signaling Regulation by RGS Proteins. *Cell*, 183(2), 503–521.e19. <https://doi.org/10.1016/j.cell.2020.08.052>

Meng, E. C., Goddard, T. D., Pettersen, E. F., Couch, G. S., Pearson, Z. J., Morris, J. H., & Ferrin, T. E. (2023). UCSF ChimeraX: Tools for structure building and analysis. *Protein science: a publication of the Protein Society*, 32(11), e4792. <https://doi.org/10.1002/pro.4792>

Ngou, B. P. M., Heal, R., Wyler, M., Schmid, M. W., & Jones, J. D. G. (2022). Concerted expansion and contraction of immune receptor gene repertoires in plant genomes. *Nature plants*, 8(10), 1146–1152. <https://doi.org/10.1038/s41477-022-01260-5>

Nguyen, L. T., Schmidt, H. A., von Haeseler, A., & Minh, B. Q. (2015). IQ-TREE: a fast and effective stochastic algorithm for estimating maximum-likelihood phylogenies. *Molecular biology and evolution*, 32(1), 268–274. <https://doi.org/10.1093/molbev/msu300>

Oliveira, C. C., Jones, A. M., Fontes, E. P. B., & Reis, P. A. B. D. (2022). G-Protein Phosphorylation: Aspects of Binding Specificity and Function in the Plant Kingdom. *International journal of molecular sciences*, 23(12), 6544. <https://doi.org/10.3390/ijms23126544>

Oliveira CC. RGS1 Phospho-Barcode: Decoding how G Signaling is modulated in plants through the phosphorylation of its components. Tese (Doutorado em Bioquímica Aplicada) - Universidade Federal de Viçosa, p. 76. 2022.

Pearlman, S. M., Serber, Z., & Ferrell, J. E., Jr (2011). A mechanism for the evolution of phosphorylation sites. *Cell*, 147(4), 934–946. <https://doi.org/10.1016/j.cell.2011.08.052>

Pronk, S., Páll, S., Schulz, R., Larsson, P., Bjelkmar, P., Apostolov, R., Shirts, M. R., Smith, J. C., Kasson, P. M., van der Spoel, D., Hess, B., & Lindahl, E. (2013). GROMACS 4.5: a high-throughput and highly parallel open source molecular simulation toolkit. *Bioinformatics (Oxford, England)*, 29(7), 845–854. <https://doi.org/10.1093/bioinformatics/btt055>

Ramazi, S., Allahverdi, A., & Zahiri, J. (2020). Evaluation of post-translational modifications in histone proteins: A review on histone modification defects in developmental and neurological disorders. *Journal of biosciences*, 45, 135.

Rosignoli, S., & Paiardini, A. (2022). Boosting the Full Potential of PyMOL with Structural Biology Plugins. *Biomolecules*, 12(12), 1764. <https://doi.org/10.3390/biom12121764>

Sun, Y., Li, L., Macho, A. P., Han, Z., Hu, Z., Zipfel, C., Zhou, J. M., & Chai, J. (2013). Structural basis for flg22-induced activation of the Arabidopsis FLS2-BAK1 immune complex. *Science (New York, N.Y.)*, 342(6158), 624–628. <https://doi.org/10.1126/science.1243825>

Syrovatkina, V., Alegre, K. O., Dey, R., & Huang, X. Y. (2016). Regulation, Signaling, and Physiological Functions of G-Proteins. *Journal of molecular biology*, 428(19), 3850–3868. <https://doi.org/10.1016/j.jmb.2016.08.002>

Toropov, A. A., & Toropova, A. P. (2020). The Monte Carlo Method as a Tool to Build up Predictive QSPR/QSAR. *Current computer-aided drug design*, 16(3), 197–206. <https://doi.org/10.2174/1573409915666190328123112>

Tunc-Ozdemir, M., & Jones, A. M. (2017). Ligand-induced dynamics of heterotrimeric G protein-coupled receptor-like kinase complexes. *PLoS one*, 12(2), e0171854. <https://doi.org/10.1371/journal.pone.0171854>

Tunc-Ozdemir, M., Li, B., Jaiswal, D. K., Urano, D., Jones, A. M., & Torres, M. P. (2017). Predicted Functional Implications of Phosphorylation of Regulator of G Protein Signaling Protein in Plants. *Frontiers in plant science*, 8, 1456. <https://doi.org/10.3389/fpls.2017.01456>

Tunc-Ozdemir, M., Urano, D., Jaiswal, D. K., Clouse, S. D., & Jones, A. M. (2016). Direct Modulation of Heterotrimeric G Protein-coupled Signaling by a Receptor Kinase Complex. *The Journal of biological chemistry*, 291(27), 13918–13925. <https://doi.org/10.1074/jbc.C116.736702>

Urano, D., Chen, J. G., Botella, J. R., & Jones, A. M. (2013). Heterotrimeric G protein signalling in the plant kingdom. *Open biology*, 3(3), 120186. <https://doi.org/10.1098/rsob.120186>

Urano, D., & Jones, A. M. (2014). Heterotrimeric G protein-coupled signaling in plants. *Annual review of plant biology*, 65, 365–384. <https://doi.org/10.1146/annurev-arplant-050213-040133>

Urano, D., & Jones, A. M. (2014). Heterotrimeric G protein-coupled signaling in plants. *Annual review of plant biology*, 65, 365–384. <https://doi.org/10.1146/annurev-arplant-050213-040133>

Vieira, I. H. P., Botelho, E. B., de Souza Gomes, T. J., Kist, R., Caceres, R. A., & Zanchi, F. B. (2023). Visual dynamics: a WEB application for molecular dynamics simulation using GROMACS. *BMC bioinformatics*, 24(1), 107. <https://doi.org/10.1186/s12859-023-05234-y>

Wang, H. C., Li, K., Susko, E., & Roger, A. J. (2008). A class frequency mixture model that adjusts for site-specific amino acid frequencies and improves inference of protein

phylogeny. *BMC evolutionary biology*, 8, 331. <https://doi.org/10.1186/1471-2148-8-331>

Wang, Y., Wang, Y., & Deng, D. (2019). Multifaceted plant G protein: interaction network, agronomic potential, and beyond. *Planta*, 249(5), 1259–1266. <https://doi.org/10.1007/s00425-019-03112-7>

Watkins, J. M., Montes, C., Clark, N. M., Song, G., Oliveira, C. C., Mishra, B., Brachova, L., Seifert, C. M., Mitchell, M. S., Yang, J., Braga Dos Reis, P. A., Urano, D., Muktar, M. S., Walley, J. W., & Jones, A. M. (2023). Phosphorylation dynamics in a flg22-induced, G-protein dependent network reveals the RGS1 phosphatase. *Molecular & cellular proteomics: MCP*, 100705. Advance online publication. <https://doi.org/10.1016/j.mcpro.2023.100705>

Watkins, J. M., Ross-Elliott, T. J., Shan, X., Lou, F., Dreyer, B., Tunc-Ozdemir, M., Jia, H., Yang, J., Oliveira, C. C., Wu, L., Trusov, Y., Schwochert, T. D., Krysan, P., & Jones, A. M. (2021). Differential regulation of G protein signaling in Arabidopsis through two distinct pathways that internalize AtRGS1. *Science signaling*, 14(695), eabe4090. <https://doi.org/10.1126/scisignal.abe4090>

Willard, F. S., & Siderovski, D. P. (2004). Purification and in vitro functional analysis of the Arabidopsis thaliana regulator of G-protein signaling-1. *Methods in enzymology*, 389, 320–338. [https://doi.org/10.1016/S0076-6879\(04\)89019-0](https://doi.org/10.1016/S0076-6879(04)89019-0)

Zelazny, E., Santambrogio, M., & Gaude, T. (2013). Retromer association with membranes: plants have their own rules! *Plant signaling & behavior*, 8(9), e25312. <https://doi.org/10.4161/psb.25312>

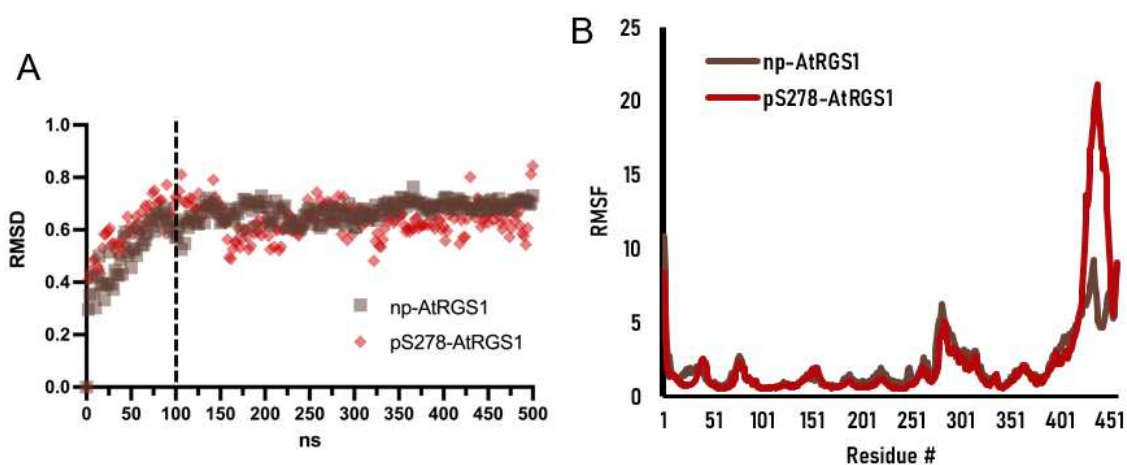
Zhong, C. L., Zhang, C., & Liu, J. Z. (2019). Heterotrimeric G protein signaling in plant immunity. *Journal of experimental botany*, 70(4), 1109–1118. <https://doi.org/10.1093/jxb/ery426>

Zipfel, C., Robatzek, S., Navarro, L., Oakeley, E. J., Jones, J. D., Felix, G., & Boller, T. (2004). Bacterial disease resistance in *Arabidopsis* through flagellin perception. *Nature*, 428(6984), 764–767. <https://doi.org/10.1038/nature02485>

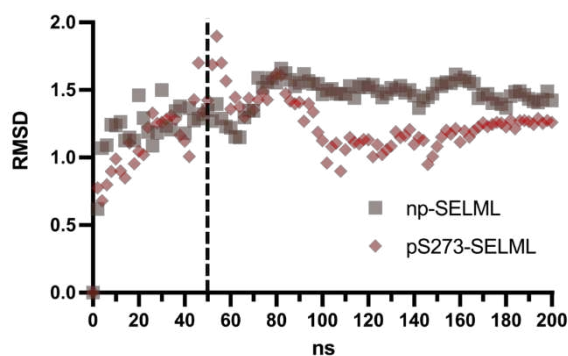
SUPPLEMENTARY MATERIAL

Supplemental Table 1 – Oligonucleotides used for cloning and site-directed mutagenesis.

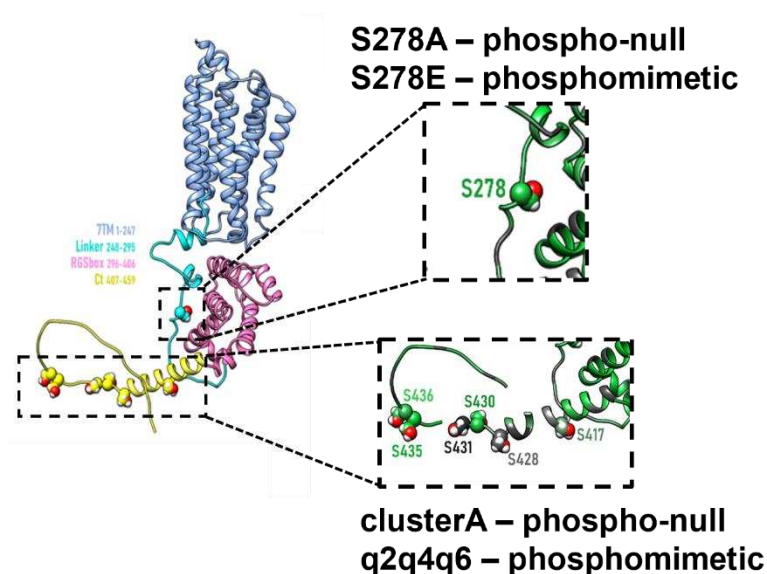
Gene	Oligonucleotide ID	Sequence (5'→3')	Application
AtRGS1	AtRGS1-Fwd-GW	CACCATGGCGAGTGGATGTGCTCTACAT	pENTR D-TOPO cloning and confirmation
	AtRGS1-NS-HiBiT-Rvs-GW	GCTAATCTTCTTGAACAGCCGCCAGC CGCTCACACCCGGACTACTGCATCTG	pENTR D-TOPO cloning and confirmation
	AtRGS1-S278E-Fwd	CATTCCCAGTgagGGATTATTATTTCGGAAG	Site-directed mutagenesis
	AtRGS1-S278A-Fwd	CATTCCCAGTgccGGATTATTATTTCG	Site-directed mutagenesis
	AtRGS1-S278-Rvs	CCTAGAGCTTGACCCATTC	Site-directed mutagenesis
	AtRGS1-q2q4q6-Fwd	caagactggaagCAGTTCAAGGCTCTGATG	Site-directed mutagenesis
	AtRGS1-q2q4q6-Rvs	gttctgcaaactcGTATCCTTCCTTATGCATTG	Site-directed mutagenesis
	AtRGS1-clusterA-Fwd	caagactggctgCAGTTCAAGGCTCTGATG	Site-directed mutagenesis
	AtRGS1-clusterA-Rvs	gagctgcaaaaagcGTATCCTTCCTTATGCATTG	Site-directed mutagenesis
	AtRGS1-quadA-Fwd	caagactggctgCAGTTCAAGGCTCTGATG	Site-directed mutagenesis
	AtRGS1-quadA-Rvs	gagctgaaaaagcGTATCCTTCCTTATGCATTG	Site-directed mutagenesis



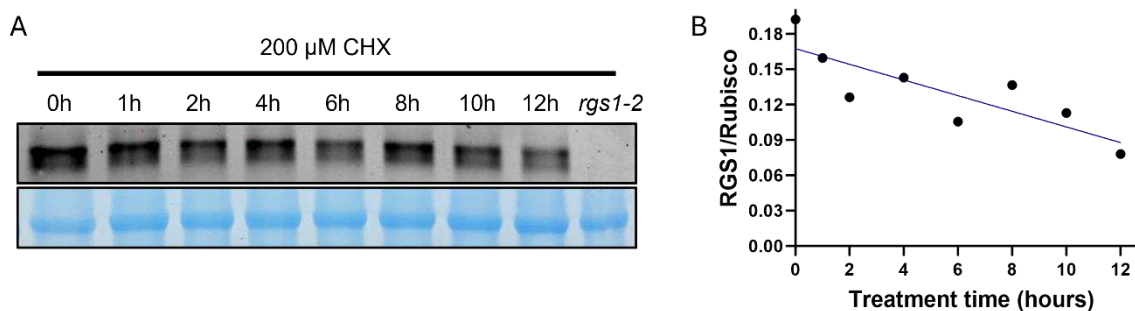
Supplemental Figure 1 – MDS analysis of AtRGS1 protein in different phosphostates. (A) Room mean square deviation (RMSD) analysis of non-phospho-AtRGS1 and phosphoS287-AtRGS1. The flattening of the RMSD curve indicates that the proteins equilibrated around 100ns after the beginning of the analysis. **(B)** Root mean square fluctuation (RMSF) analysis from the same two proteins. The pS278-AtRGS1 peak close to the C-tail residues indicates a higher freedom of movement and flexibility in that region.



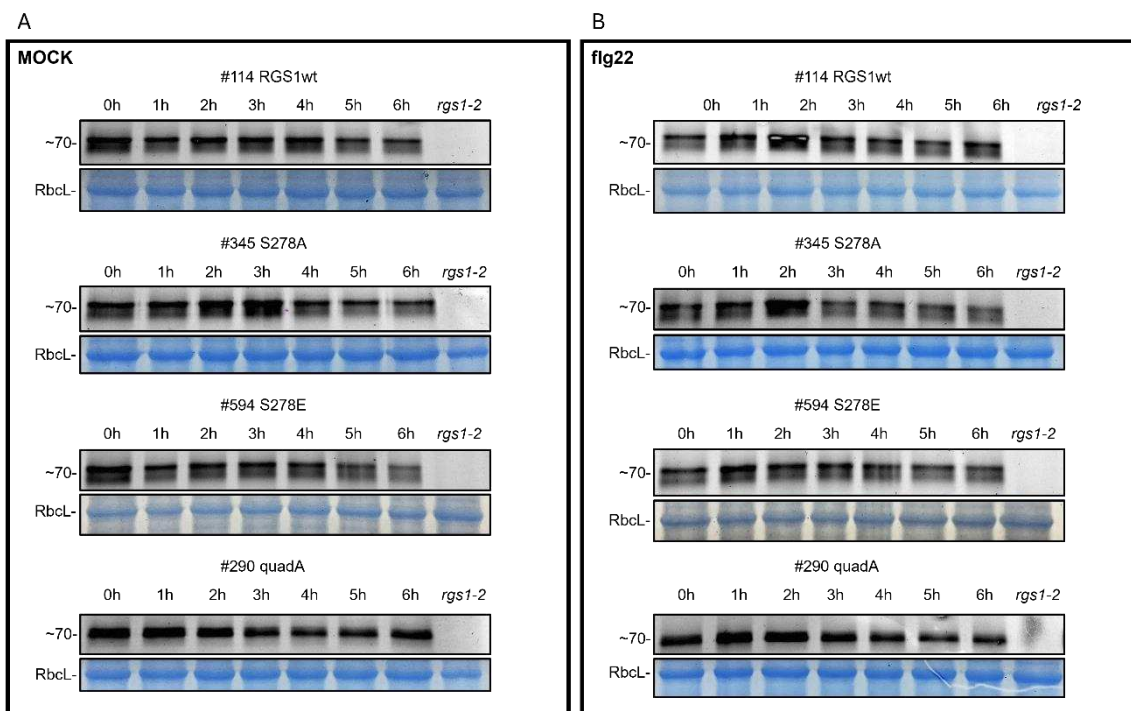
Supplemental Figure 2 – MDS analysis of RGS-SELML protein in different phosphostates. RMSD analysis of npRGS1-SELML and pS273-RGS-SELML. The flattening of the RMSD curve indicates that the proteins equilibrated around 50 ns after the beginning of the analysis.



Supplemental Figure 3 - Schematic 3D structure showing the phosphorylation sites positions.

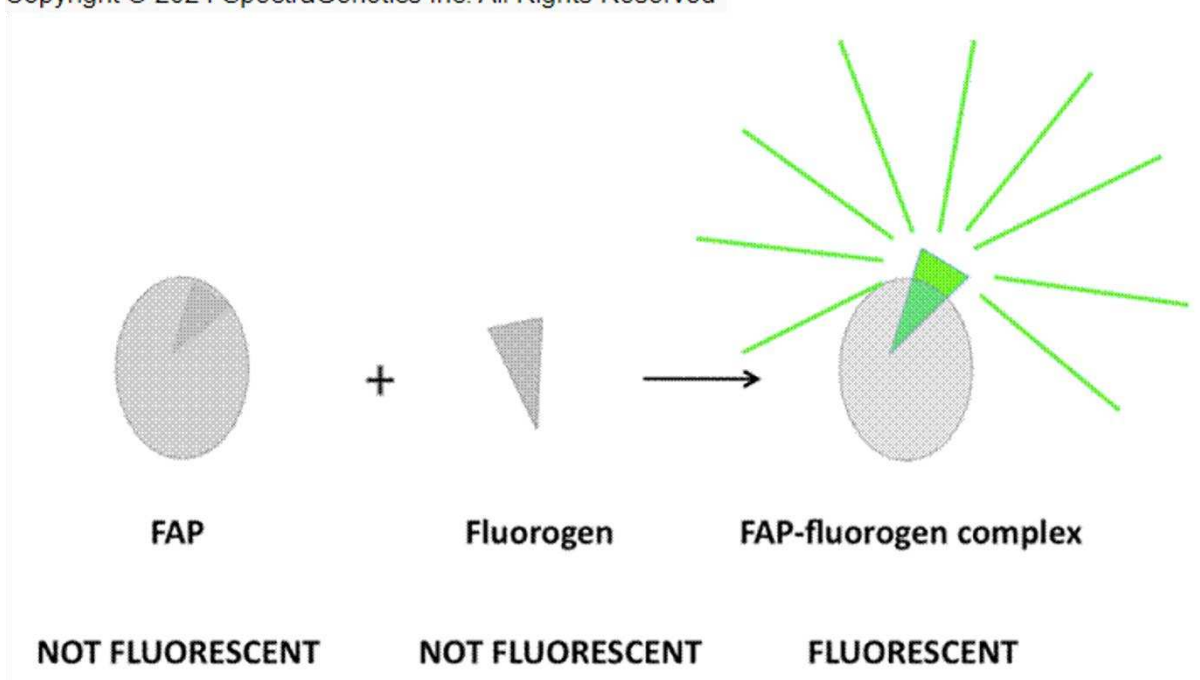


Supplemental Figure 4 - AtRGS1 stability over time. (A) Western blot analysis of AtRGS1 stability along 12 hours. Cycloheximide (CHX) was used for protein synthesis inhibition, and RbcL was used as the loading control. (B) Western blot quantification of AtRGS1 decay.

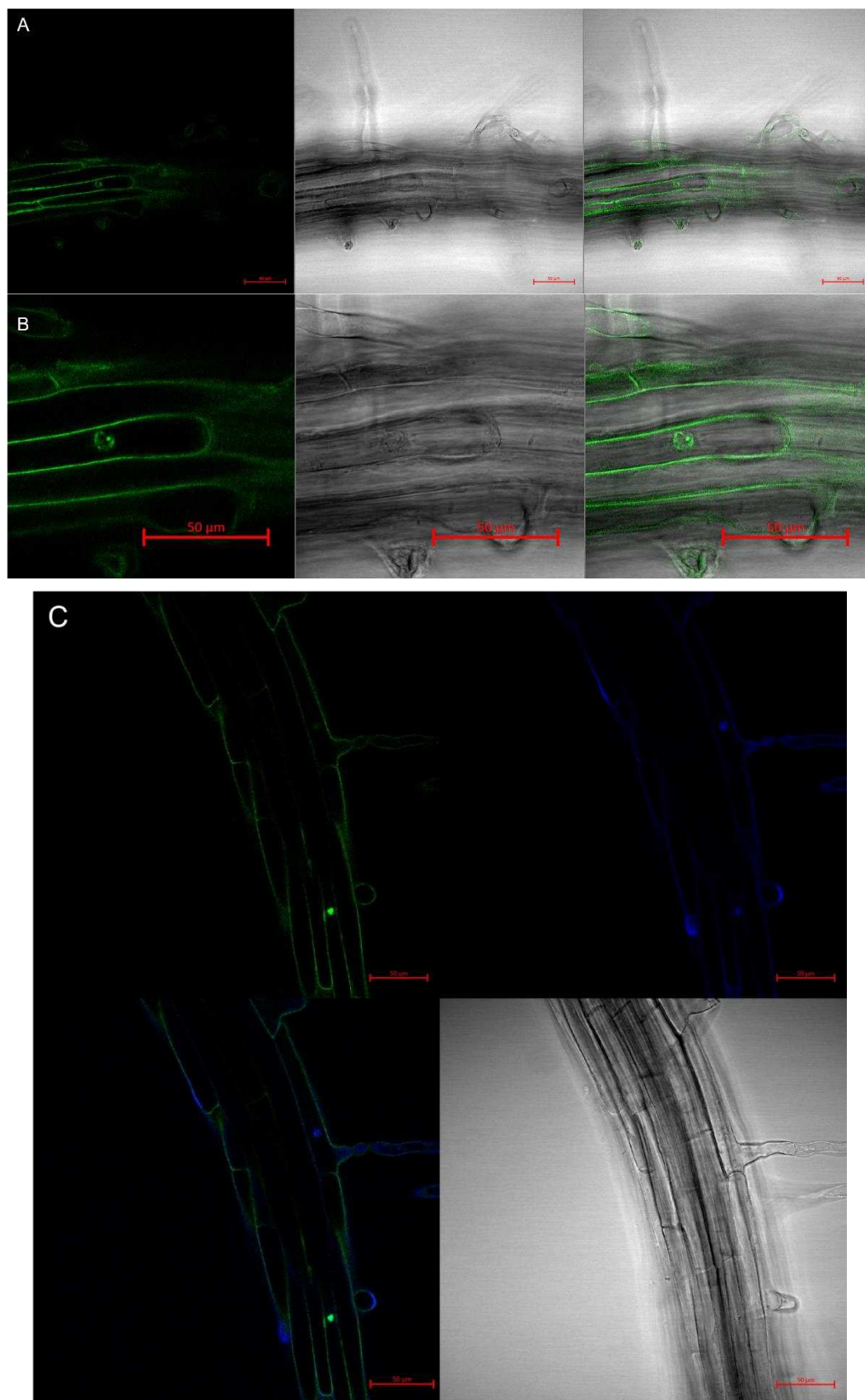


Supplemental Figure 5 - AtRGS1 wild type and phosphomimetic mutants' stability over time. Western blot analysis AtRGS1 stability along 6 hours. Cycloheximide (CHX) was used for protein synthesis inhibition, flg22 was used as a mimetic elicitor, and RbcL was used as the loading control. **(A)** Western blot of AtRGS1^{WT} and phosphomimetics decay only under CHX exposure. **(B)** Western blot of AtRGS1^{WT} and phosphomimetics decay under CHX and 100nM of flg22 exposure.

Copyright © 2024 SpectraGenetics Inc. All Rights Reserved

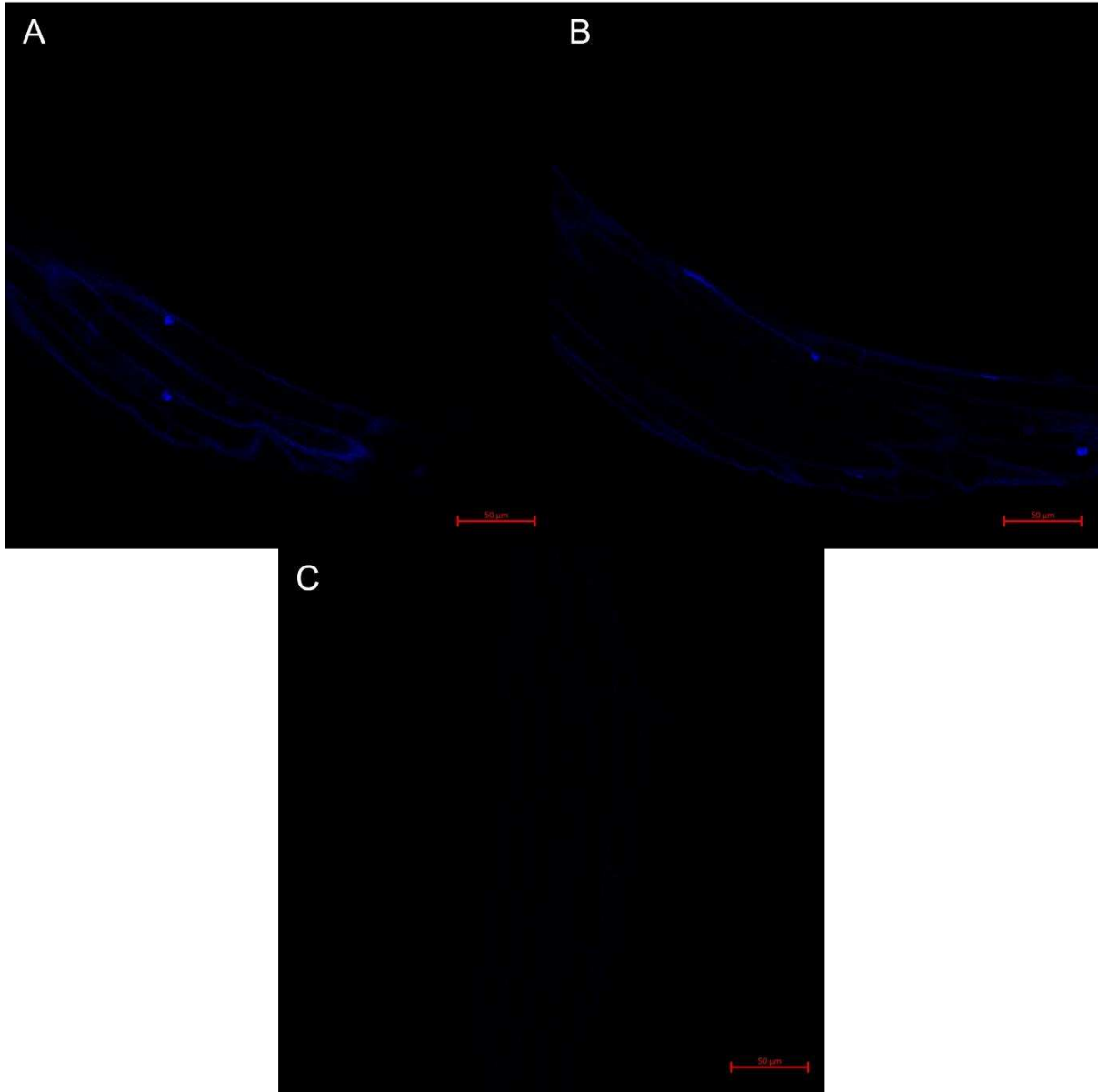


Supplemental Figure 6 – Schematic representation illustrating the mechanism of FAP-fluorescence.

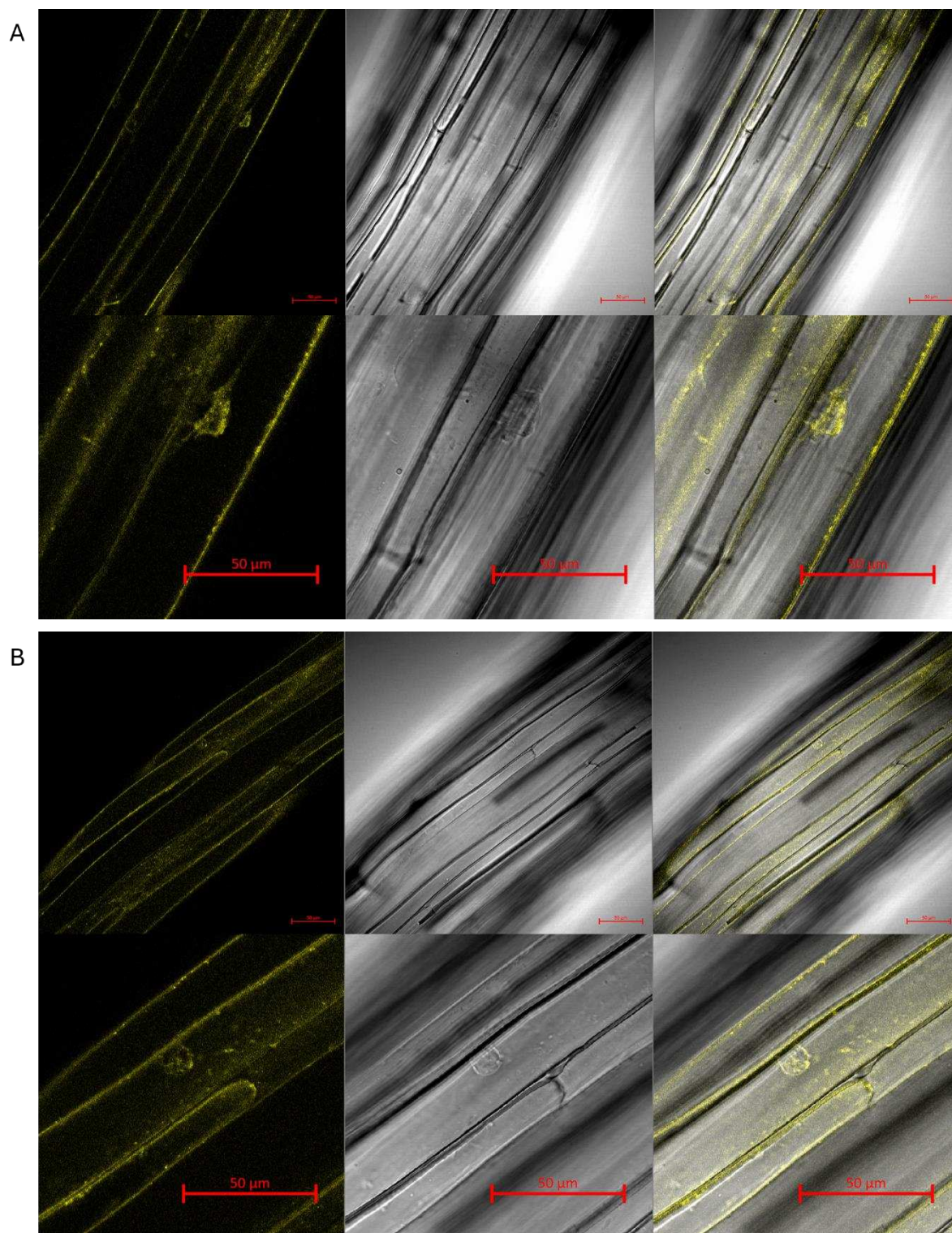


Supplemental Figure 7 – FAP-Beta-RGS1-WT nuclear localization. (A) Representative processed confocal images of FAP-Beta-RGS1 fluorescence within the envelope nuclear. (B) Zoom-in image in the

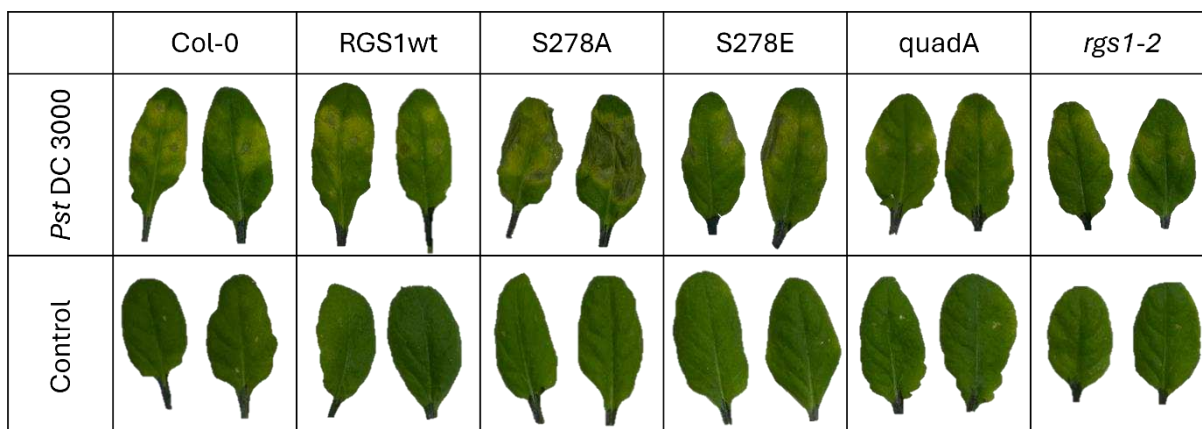
bottom to provide a better observation of the nucleus. **(C)** Colocalization of FAP-Beta-RGS1 fluorescence and Hoechst staining. Scale bar - 50 μm .



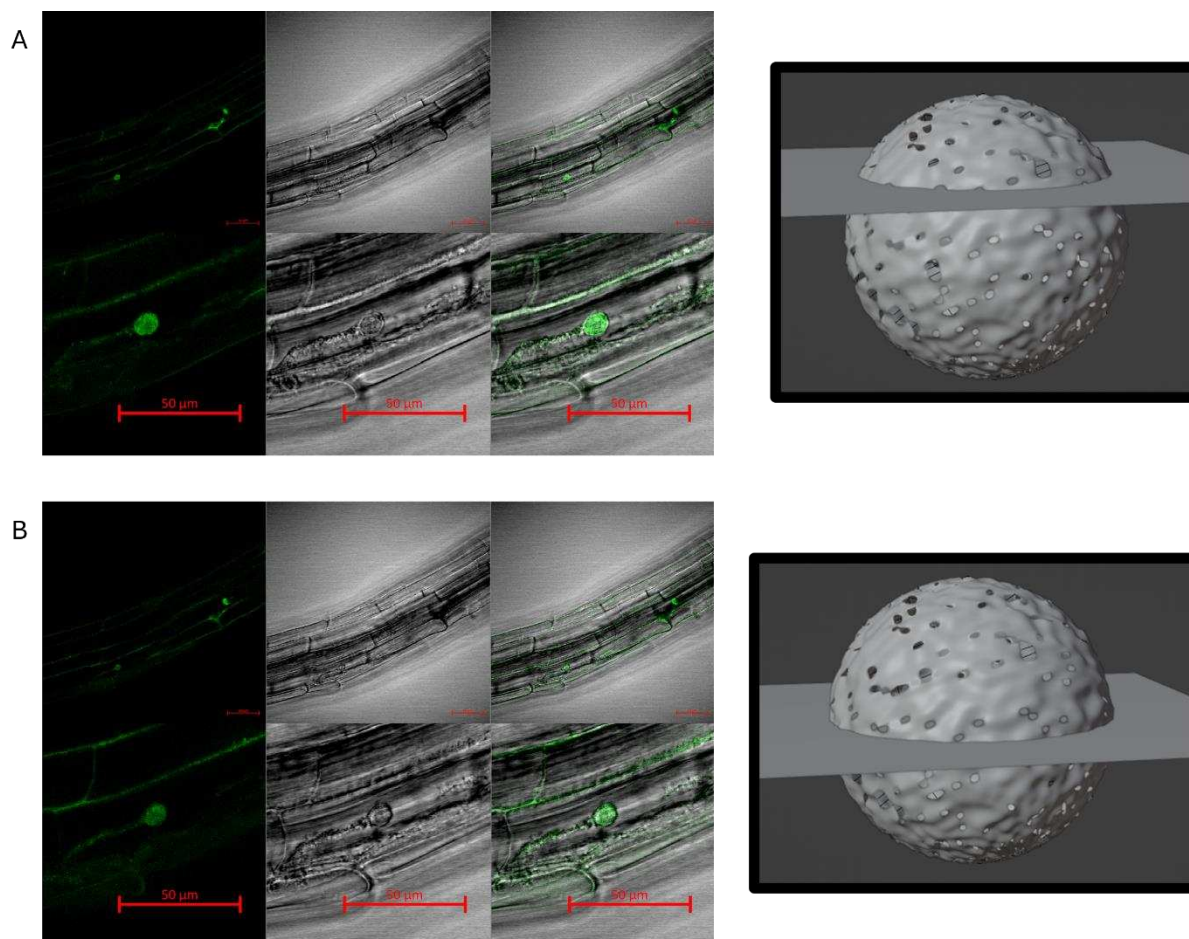
Supplemental Figure 8 – Controls of FAP-Beta confocal imaging. **(A-B)** Representative processed confocal images of Col-0 seedlings incubated with Hoechst nuclear marker, evidencing staining in the nucleus and membranes even after water-wash steps. **(C)** FAP-Beta-RGS1^{WT} seedlings without fluorogen addition, demonstrating that there is no fluorescence overlapping by FAP-Beta and Hoechst marker. Scale bar - 50 μm .



Supplemental Figure 9 – RGS1^{WT}-YFP nuclear localization due flg22 induction (A-B). Representative processed confocal images of different RGS1^{WT}-YFP seedlings under 1 hour of Flg22 treatment (zoom-in at the bottom images). Scale bar - 50 μm.



Supplemental Figure 10 – Phosphorylation of serine residues affects AtRGS1 response to bacterial infection. Disease symptoms on leaves post *Pst* DC3000 infection. Images were taken at 5 dpi. n ≈ 3.



Supplemental Figure 11 – FAP-Beta-RGS1-WT is located on the nucleus surface. Representative processed confocal images of FAP-Beta-RGS1-WT under 1 hour of Flg22 treatment in different depth layers. **(A)** At the left side, a confocal image showing the external layer of the nucleus (zoom-in at the bottom images). On the right side, a cartoon representing confocal images. **(B)** At the left side, a confocal image showing the middle layer of the nucleus (zoom-in at the bottom images). On the right side, a cartoon representing confocal images. Scale bar - 50 μm.

GENERAL CONCLUSION

Plants, as sessile organisms, must perceive the information around them to make the best decisions that enable them to survive, grow, and thrive. A signal or molecule should be recognized by the plant cell to activate a response during a certain period. Therefore, specific pathways should be activated in order to maintain the cell-environment adjustment.

In this work, we presented two crucial signaling pathways essential for cell development, survival, and stress responses. Firstly, we described the conserved and unique mechanisms activated by ER sensors in plants and how they modulate the cell response to different types of stress. Furthermore, under prolonged stress, ER signaling can trigger autophagy or programmed cell death responses. Although these mechanisms are not fully understood, many factors have been elucidated, and their connections with other pathways increase their relevance in cell function. However, some unanswered questions regarding ER-mediated signaling may guide scientists in the near future: What is the critical point at which the cell activates the cell death response under ER stress? Does the developmental stage implicate different responses of the involved factors?

Secondly, we leveraged *in silico* molecular simulations, *in vivo* interaction assays, and RGS1 transgenic lines to investigate the RGS1 structure and the phosphorylation effect on RGS1 function. We demonstrated the conservation of specific amino acid residues of RGS1 among different species and highlighted their crucial roles in RGS1 function. We identified the S278 residue, often overlooked due to its location in the flexible linker region, as an essential player for RGS1 function. Consequently, we evaluated the role of the S278 residue and its phosphomimetic and phospho-null mutants in RGS1 structure, stability, internalization, and cell function. Our findings indicated that the phosphorylation of S278 influences the structure and interactions of the RGS1 protein. The phosphomimetic exhibited a decreased interaction pattern with AtGPA1, although the interaction with AtGPA1 Y166 phosphomimetic was stabilized, implicating a more complex phosphorylation code. S278 residue phosphorylation is also crucial for RGS1 internalization, and nuclear translocation under sugar and flg22 treatments. Moreover, we demonstrated that RGS1 stability in the cell is related to S278 phosphorylation, as the phospho-null protein displayed higher stability compared to RGS1^{WT} and the phosphomimetic.

Additionally, S278 phosphorylation is important for plant responses under bacterial infection.

Therefore, our data imply that the conservation of specific amino acid residues, such as S278, is extremely relevant to RGS1 structure dynamics, as well as the modulation of RGS1 interaction and activity. A deep understanding of this residue and its influence on other residues will lead us to unveil part of the heterotrimeric-G phospho-barcode.